JOURNAL OF THE

Electrochemical Society

Vol. 103, No. 6 June 1956

AS PARTNERS IN YOUR PROGRESS . . .

SERVICE – is a *plus* factor!

Our service engineers are thoroughly familiar with electrothermic and electrochemical operations. They are competent to render high level technical advice to electrode, anode, carbon brick and mold stock customers.

The alertness of these service engineers in anticipating customer needs and wishes is a characteristic *plus factor* in the trustworthiness of GLC carbon and graphite products.

The high degree of integration between discoveries in our research laboratories, refinements in processing raw materials and improved manufacturing techniques is further assurance of excellent product performance.

ELECTRODE GLC® DIVISION

Great Lakes Carbon Corporation

ADMINISTRATIVE OFFICE: 18 East 48th Street, New York 17, N. Y. PLANTS: Niagara Falls, N. Y., Morganton, N. C. OTHER OFFICES: Niagara Falls, N. Y., Oak Park, Ill., Pittsburgh, Pa. SALES AGENTS: J. B. Hayes Company, Birmingham, Ala., George O. O'Hara, Wilmington, Cal. SALES AGENTS IN OTHER COUNTRIES: Great Northern Carbon & Chemical Co., Ltd., Montreal, Canada; Great Eastern Carbon & Chemical Co., Inc., Chiyoda-Ku, Tokyo, Japan

Journal of the
Electrochemical Society

JUNE 1956 VOL. 103 · NO. 6

CONTENTS

Published monthly by The Electrochemical Society, Inc., Mount Royal and Guilford Aves., Baltimore 2, Md., combining the JOURNAL and TRANSACTIONS OF THE ELECTROCHEMICAL SOCIETY. Editorial offices: 216 West 102nd Street, New York 25, N. Y Statements and opinions given in articles and papers in the JOURNAL OF THE ELECTROCHEMICAL SOCIETY are those of the contributors, and The Electrochemical Society assumes no responsibility for them. Nondeductible subscription to members $5.00; subscription to nonmembers $18.00. Single copies $1.25 to members, $1.75 to nonmembers. Entered as second-class matter November 15, 1947, at the Post Office at Baltimore, Md., under the act of August 24, 1912.

The Graduate Program in Chemistry

TRAINING the Ph.D. candidate in science is a serious matter today. Few students can afford the luxury of the graduate course unless they are subsidized by teaching or research assistantships. The long years of confined work and comparative poverty can create problems in social and family life, sometimes even in health. The same thing is, of course, true in all the professional schools.

The university departments have these problems very much in mind in the periodic reappraisals of their programs. How can the student be directed to make best use of his time? Should he spend a year, or more, solely in textbook work? How much routine laboratory work should he do before starting experimental research? Should there be a single comprehensive examination—a blockbuster—or many shorter quizzes? Should the department offer many specialized courses, or rely on a few fundamental subjects?

Naturally, each department must work out its own formula, with its own students, its financial and material resources, and its own professorial staff in mind. There are, however, a few general principles for guidance. Perhaps only half, or less, of the first-year class is expected to complete the Ph.D. program. Further, most of them were uncertain, as undergraduates, of continuing in graduate school, and only a few made serious efforts to prepare well for advanced work. Therefore, the first-year work should be comprehensive and well balanced, with much review and demonstration of basic principles, and with modest extension to more advanced theory, concepts, and applications. This is the principle of "progressive repetition," as sound for most Ph.D. candidates as for the lower grades. The occasional exceptional student will not be discouraged; if the professors are alert he will waste no time.

After a successful first year, the competent student should be increasingly able to absorb and appreciate more advanced material. It is not necessary that he learn every intricacy of quantum mechanics, heterocyclic reaction mechanism, or theory of electrode processes. He should become well acquainted in a number of such fields, and, further, become able to orient them properly with respect to theory and practice. It is important that he become accustomed to study and read, to think and imagine and discuss, to learn the technique of well-planned experimentation, to wax emotional about his own special field, and to enjoy it all. His Ph.D. *can* mean more than a few years of routine note-taking and examination-passing. Whether it does will depend very much on the professional atmosphere of his department and its staff.

How much time should the graduate student spend on his studies? Years ago, Kekulé was advised by his teacher, Liebig, that no one could hope to do anything in chemistry unless he ruined his health with study. It is said that Arrhenius received similar advice, but missed the last two words; so he promptly joined the Aurora Club, which had but one working rule—its meetings must never break up before dawn. While advice along these lines today should no doubt be moderate, the earnest graduate student must be prepared to forego many normal activities during his few years of opportunity, or at least to concentrate them in occasional well-earned vacations.

—CVK

6 Reasons Why

SULFUR HEXAFLUORIDE *is preferred* For Gaseous Insulation!

Designs can be simplified, electronic equipment miniaturized, production and operating costs reduced when B&A Sulfur Hexafluoride is used as the dielectric. That's because it has proved superior to other gaseous insulation, and to oil insulation in many applications. One of the heaviest gases known, B&A Sulfur Hexafluoride is easily managed, nonflammable, nontoxic, safe.

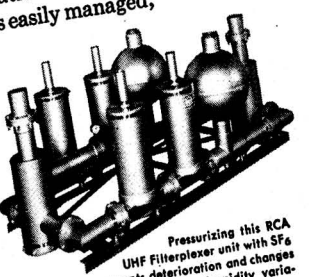

Pressurizing this RCA UHF Filterplexer unit with SF_6 gas prevents deterioration and changes in tuning caused by humidity variations.

Its advantages include:

- High Dielectric Strength—More than twice that of Air, Nitrogen or Carbon Dioxide, at one atmosphere.
- High Density—Transformers containing SF_6 often can be opened and serviced without need for recharging.
- Arc Quenching—High dielectric strength minimizes arcing . . . results in rapid recovery of strength after arcing.
- Efficient Over Wide Temperature Range—Dielectric strength remains substantial at temperatures as low as minus 63°C.
- Cooler Operation—high heat transfer coefficient results in reduced operating temperatures invaluable for miniaturized equipment.
- Safe—Nonflammable, nontoxic, chemically and physiologically inert.

IMPORTANT NEW TECHNICAL BULLETIN

For the full story of SF_6, its advantages, properties, and applications as gaseous insulation, send for new, illustrated technical bulletin. It is packed with information that can be highly important to your operations.

BAKER & ADAMSON®
Fine Chemicals
GENERAL CHEMICAL DIVISION
ALLIED CHEMICAL & DYE CORPORATION
40 Rector Street, New York 6, N. Y.

Clip to your letterhead and mail!

BAKER & ADAMSON® PRODUCTS
GENERAL CHEMICAL DIVISION, Allied Chemical & Dye Corporation
40 Rector Street, New York 6, N. Y.

☐ Without obligating me, please send your new, illustrated booklet on Sulfur Hexafluoride for gaseous insulation (Technical Bulletin TB-85602).

☐ I would like information about other B&A Electronic Grade Chemicals.

NAME_____ POSITION_____

COMPANY_____

ADDRESS_____

CITY_____ ZONE____ STATE_____

JE 6

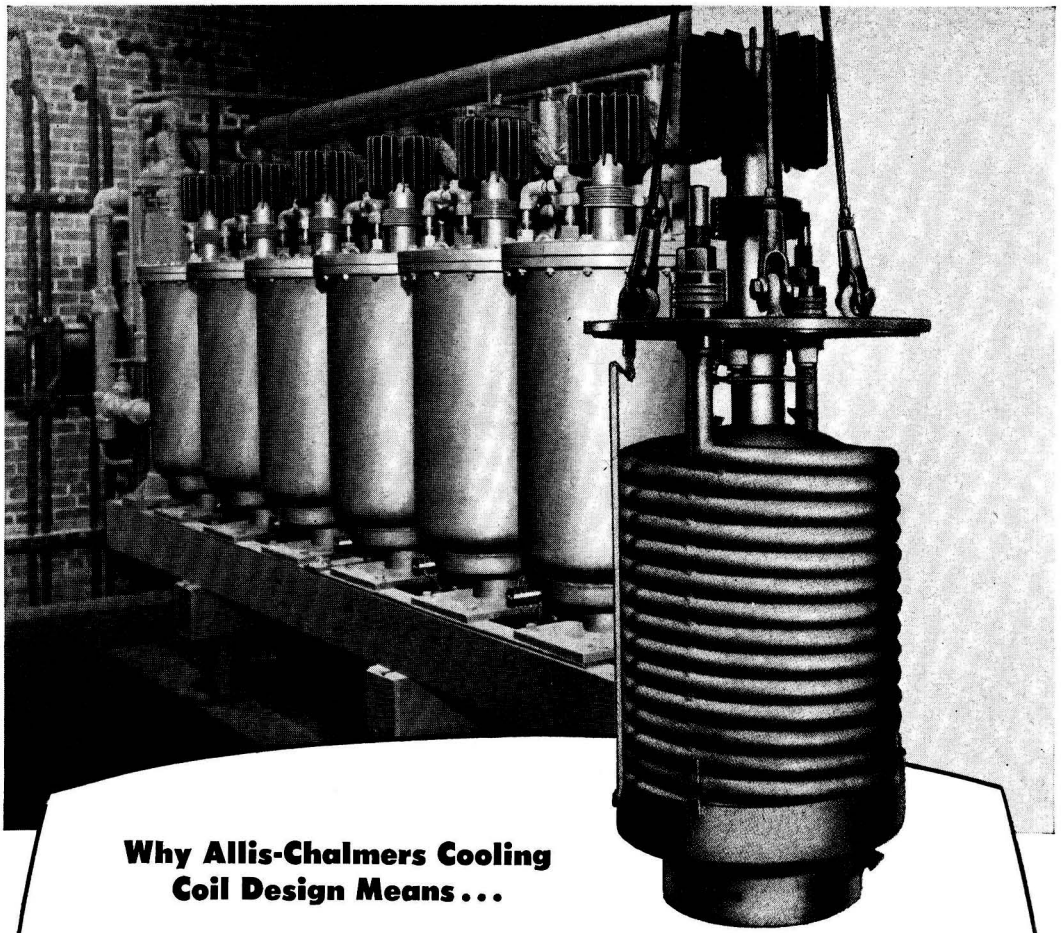

Why Allis-Chalmers Cooling Coil Design Means . . .

Better Rectifier Operation

More Efficient Heat Transfer results from internal cooling coil. The steel coil surrounds active parts, offering more cooling surface and better heat transfer than other types. Unit maintains more uniform temperature and mercury vapor pressure.

Simplified Maintenance results from Allis-Chalmers unique unit construction. All active components are attached to the anode plate for easy withdrawal, dismantling, and re-assembling — as illustrated above.

Positive Arc Barrier is formed by the cooling coil, which is insulated from the tank. The main arc is confined within the coil, preventing arc transfer to the tank.

Years of Operation in hundreds of installations have proved the reliability, ease of operation, and simplified maintenance of Allis-Chalmers mercury arc rectifiers. You can get complete information at your nearby A-C office, or write Allis-Chalmers, Industrial Equipment Division, Milwaukee 1, Wisconsin.

LIVE BETTER ELECTRICALLY

ALLIS-CHALMERS

A-C ALLIS-CHALMERS

A-5084

Anodic Transients of Copper in Hydrochloric Acid

RALPH S. COOPER

Physics Department, University of Illinois, Urbana, Illinois

ABSTRACT

Anodic transients for the system Cu | HCl were studied using horizontal anodes shielded to prevent convection. With the exception of the appearance of a second plateau the results are in quantitative agreement with Müller's "Bedeckungstheorie." The reaction occuring during the first plateau is

$$Cu + Cl^- \rightarrow CuCl + e^-$$

The second plateau is due to the initiation of a new reaction involving the OH^- ion. Potential measurements and visual observation indicate it to be

$$2\,Cu + 2\,OH^- \rightarrow Cu_2O + H_2O + 2e^-$$

Studies made with $0.5N$–$6N$ hydrochloric acid show the layer thickness to be given by a relation of the form $\delta = Di_I^{-m}$ with m independent of concentration and D proportional to it. These results were compared with some obtained with vertical unshielded anodes to determine the effect of convection. For rapid transients (< 3 sec) Müller's theory held with both types of anode. Otherwise results were qualitatively similar with the exception of the appearance of overshoot and a steady state with the unshielded anodes.

INTRODUCTION

An understanding of the fundamental mechanisms involved in layer formation at anodes would be of great value in such fields as corrosion, passivity, polarization, electrolytic rectification, refining, and polishing. Previous studies at this laboratory dealt with Fe | H_2SO_4 (1, 2) and Cu | 2N HCl (3) systems. Current and potential transients were investigated and in the latter system the anodic layer was identified as CuCl. The present paper is a continuation of the work on the Cu | HCl system and has four major objectives: (*a*) identification of the processes taking place; (*b*) application of Müller's theory (4, 5) to the prediction of the current transient; (*c*) a study of the effect of hydrochloric acid concentration; and (*d*) an investigation of the influence of convection.

Müller's theory is based on two types of layer growth; first, the spread of a solid layer of constant thickness (6) across the anode face until only small pores in layer remain, and, second, the increase in depth of the layer with the pore area constant. If a high current density is applied to an anode, a saturated solution of the anode salt will be formed in the neighborhood of the electrode surface and subsequently a solid film of the salt will be deposited on the anode face. For the initial process Müller (6) assumes that (*a*) the solution and diffusion of the salt is negligible, (*b*) the solid film spreads from random nuclei [as has been directly observed (3)], (*c*) this film maintains a constant thickness, (*d*) the anode potential is constant, i.e., neglecting concentration polarization, and (*e*) the conductivity of the salt is negligible, thus causing the current to flow only through the uncovered areas until they diminish in size to small pores in an otherwise complete layer. The resistance of the layer-pore system is relatively small until about 99% of the surface is covered, at which time the resistance increases sharply, becoming the controlling one in the circuit and causing the current to decrease. The current-time behavior is represented by the equation:

$$t = \tau + A\left[\frac{-1}{i_I - i} + \frac{1}{i_I}\ln\left(\frac{i_I - i}{i}\right)\right] \qquad (I)$$

where i_I is the total current during the first plateau,[1] and τ and A are constants for a given transient. τ is a measure of the duration of the current plateau, and A is inversely related to the rate at which the current decreases at the termination of the plateau. The form of this relation for several values of the parameters is shown in Fig. 1. By substituting $x = i/i_I$

$$t - \tau = +\frac{A}{i_I}\left[-\frac{1}{1-x} + \ln\left(\frac{1-x}{x}\right)\right] = +\frac{A}{i_I}f(x) \qquad (II)$$

Thus, all transients obeying this law would have the same form (Fig. 2) except for the multiplicative factor A, which in effect expands or contracts the time scale. The validity of the relation and the constants A and τ is determinable by plotting $f(x)$ vs. t for a given transient. This should result in a straight line of slope $-i_I/A$ and intercept τ on the t axis. These constants contain the thickness of the layer δ, the conductivity of the solution in the pores κ, and other physical properties of the system. Solving for δ and κ:

[1] Unfortunately there is conflicting nomenclature in the literature. i_I here represents the total current (not current density) during the first plateau in agreement with references (2) and (3), while Müller used i_∞ for this quantity. i_∞ here refers to the value of i immediately upon closing the circuit. A is a constant, while the symbol S is used to denote areas. Müller used F in place of S; C for τ and μ for t_+. The general nomenclature, especially the usage of E, V, and ϵ is consistent with references (2) and (3) as this work is a continuation of the latter.

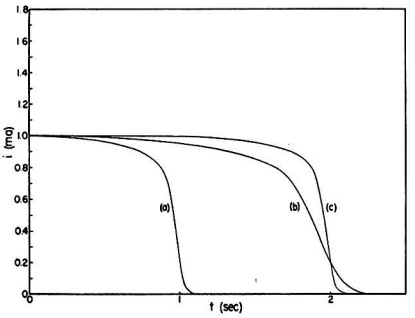

FIG. 1. The shape of current transients according to Müller. i_I = 1 ma. Curve (*a*) τ = 1 sec, A = 0.02 ma-sec; curve (*b*) τ = 2 sec, A = 0.06 ma-sec; curve (*c*) τ = 2 sec, A = 0.02 ma-sec.

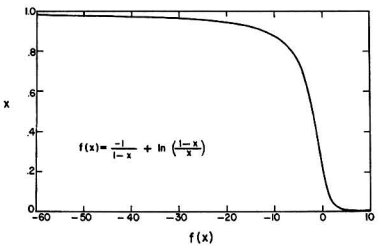

FIG. 2. The form of the current transient, according to Müller; i vs. t has the same form with t as the abscissa.

$$\delta = \frac{\tau k(1 - t_+)i_I}{\rho S} \qquad \text{(III)}$$

$$\kappa = \frac{\tau^2 i_I^2 k(1 - t_+)}{A\rho S^2(R + r_o)} \qquad \text{(IV)}$$

k is the equivalent weight of the precipitated salt divided by the Faraday constant, ρ is its density, t_+ is the transference number of the cation, and S is the apparent area of the electrode. $(R + r_o)$ is the total resistance initially present in the circuit. All quantities appearing in equations (III) and (IV) are assumed to be constant for this phase of the transient.

As the pore area becomes smaller the current density in the pores rises, and instead of the pores closing entirely, the layer grows in depth, with the pore area constant. Müller assumes the layer becomes deeper by the anodization of the metal at the base of the pores only, but no mechanism for this is given in his work. The transition from the spreading process to the growth in depth is a relatively sharp one, but no theory has been developed which predicts at what point it occurs.

On the basis of Müller's assumption, the increase in layer depth (7) is governed by the relations

$$t - t_1 = B\left(\frac{1}{i^2} - \frac{1}{i_1^2}\right) \qquad \text{(V)}$$

$$B = \frac{\kappa(E - \epsilon)s_p^2}{k(1 - t_+)} \qquad \text{(VI)}$$

where B is a constant, E is the applied voltage, ϵ the anode potential, and s_p is the total area of the pores in the solid layer. i_1 is the value of the current at any particular time t_1 during the period of growth in depth. A plot of i^{-2} vs. t results in a straight line of slope B^{-1} for the period during which this process is occurring. The pore area may be calculated from B and compared to that computed for the spreading process at the time that the transition occurs.

Müller found these relations to hold in many simple acid-metal systems. However, the Cu/HCl system has several complicating features which are interrelated. The most apparent deviation is the appearance of a second plateau. This is interpreted as the occurrence of a second electrode reaction. Next in importance is the complex ion formation of dissolved CuCl as $CuCl_2^-$ and $CuCl_3^=$. This is accompanied by a strong dependence of solubility upon Cl^- concentration (and hence on hydrochloric acid concentration), resulting in a large variation in conductivity, as CuCl is only slightly soluble in water. The electrode potential, ϵ, varies for several reasons. It is a function of the concentration and the $CuCl_2^-$ content of the acid in the immediate neighborhood of the anode, which is different than the bulk values because of the Nernst diffusion layer. The presence of a solid film also alters ϵ. Finally, the transference number of the cation may change as the H^+ is replaced by Cu^+ near the anode face. The rates of the reactions involved are believed to be too rapid to produce observable effects in these experiments.

EXPERIMENTAL

Apparatus.—The basic circuit used was that described previously (3).

For very fast interruption experiments an apparatus was devised using a pair of Westinghouse No. 275c relays (Fig. 3). A variable resistance was placed in series with one relay and both relays were powered by the same 22.5 v dry cell battery. By varying the resistance, one relay (A) could be adjusted to close from 0 to 20 msec after the other (B). The circuit was broken only for the period when only one relay was closed. The cell circuit could thus be opened conveniently for periods as short as 50 μsec to observe the electrode potential and resistance. A motor driven switch was placed in the battery circuit so

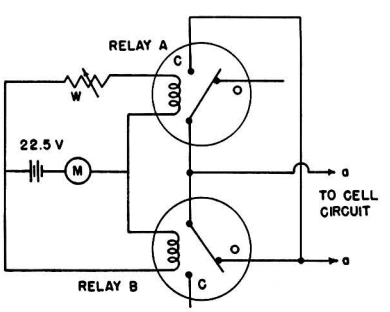

FIG. 3. Interruption circuit. M, motor driven switch. Both relays are shown in the open position, O. When the relays are energized relay B closes first, A shortly after, breaking circuit a-a momentarily.

that the interrupting mechanism could be actuated up to six times per second during the course of a transient. In addition, this device was used in conjunction with a Tektronix 512 oscilloscope and a 35 mm still camera, to obtain information of the very early stages ($<10^{-3}$ sec) of transients and of potential decays.

The cathode was of platinized platinum, 10 cm² in area, the potential of which was constant within 0.01 v. An 0.1*N* calomel electrode placed very close to the cathode was used as reference. All potentials given here are with respect to this reference unless otherwise noted. The applied voltage E is defined to include the potential of the cathode, which was nonpolarizable under currents of 50 ma or less. The open circuit anode potential was approximately −0.35 v on this scale so that applied voltages above this value, even if negative, were anodic. The internal resistance r represents the total resistance between the tip of the reference and the anode metal, and includes the resistance of the bulk of the solution and of all liquid and solid anode films. V is the potential of the anode metal with respect to the reference cell and includes the IR drop in the electrolyte and film.

In 2*N* hydrochloric acid the reference showed a liquid junction potential of 0.06 v when checked against an Ag/AgCl electrode. Thus, the platinized platinum hydrogen electrode displayed a potential of −0.40 v instead of −0.335 v. The liquid junction potential was negligible in 0.1*N* hydrochloric acid. Most of the anodes used were copper wire and rolled rod. A few measurements were made with single crystals of copper, but no significant differences were observed. Anodes of various areas were investigated but were usually of 0.176 cm² cross section. They were screwed or soldered into brass rods, with all but the face covered with some form of insulation. The most satisfactory insulation consisted of seven coats of Micro Supreme Stop Off Laquer HR-302 (Michigan Chrome Company), but even shellac and paraffin, although not as durable, produced the same results. The construction of shielded anodes is shown in Fig. 4. These showed no tendency for preferential etching at the sharp edge, even after prolonged use.

Procedure.—In the previous work anodes were polished with 4/0 emery paper before each run. In a study of the effect of varying the electrode area, it was observed that reproducibility was improved if several runs were made with the same anode before taking data. This removes the material severely cold worked by the mechanical polishing. Thus, the procedure was as follows.

An anode was ground down with 2/0 and 4/0 emery paper and up to 20 runs were made; no data were taken until the fourth run. Between each run the anode and/or solution was agitated to permit the solution of the CuCl layer, which could be detected by its effect on the open circuit potential of the electrode. In solutions 1*N* or less, the layer was more difficultly soluble, and in these cases the anode was removed and cleaned with 2*N* HCl. Air saturated solutions were made from 'Baker Analyzed' Reagent grade HCl, and were maintained at 25 ± 1°C. Each run was made with a constant applied voltage, E, and fixed external resistance, R.

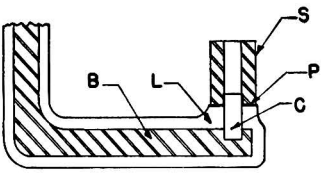

FIG. 4. Detail of shielded anode. *C*, copper specimen; *B*, brass support; *L*, 7 coats of lacquer; *S*, Lucite shield; *P*, parafin seal.

RESULTS AND DISCUSSION

Shielded Anodes in 2N HCl

General nature of transients.—The results presented in this section were obtained, unless otherwise specified, by using a shielded anode of 0.176 cm² cross section and zero external resistance. The current transients are qualitatively similar to those obtained previously (3) for unshielded anodes. Two examples are shown in Fig. 5. In Fig. 5*a* is a transient made with small applied voltage (−0.24 v), which is a low-current, slow transient with an initial decrease before the stationary current of the first plateau is reached. This is followed by a single slow decrease in current. With greater applied voltages the initial current becomes larger and the time (τ) to the current decrease shorter. At about 0.5 v a second plateau becomes clearly discernible, although it is present at applied voltages (E) as low as 0 v, and can be better observed with a larger (R = 150 Ω) external resistance. A typical transient of this type is shown in Fig. 5*b*. It has two plateaus and a region where the i^{-2} law holds. A set of characteristic curves (Fig. 6) can be drawn relating i and V (the anode potential including IR drop in the solution) for the stationary values on the first (i_I, V_I) and second (i_{II}, V_{II}) plateaus.

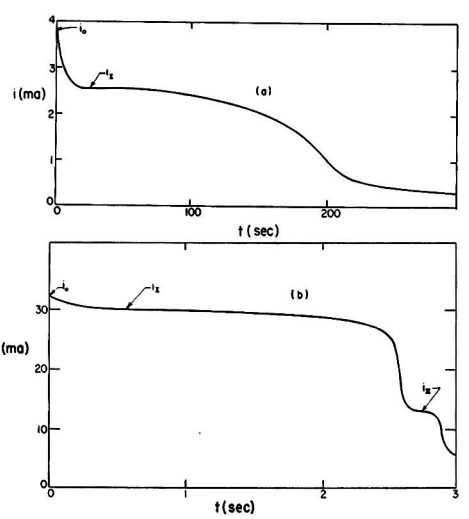

FIG. 5. Typical transients in 2*N* HCl; shielded anode 0.176 cm². (*a*) E = −0.24 v, R = 0 Ω; (*b*) E = +0.4 v, R = 150 Ω.

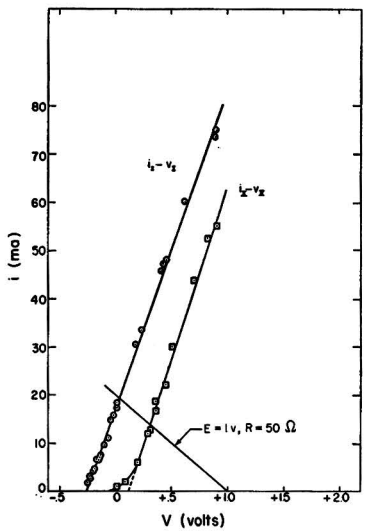

FIG. 6. Characteristic curves for shielded anode (0.176 cm²) in 2*N* HCl, showing locus of stationary values of current and voltage on first plateau (i_I, V_I) and second plateau (i_{II}, V_{II}). No steady state exists. A typical "load line," with $E = 1$ v, $R = 50\ \Omega$ is shown.

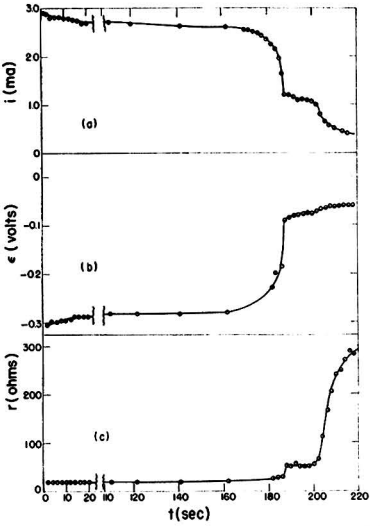

FIG. 7. Results of interruption experiments 2*N* HCl; $E = 0.2$ v; $R = 150\ \Omega$. (*a*) i vs. t; (*b*) ϵ vs. t; (*c*) r vs. t.

Since Ohm's laws applied to the circuit results in the equation

$$V = E - iR \qquad \text{(VII)}$$

the $i - V$ relation for any given transient can be represented by a "load line" (3) of slope $-1/R$ and intercept, E. For $R = 0\ \Omega$ the load line is vertical, and an example with $E = 1.0$ v, $R = 50\ \Omega$ is shown in Fig. 6. The intersection of the load line with the characteristic curve gives the values of i and V on the plateaus. The i_I, V_I and i_{II}, V_{II} curves are straight lines, with slopes representing resistances of about 14 ohms, that of the solution in the cell. No steady state is reached within 10 min. Interruption experiments were performed to determine the electrode potential (ϵ) and resistance (r). Fig. 7 shows i, ϵ, and r, as functions of time for $E = 0.2$ v, $R = 150\ \Omega$. It may be noted that r is constant on the second plateau at a value larger than r_o, which is somewhat different from the previous results. The variations in ϵ and r are discussed later.

Initial current peak.—When a copper rod is placed in 2*N* hydrochloric acid free of Cu^+ ion, its potential cannot be determined by the Nernst equation, but is partially the result of local action cells (8). The potential is dependent upon the very small amount of Cu^+ which goes into solution and upon its rate of removal by diffusion. Thus, while the observed potential is -0.44 v for vertical unshielded electrodes, the shielded anode displays a potential of -0.35 v (which approaches -0.44 v upon vigorous stirring of the solution). These potentials may vary as much as ± 0.02 v, but such variations have negligible effect upon the transients. For both types of electrodes in 2*N* hydrochloric acid saturated with CuCl, the observed potential is -0.27 v. This value may be calculated from the Nernst equation. Therefore, for a transient in pure hydrochloric acid there is initially a short period during which the acid is becoming saturated with CuCl, and ϵ is changing from -0.35 v to -0.27 v. During this time, the interruption experiments (Fig. 7) show that r is constant, and hence the initial current peak is due entirely to changes in ϵ. The current is given by Ohm's law for the circuit

$$i = \frac{E - \epsilon}{R + r} \qquad \text{(VIII)}$$

Thus, for large applied voltage (E) (and hence large i_o, i_I) the effect of an 0.08 v change in ϵ is relatively small. Also for large initial currents, the solution near the anode becomes saturated more quickly and so the transition from i_o to i_I is of shorter duration.

The first plateau.—During the first plateau the potential is steady at the value of -0.27 v; the resistance r remains as its initial value. This can be accounted for completely by the ohmic resistance of the solution. The shield contains a cylinder of acid 1.2 cm long and 1.76 cm² in cross section. If one adds the radius of the cylinder to correct roughly for the end effects, and uses the value of 0.56 Ω^{-1}cm^{-1} for the bulk electrolytic conductivity (9, 10) one obtains a value of 14 ohms. This compares well with the values obtained by interruption methods 17 ± 4 ohms (Fig. 7) and from the slope of i_I, V_I curve 14.3 ± 0.5 ohms. The large uncertainty in the value from the interruption experiment is due to the small potential drop of only 0.045 ± 0.01 v in the example given. One with a potential drop of 0.415 v gave $r = 14.2 \pm 0.5\ \Omega$. As the layer nears completion, the resistance increases as expected. However, the potential ϵ also begins to change, becoming less negative. The effect of this change depends upon the amount of shift in ϵ compared to the total potential applied to cell. ϵ changes only by about 0.2 v at the maximum, while E may be chosen at will and has been

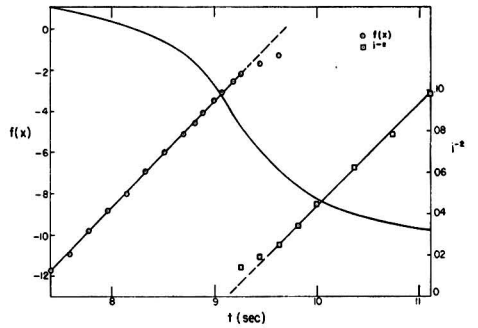

FIG. 8. The validity of Müller's laws. $f(x)$ vs. t and i^{-2} vs. t for shielded anode $E = 0$ v; $R = 0\ \Omega$.

made as high as 4.5 v in this study. Thus, the variation of ϵ may be expected to cause some deviation from the ideal behavior previously derived. Nevertheless, the linear relation between $f(x)$ and t holds well for $E = 0$ (Fig. 8) and even lower.

The solid product was identified previously as CuCl (3). The potential of the first plateau (−0.27 v) has been noted to be identical with the potential of a copper electrode in $2N$ hydrochloric acid saturated with CuCl. There are two possible net reactions:

$$Cu + 2\ Cl^- \rightarrow CuCl_2^- + e^- \qquad (IX)$$

and

$$Cu + Cl^- \rightarrow CuCl + e^- \qquad (X)$$

For saturated solutions of CuCl in HCl nearly equal potentials are calculated from the Nernst equation for the two reactions. Including liquid junction potentials the result is −0.27 v for reaction (IX) and −0.28 v for reaction (X) in $2N$ hydrochloric acid saturated with CuCl. It is to be expected that during the period when the hydrochloric acid is unsaturated, reaction (IX) alone takes place.

When the solution is saturated, the electrode should assume the Cu/CuCl/Cl⁻ potential. To check this both a Cu and Ag/AgCl electrode were immersed in various concentrations of hydrochloric acid saturated with CuCl. The difference in standard potential of the Ag/AgCl/Cl⁻ and Cu/CuCl/Cl⁻ electrodes is 0.100 v and the experimental value is within ±0.01 v of this, down to $0.05N$ hydrochloric acid. This indicates that the anode is behaving as a Cu/CuCl/Cl⁻ electrode. During the transient, changes of composition in the diffusion layer take place, altering the concentration of the potential determining species at the anode face and introducing a small free diffusion potential.

Taking the solid product as CuCl one can compute the layer thickness δ and the conductivity (κ) in the pores for a series of transients. i_I, τ, A, δ, and κ for a wide range of transients are tabulated in Table I. First, consider τ, which is related to the length of the first plateau. A plot of $\log \tau$ vs. $\log i_I$ (Fig. 9) gives a straight line, indicating the relation,

TABLE I. *Results in 2N HCl*

E volts	R Ω	i_I ma	τ sec	$A \times 10^3$ ma-sec	$\delta \times 10^3$ cm	$\kappa \times 10^3$ $(\Omega\ cm)^{-1}$
0.10	0	21.6	5.70	1.94	0.21	5.7
0	0	15.7	9.70	3.01	0.25	5.1
−0.10	0	9.52	22.8	5.10	0.36	6.2
−0.15	0	6.60	42.5	7.09	0.48	8.0
−0.20	0	4.64	81	13.7	0.62	7.0
−0.20	0	4.52	84	13.0	0.63	7.4
−0.24	0	2.55	210	24.0	0.89	7.9
0.20	150	2.74	193	3.23	0.89	6.1
0.50	50	11.0	16.6	1.78	0.30	2.8
0	50	4.06	92	2.31	0.62	9.3

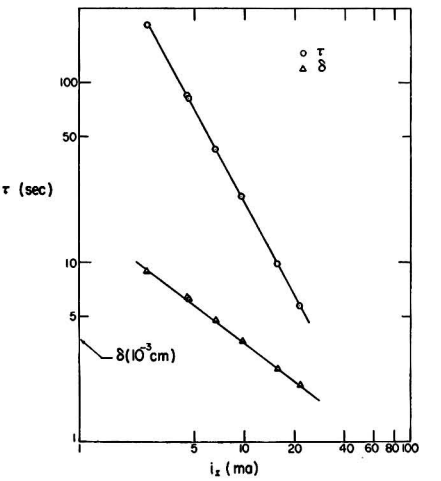

FIG. 9. The duration of the first plateau (τ) and the layer thickness (δ) as functions of i_I ($2N$ HCl).

$$\tau = 1025\ i_I^{-1.685} \qquad (XI)$$

i_I in milliamperes. δ, the layer thickness, can be computed from τ and is given by

$$\delta = 1.70 \times 10^{-3}\ i_I^{-1.685}\ \text{cm} \qquad (XII)$$

Müller found a variation of δ with i_I of this form with various exponents in many systems which he explained on the basis of crystallization of smaller particles at higher current densities, and consequently higher supersaturation at the anode face. That δ depends on the current density only, rather than total current, may be seen from Fig. 10, in which data for a shielded anode of 0.176 cm² cross section, taken with various values of R, are shown and compared with the results obtained from a smaller unshielded one (0.021 cm²), adjusted to the same current density. δ ranged from 24×10^{-3} to 0.1×10^{-3} cm in this study, and was computed on the basis of $t_+ = 0$, i.e., that H^+ and Cl^- were carrying most of the current during the major portion of the current plateau. This is reasonable in view of the fact that the Cu in solution is present almost entirely as $CuCl_2^-$ and $CuCl_3^=$ complexes (11, 12).

The conductivity (κ) of the solution in the pores is found to vary between 8.0×10^{-3} and $4 \times 10^{-3}\ \Omega^{-1}cm^{-1}$. The conductivity of $2N$ hydrochloric acid is $0.56\ \Omega^{-1}cm^{-1}$

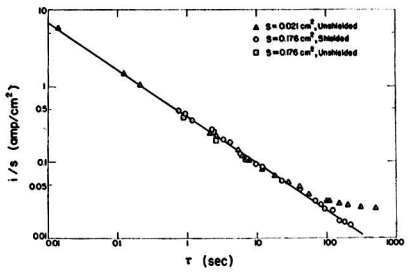

FIG. 10. τ vs. current density, showing identical results for large and small anodes and the effect of convection on unshielded anodes at low current densities (2N HCl).

and that of saturated aqueous CuCl approximately 1.5 $\times 10^{-4}\ \Omega^{-1}\text{cm}^{-1}$, while the conductivity of the solution in the pores lies somewhere in between, at about the geometric mean of the two. A qualitative understanding of this may be based on concentration changes occurring in diffusion layer during the transient. The concentration of hydrochloric acid at the anode appears to decrease according to the Schlieren observation made earlier (3) and this is to be expected from the depletion of Cl^- ions by formation of CuCl. Thus, if the major portion of the concentration change occurs before the current drops, the conductivity in the pores may be expected to have a roughly constant low value for the relatively short duration of the current decrease at the end of the plateau.

The observed value of κ is equivalent to a hydrochloric acid concentration of 0.02N. If κ lessens during the decrease of the current, then the slope of the $f(x)$ vs. t curve should become smaller and this behavior is confirmed by observation, especially with large external resistance R. Also decreasing hydrochloric acid concentration decreases CuCl solubility, thus tending to precipitate it from solution. Despite these aberrations the theory apparently does hold quantitatively for most of the conditions studied, and qualitatively for the rest. In most cases a precise value of $A(\pm 5\%)$ can be found to fit the current transient. Since A is proportional to δ^2, a plot of log A vs. log i_I (Fig. 11) should be a straight line of slope -1.36. Actually, such a plot has a slope of -1.19, the difference being due to the variation with the external parameters (E and R) of the conductivity in the pores.

The second plateau.—For applied voltages of 0.1 v or more the decrease in current is interrupted by a second plateau. The locus of the i_{II}, V_{II} values are shown in Fig. 6. In 2N hydrochloric acid the second plateau is much shorter than the first and less reproducible in all features. At times it is only a small inflection or discontinuity in slope. Interruption experiments show that ϵ changes after the first plateau and rises to the value of -0.05 v on the second, during which it remains constant. The resistance also is constant during the plateau period. The i_{II}, V_{II} curve approaches a straight line (for large currents), with an intercept of + 0.11 v. However, potential decay and interruption experiments always give the value of ϵ to be -0.05 v during the second plateau. In earlier work (3) it was observed that the first decrease was due to the sudden change of ϵ (assumed due to the formation of a very

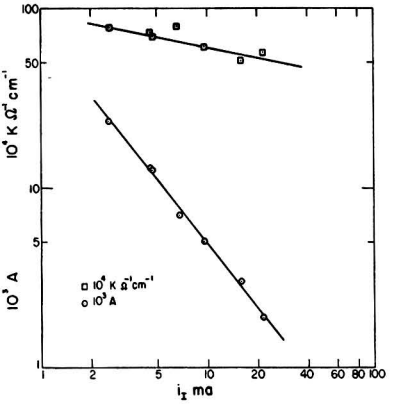

FIG. 11. κ and A vs. i_I (2N HCl)

thin complete layer of CuCl over the surface) and that there was a slight delay before r increased, thus causing a second decrease in current. The explanation of the second plateau postulated here is that a new reaction occurs on the second plateau, forming a solid layer at the base of the pores in the CuCl layer. It was observed that the second plateau became more prominent as the concentration of the acid was reduced. In 0.5N HCl the second plateau was more prominent and reproducible than at higher concentrations and lasted 4 or more times as long as the first plateau. This is a strong indication that the reaction occurring during the second plateau involves the OH^- ion. Next, consider the situation just before the second plateau begins. The conductivity of the solution in the pores has been shown to be about $6 \times 10^{-3}\ \Omega^{-1}\text{cm}^{-1}$ which corresponds to $1.5 \times 10^{-2}N$ HCl. In addition, the composition of the solution in the pores is probably nonuniform due to diffusion caused concentration gradients which are likely to be set up, especially under such large current densities as 3 amp/cm². However, since the solid CuCl layer can act as a source of CuCl, the minimum conductivity should be that of a saturated solution of CuCl. Even if the hydrochloric acid concentration at the anode surface were as high as the average in the pores, of the order of $10^{-2}N$, it would permit the reaction:

$$2\ \text{Cu} + 2\ \text{OH}^- \rightarrow \text{Cu}_2\text{O} + \text{H}_2\text{O} + 2e^- \qquad \text{(XIII)}$$

The possibility of Cu_2O formation is also indicated by the presence of a reddish-brown powder observed on anodes upon removal from solution after electrolysis in 0.5N hydrochloric acid. The equilibrium potential of this reaction in $10^{-2}N$ HCl is +0.03 v, neglecting liquid junction and free diffusion potentials which may be of the order of ± 0.06 v. Any migration effects would cause the concentration of the HCl at the anode surface to be less than the average concentration in the pores, which would favor the above reaction at lower potentials. The major problem in comparing the experimental and theoretical electrode potential is caused by the unknown value of the concentration potential across the diffusion layer adjacent to the anode. CuOH and basic salts are the only other possibilities. Nevertheless, it appears clear that the forma-

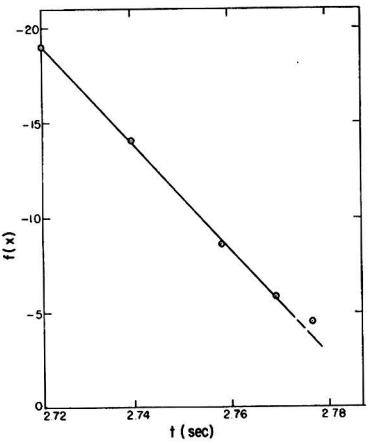

FIG. 12. The validity of Müller's law for the second plateau, 2*N* HCl, unshielded anode.

tion of Cu_2O is consistent with the observed potential for the second plateau. In addition the shape of the current-time curve during the drop after the second plateau indicates that Müller's theory holds here also. Fig. 12 shows an example, taken with a small unshielded anode in 2*N* HCl.

Layer growth in depth.—Following the last plateau, and in certain cases between the first and second plateaus, the transient is observed to follow Müller's depth increase law. An example of this is shown in Fig. 8, where i^{-2} is plotted against t for a shielded anode with only one plateau. This line represents equation (V) and from its slope the pore area, s_p, may be found. The value of κ used ($5.1 \times 10^{-3}\ \Omega^{-1}\text{cm}^{-1}$) was determined from the first plateau. t_+ was assumed to be zero and ϵ to be -0.27 v. This resulted in value for s_p of 2.5×10^{-3} cm², which is 1.4% of the total apparent area of the anode. The value of the pore area thus obtained may be compared with that computed for the sideways growth at the time of transition to the new process. For the example shown, the transition begins at about 9.3 sec, there being a period of about 0.2 sec during which the change is completed. Evaluating s_p at the middle of this period, one obtains $s_p = 2.3 \times 10^{-3}$ cm². This is rather good agreement; in view of the assumptions and uncertainties a difference of 20% is still satisfactory. This value of the pore area indicates a large actual current density of 3.3 amp/cm² in the pores.

Effect of Concentration

If the concentration of hydrochloric acid is varied, the characteristic curves are altered in a predictable way. The slope of the i_I, V_I curve is proportional to the specific conductance of the acid, and the intercept on the V axis is the value of the corresponding Cu | CuCl | Cl^- potential. This is shown in Fig. 13 and Table II. The duration of the first plateau increases with increasing acid concentration. At all concentrations investigated (0.5*N*–6*N*) the length of the plateau is given by a relation of the form $\tau = D' i_I^{-m}$, (Fig. 14). m is approximately constant and D' is

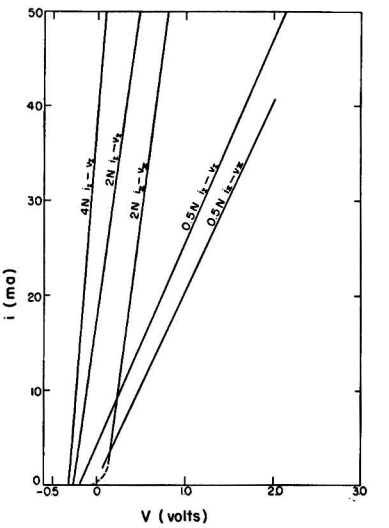

FIG. 13. Characteristic curves for several acid concentrations.

TABLE II

HCl	0.5*N*	2*N*	4*N*	Source
r_0	56	14	9.6	Characteristic curves
r_0	44	14	9.6	Conductivity calculations
ϵ_I	−0.21	−0.27	−0.32	Characteristic curves
ϵ_I	−0.22	−0.27	−0.32	Potential calculations
ϵ_I	−0.22	−0.275	−0.32	Potential of Cu | CuCl satd. HCl
ϵ_{II}	−0.05	−0.05	—	Interruption experiments
ϵ_{II}	−0.05	+0.11	—	Characteristic curves

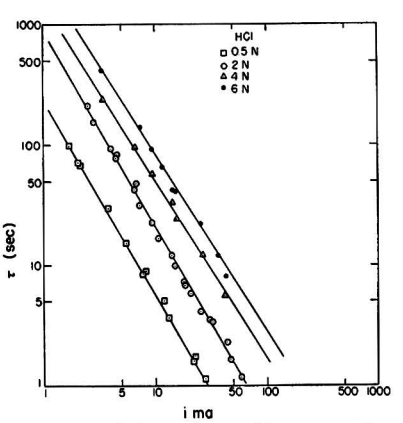

FIG. 14. τ vs. i_I for various acid concentrations

roughly proportional to the concentration. The length of the second plateau is the feature of the transient most dependent upon acid concentration. It barely appears in 4*N* and 6*N* acid, but is very prominent in 1*N* and 0.5*N* HCl. With lower acid concentrations the H^+ is depleted

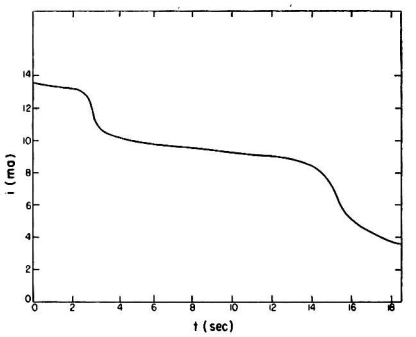

FIG. 15. i vs. t showing long second plateau in 0.5N HCl

more quickly at the anode surface, the oxide formation probably begins sooner and has a greater area upon which to form. An example in 0.5N HCl is shown in Fig. 15. Interruption experiments, performed on an exactly similar transient, resulted in a value of -0.05 v for the open circuit potential (ϵ_{II}) during the second plateau. This is the same value as that obtained by extrapolating the i_{II}, V_{II} line (Fig. 13) and the same as that obtained by interruption experiments in 2N HCl. Interruption experiments show the open-circuit potential during the first plateau, ϵ_I, to be -0.20 v in 0.5 N hydrochloric acid, in agreement with the value obtained by extrapolation of the i_I, V_I line and by potential measurements of a copper electrode in hydrochloric acid saturated with CuCl. Thus, ϵ_I varies with hydrochloric acid concentration while ϵ_{II} does not. This tends to confirm the view that the second plateau is the result of the initiation of a new electrode reaction, corresponding to the depletion of H^+ ion at the anode surface.

Unshielded Anodes

Except for steady-state behavior, the results obtained with both shielded and unshielded anodes have been found to be qualitatively, and in many cases, quantitatively, the same. The general temporal behavior is the same, both showing one or two plateaus according to the values of external parameters E and R. The chief difference between the two cell geometries is the effect of convection. Re-examining Fig. 10, it may be noted that the shielded and unshielded anodes give quantitatively identical results except at very low current densities where the plateau is very long in duration, greater than 20 sec. Only then do the unshielded electrodes show quantitatively different results. The convection current is the result of a saturated solution of cuprous ion complexes which is denser than the surrounding hydrochloric acid. Convection carries away some of the products of solution of the layer and hence retards its completion. For low currents, the layer is removed as fast as it is formed and thus is never completed. However, τ and Q, the total charge having flowed during the first plateau, are functions only of i_I for anodes of a given size and geometry as shown in Fig. 16, for vertical unshielded anodes of 0.021 cm² cross section. As was assumed by Stephenson (13) the dissolution may be considered equivalent to a removal current i_r, and so Q may be considered as a function of $(i_I - i_r)$.

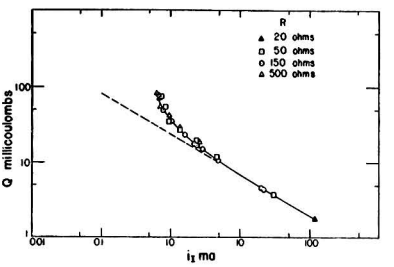

FIG. 16. Q vs. i_I, showing effect of convection (2N HCl)

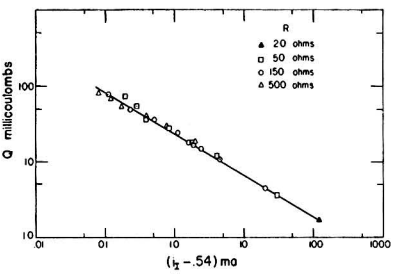

FIG. 17. Q vs. $(i_I - 0.54)$, corrected for removal current

For the geometry mentioned above, the correction is negligible for $i_I > 5$ ma and by taking i_r to be 0.54 ma, the unshielded anode (Fig. 17) displays a linear relation between log Q and log i_I over the entire range, exactly similar to the case of shielded anodes.

Two other effects of convection are the production of overshoot and of a steady state. With shielded anodes a steady state is never achieved within 10 min, the current dropping slowly to very low values instead, while, with unshielded ones of 0.02 cm² cross section, convection and diffusion are able to maintain steady-state current densities of the order of 0.1 amp/cm². Overshoot, the appearance of a current minimum after the plateaus, was absent in shielded anode transients while almost invariably present in both vertical and horizontal unshielded ones. This type of overshoot is interpreted as due to the variation of solubility of CuCl in hydrochloric acid at the anode surface brought about by convection. The minimum rarely appears before 3 sec of the transient have elapsed, at which time the effects of convection are first observed (using Schlieren methods). For a rapid transient ($\tau < 3$ sec) the Cl^- at the anode surface is quickly depleted, reducing the solubility of the layer and consequently permitting only a small current to flow. However, convection both carries away the products of solution and replenishes the solvent ion (Cl^-) at the anode surface, tending to establish a thinner, less resistant layer and, thus, the current rises to the steady-state value, completing the overshoot. Overshoot occurs with unshielded anodes also when the current decreases rapidly (e.g., because of completion of a solid layer) since the diffusion convection layer (~ 0.5 mm thick) is slow in its response to the change in the boundary condition (i). An example of this is overshoot which occurs following the current decrease after a long (30 sec) plateau. The reduced

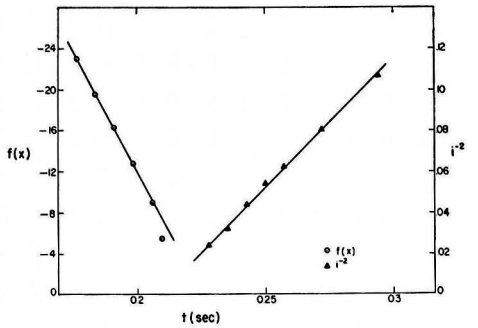

FIG. 18. The validity of Müller's laws for an unshielded anode, 2*N* HCl, E = 1.0 v, R = 50 Ω.

current is in equilibrium with a lower Cl^- concentration gradient, and hence with a higher Cl^- concentration at the surface. As before the layer resistance decreases as the system tends toward equilibrium, producing overshoot. This type of overshoot does not occur with shielded anodes because diffusion alone is not sufficient to establish equilibrium (steady-state) conditions. Transients whose significant events occur before 3 sec are identical for all cell geometries. Both of Müller's laws are found valid, as are shown by the example in Fig. 18. Thus, correct quantitative results may be expected in general for short transients independent of cell geometry.

Reproducibility

Polishing with 4/0 emery paper gave anodes which were not completely satisfactory in their reproducibility, especially for such quantities as the length of plateaus. For unshielded anodes i_I, i_∞, and i_{II} could be reproduced to 2% deviation from the mean, but τ and Q varied as much as 20%. Electrolytic polishing of the anode in 50% phosphoric acid for 5 min improved the results only slightly. An investigation of the effect of repeated use of a single anode without removing it from solution showed that the electrolytic anodization formed by dissolution of the copper produced a uniform reproducible surface. The anodization removes the cold worked surface produced by the mechanical polishing. One test was made by repeatedly using the anode with E = 0.3 v and R = 500 Ω for 11 runs. The first run (with a mechanically polished surface) had a plateau of 20-sec duration while all the runs with an anodized surface had plateaus of 27 sec to within 0.5 sec, which was the limit of precision of measurement. For all runs, i_I, i_{II}, and i_∞ had mean deviations of 1%, which also was the limit of precision. The open-circuit potential varied from −0.34 to −0.40 v without affecting the results. However, the more sensitive features of the transient, e.g., the shape of drop and the second plateau, changed during the first 3 runs. The second plateau appeared clearly for the first time in the 4th run, i.e., the anode having been etched 3 times by previous use. From the 4th run to the 11th and last, the transients were identical in all respects to within the limits of measurement. Results obtained on different days with anodized anodes agreed to within 2%.

SUMMARY

When a copper electrode, shielded to prevent convection, is made anodic in hydrochloric acid the transient current behavior is essentially as predicted by Müller, with the exception of a second plateau due to the initiation of a new reaction. The transient begins with a decreasing current as the solution near the anode becomes saturated with CuCl. There follows a period of constant current, during which a solid layer of CuCl is being deposited on the anode face, spreading sideways from random nuclei. This is terminated by a drop in the current as the layer is completed, leaving small pores in it. A second current plateau appears during which a new reaction takes place. The effect of acid concentration, the observation of a red-brown deposit, and the measured electrode potential indicate this to be the formation of Cu_2O. Finally, the layer grows in depth with constant pore area. The duration of the first plateau and thickness of the CuCl layer can be correlated with the current during the plateau. Studies with unshielded anodes give results which are qualitatively similar except for overshoot and steady-state behavior. For fast transients (<3 sec) both types of anodes show quantitatively identical behavior.

ACKNOWLEDGMENTS

This work was supported by the Office of Ordnance Research under contract DA-11-022-ORD-939. The author is greatly indebted to Professor J. H. Bartlett for his encouragement and aid and to Professor Sherlock Swann, Jr., for his careful and considerable help with the manuscript. Thanks are due also to Mr. James Briggs, who designed and built the interruption relay.

Manuscript received August 26, 1955.

Any discussion of this paper will appear in a Discussion Section to be published in the December 1956 JOURNAL.

REFERENCES

1. J. H. BARTLETT, *Trans. Electrochem. Soc.*, **87**, 521 (1945).
2. J. H. BARTLETT AND L. STEPHENSON, *This Journal*, **99**, 504 (1952).
3. J. H. BARTLETT AND L. STEPHENSON, *ibid.*, **101**, 571 (1954).
4. W. J. MÜLLER, "Die Bedeckungstheorie der Passivitat der Mettale und ihre experimentalle Begrundung," Verlag Chemie (1933).
5. W. J. MÜLLER, *Trans. Faraday Soc.*, **27**, 737 (1931).
6. W. J. MÜLLER AND K. KONOPICKY, *Monatsh. Chem.*, **48**, 711 (1927).
7. W. J. MÜLLER AND K. KONOPICKY, *ibid.*, **50**, 385 (1929).
8. O. GATTY AND E. C. R. SPOONER, "Electrode Potential Behavior of Corroding Metals in Aqueous Solution," pp. 22 and 182, Clarendon Press, Oxford (1938).
9. B. B. OWEN AND F. H. SWEETON, *J. Am. Chem. Soc.*, **63**, 2811 (1941).
10. R. A. ROBINSON AND R. H. STOKES, "Electrolyte Solutions," p. 361, Butterworths Scientific Publications, London (1955).
11. A. A. NOYES AND M. CHOW, *J. Am. Chem. Soc.*, **40**, 739 (1918).
12. K. S. CHANG AND Y. CHA, *J. Chinese Chem. Soc.*, **2**, 298 (1934).
13. L. P. STEPHENSON, Ph.D. Thesis, University of Illinois, p. 79 (1953).

Electrokinetic Potentials on Bulk Metals by Streaming Current Measurements

II. Gold, Platinum, and Silver in Dilute Aqueous Electrolytes

RAY M. HURD AND NORMAN HACKERMAN

Defense Research Laboratory and Department of Chemistry, The University of Texas, Austin, Texas

ABSTRACT

The electrokinetic (ζ) potentials of platinum, gold, and silver in contact with distilled water were found to be 60.8, 61.0, and 49.0 mv, respectively. The ζ potentials of these metals were also measured as a function of concentrations of KCl and KOH. Maxima were observed in all cases except that of gold in KCl solutions. These maxima are qualitatively related to the solubilities of the corresponding chlorides and hydroxides.

INTRODUCTION

In a previous paper (1), a method was described whereby the electrokinetic potentials of bulk metals could be obtained from streaming current measurements.[1] The method consisted essentially of using a recording milli-microammeter of low internal impedance, so that the streaming current was shunted through an external circuit rather than returning through the capillary itself. By this means the troublesome "shorting" resistance of the metal capillary was eliminated as a factor in the electrochemical circuit. For a complete description of the circuitry and a proof of the method, reference should be made to the first paper.

EXPERIMENTAL

Short lengths of platinum, gold, and silver seamless drawn tubing with nominal internal diameters of 0.005 in., 0.010 in., and 0.015 in. were furnished by the Baker and Company platinum works. Capillaries of various lengths were cut from each piece of tubing and sealed into small bore Pyrex glass tubing with Apiezon "W" hard wax. A sketch of a typical finished capillary is shown in Fig. 1*a*. The ends of the capillary were ground down to a knife edge, and the sealing wax was made to cover as much of the external wall as possible. The inside walls of the capillaries were cleaned by rinsing with warm dilute HNO_3, followed by a prolonged rinsing with distilled water. The finished capillaries were then stored in distilled water to allow the metal-water interface to reach an equilibrium state, which was found to require about 24 hr.

Since the streaming current is directly proportional to the square of the capillary radius, it was essential that accurate measurements of this value be obtained. It was calculated from Poiseuille's law from measurements of water flow rate through the capillaries at a series of applied pressure differences. The length of each capillary was measured with a traveling microscope. A summary of the pertinent data for all capillaries is given in Tables I, II, and III. The values of the critical dimensional factor (ratio of length to radius squared) are accurate to within $\pm 0.5\%$.

In order to measure the streaming current directly, it is important that the total resistance (ionic plus electronic) from one end of the capillary through the external circuit to the other end of the capillary be kept as low as possible. This places the following restrictions on electrode construction and location:

(*A*) The electrode reactions must not polarize the electrodes. Because the current is extremely low ($\sim 10^{-10}$ amp), this causes little difficulty. Smooth platinum gauze with a total area of approximately 1 cm^2 exposed to the solution is adequate, and does not introduce any contaminants into the solution.

(*B*) The electrodes must be placed as close to the ends of the capillary as possible in order to minimize the ionic resistance. This was accomplished by sealing the gauze electrodes into the 7 mm glass tubing which constituted the fluid flow circuit, and then joining the capillary to the glass tubing by means of short pieces of flexible Tygon tubing as shown in Fig. 1*b*.

The apparatus for controlling and measuring the pressure difference applied to the capillary is shown in Fig. 2. Pressure was supplied by means of tank helium, and was measured by reading the height of the water column. The dimensions of the capillaries were such that fairly low pressures (<100 cm H_2O) were necessary to avoid turbulent flow.

A conductivity cell (D, Fig. 2) was incorporated directly into the fluid flow path so that a continuous check could be maintained against possible contamination of the solution.

The water used in all determinations was obtained by twice redistilling the "stock" distilled water obtained from a Barnstead still. The final distillation was made from dilute permanganate in order to destroy organic contaminants. No special efforts were made to obtain water with the same value of specific conductivity for each run;

[1] As pointed out in the previous paper (1), this method was used first by Eversole and Boardman (2). It has been brought to the attention of the authors that subsequent work using streaming current methods has been done by Neale and Peters (3) and Buchanan and Heymann (4).

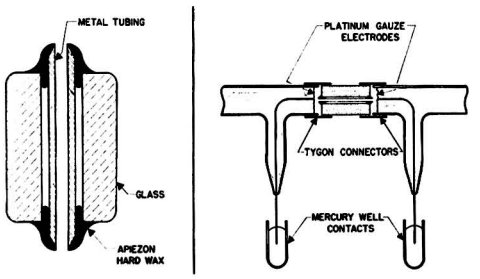

FIG. 1. Typical capillary construction and mounting. (*a*) (left), typical capillary construction; (*b*) (right), electrodes and contacts.

TABLE I. *Gold capillaries in distilled* H_2O

Dimensions	Ratio, l/r^2	t	$I/\Delta P \times 10^{12}$	ζ
		°C		mv
$r = 7.02 \times 10^{-3}$ $l = 1.521$	3.09×10^4	22.0	4.5	61.0
$r = 1.38 \times 10^{-2}$ $l = 1.724$	1.10×10^4	22.0	12.7	61.1
$r = 1.89 \times 10^{-2}$ $l = 3.251$	9.09×10^3	18.0	14.1	61.9
$r = 1.89 \times 10^{-2}$ $l = 5.50$	1.54×10^4	24.5	9.4	60.0

TABLE II. *Platinum capillaries in distilled* H_2O

Dimensions	Ratio, l/r^2	t	$I/\Delta P \times 10^{12}$	ζ
		°C		mv
$r = 6.81 \times 10^{-3}$ $l = 1.502$	3.24×10^4	18.0	3.88	60.8
$r = 1.29 \times 10^{-2}$ $l = 1.527$	9.13×10^3	17.0	13.2	60.0
$r = 1.87 \times 10^{-2}$ $l = 3.198$	9.15×10^3	21.0	15.0	61.5
$r = 1.87 \times 10^{-2}$ $l = 5.50$	1.57×10^4	21.0	8.7	61.5

TABLE III. *Silver capillaries in distilled* H_2O

Dimensions	Ratio, l/r^2	t	$I/\Delta P \times 10^{12}$	ζ
		°C		mv
$r = 6.64 \times 10^{-3}$ $l = 1.721$	3.90×10^4	25.0	2.80	44.8
$r = 1.17 \times 10^{-2}$ $l = 1.821$	1.32×10^4	19.0	8.14	50.6
$r = 1.87 \times 10^{-2}$ $l = 3.142$	9.03×10^3	16.0	10.4	48.0
$r = 1.87 \times 10^{-2}$ $l = 5.50$	1.58×10^4	20.0	7.2	52.5

however, the conductivity was less than 2.0×10^{-6} in all cases.

All runs were made at room temperature, which varied throughout the range 15°–25°C. From the data, the ζ-potential was essentially independent of temperature in this interval. It was of course necessary to measure the temperature of the solution in order to use the proper value for viscosity.

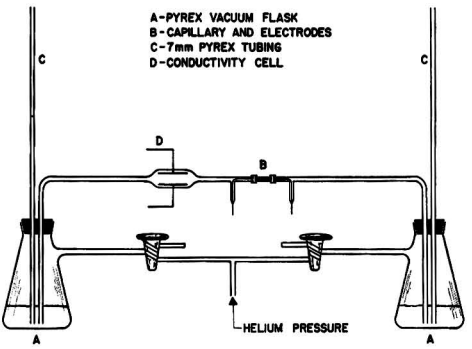

FIG. 2. Fluid flow system

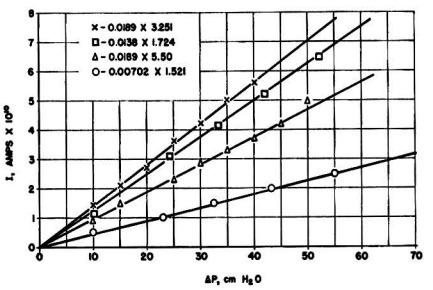

FIG. 3. Gold capillaries in distilled water

The dilute electrolyte solutions were prepared from reagent grade chemicals.

RESULTS AND DISCUSSION

ζ-Potential at the gold-water interface.—Curves of streaming current vs. pressure drop across the gold capillaries are shown in Fig. 3. In a previous paper (1) results were shown with flow in both the left-to-right and the right-to-left directions; however, after enough curves of that type were taken to show definitely that the two segments were always of the same slope, runs were made with flow in one direction only.

With these and all other capillaries tested (platinum and silver), the electrode *toward* which the fluid was flowing became more positive, which means that the excess ions traveling with the fluid flow were cations. For such a case, the ζ-potential is given a negative sign by convention.

Pertinent data and calculated ζ-potentials[2] for the gold capillaries are summarized in Table I. The mean value for the ζ-potential, 61.0 ± 1.0 mv, was obtained only after the capillaries had been in contact with the water long enough to reach an equilibrium condition. If the runs were made too soon after cleaning with dilute HNO_3, the ζ-potentials were invariably larger and inconsistent. By prolonging the time of contact with the HNO_3 solution, a ζ-potential of 134 mv was obtained for one of the capillaries; this value decreased slowly with storage in

[2] From the equation $\zeta = [4\eta/D][l/r^2][I/\Delta P]$. *See* reference (1).

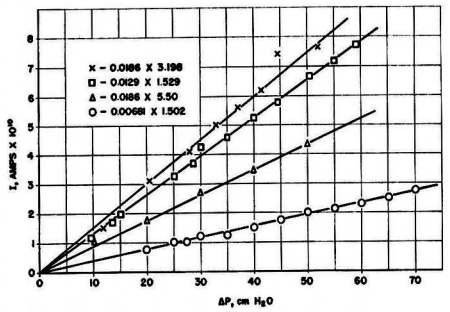

FIG. 4. Platinum capillaries in distilled water

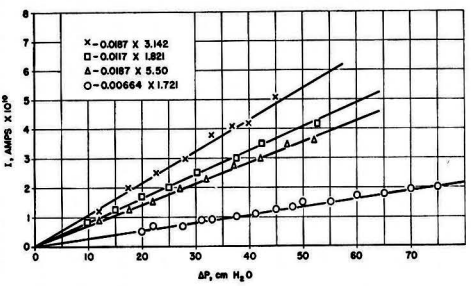

FIG. 5. Silver capillaries in distilled water

distilled water, until the equilibrium potential was reached after approximately nine days. With capillaries subjected to the usual cleaning procedure, the interface attained the equilibrium state after only one or two days, and no further changes were noted even after storing in water for as long as thirty days.

The higher ζ-potentials observed immediately after rinsing with HNO_3 were observed also with silver and platinum, and are attributed to a more highly oxidized state of the surface than is present after equilibrium is reached. This fits well with the description of the metal-solution interface given by de Boer and Verwey (5), who attribute the negative ζ-potential to a layer of oxygen chemically adsorbed on the surface. Electrophoretic measurements have shown that, by carefully excluding all oxygen during the preparation of platinum sols, it was possible to reverse the sign of the ζ-potential (6). Streaming current measurements on bulk metals to confirm these results could probably be made, and should be an object of future research.

ζ-Potential at the platinum-water interface.—The curves of streaming current vs. pressure drop for the four platinum capillaries in distilled water are shown in Fig. 4. Table II summarizes the data and gives the calculated ζ-potentials, the mean value of which is 60.8 ± 1.0 mv. It is somewhat surprising that the ζ-potentials for gold and platinum are practically identical, even though one would not expect them to be very different.

ζ-Potential at the silver-water interface.—Whereas the values of the ζ-potential for gold and platinum were remarkably consistent from one capillary to another, considerably more variation was found among the silver capillaries. The curves for the four capillaries in distilled

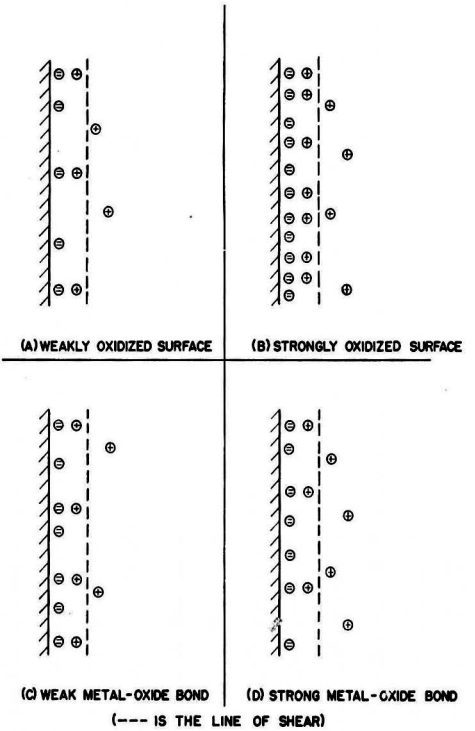

FIG. 6. Ionic distribution at the metal-solution interface.

water are shown in Fig. 5, and a summary of the data is given by Table III. The ζ-potential for silver is 49.0 ± 4.0 mv, a value significantly lower than that found for gold and platinum. An explanation of this may arise from the fact that the silver-oxygen bond in the oxide layer is somewhat weaker than the corresponding platinum and gold bonds with oxygen. Most authors are in agreement that the ionic distribution at the metal solution interface can be shown pictorially as in Fig. 6, in which the double negative charges represent the oxide layer and the positive charges the counter ions in solution. For a double layer structure of this type, one may draw the following qualitative conclusions:

(*A*) For a given metal, a more highly oxidized surface results in a higher number of positive ions per square centimeter in the movable part of the double layer (compare Fig. 6*a* and 6*b*).

(*B*) A weaker bond between the metal ion and the oxide ion results in a stronger bond between the oxide ion and the counter ion in solution, thus leaving fewer excess positive ions in the movable part of the double layer (compare Fig. 6*c* and 6*d*).

Both of these conclusions are in agreement with the results described above. That is, assuming the silver-oxygen bond to be weaker than the corresponding gold- and platinum-oxygen bonds, then the original highly oxidized surface produced by nitric acid cleaning will be dissolved to a greater extent in the case of silver. The greater ease with which the oxide is removed from the

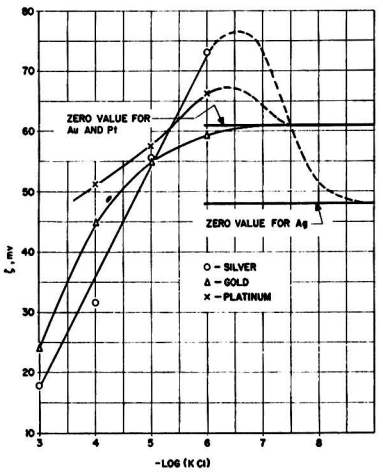

FIG. 7. Metal capillaries in dilute KCl

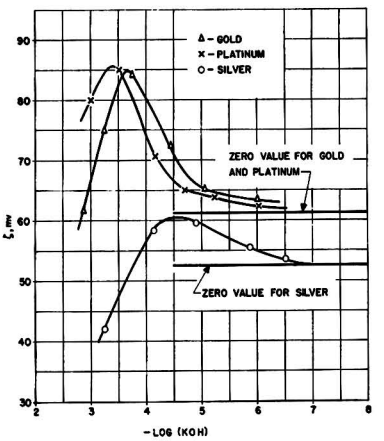

FIG. 8. Metal capillaries in dilute KOH

silver surface would also explain the greater variation in ζ-potential from capillary to capillary. Thus, either of the double-layer configurations (A) and (B) (Fig. 6) may explain the results obtained In all likelihood, both mechanisms contribute. However, in view of the fact that actual equilibrium data on the surface oxidation states are unavailable, these mechanisms can be presented only as *possible* explanations.

ζ-Potentials at the interface metal-dilute KCl.—Streaming current measurements were made on one capillary of each metal, using dilute solutions of KCl as the liquid phase. KCl concentrations of 10^{-6}, 10^{-5}, 10^{-4}, and $10^{-3}N$ were used. Results are shown in Fig. 7, in which the ζ-potentials are plotted against the negative logarithm of the KCl concentration. It is notable that the effect of KCl on the ζ-potential is at least qualitatively related to the solubility of the corresponding metal chloride. Thus, silver, which forms a very insoluble chloride, shows a marked maximum in ζ at low chloride concentrations; platinum, which forms a sparingly soluble chloride, shows a much smaller maximum; and gold, whose chlorides are very soluble, shows no increase in ζ at all. The maxima in the case of silver and platinum are ascribed to filling in, by chloride ions, of vacant spots in the oxide layer, thus yielding the same effect as a more highly oxidized surface. The tendency of these metals to form coordination complexes with chloride ions may also be of importance here, but the correlation is not as evident as the solubility relationship.

The decreasing ζ-potentials at the higher KCl concentrations is a general phenomenon encountered with almost all solid surfaces and electrolytes, and is due to the fact that solutions with high ionic strengths "compress" the entire double layer to the extent that only a small amount of the total potential drop remains in the diffuse part of the layer.

ζ-Potentials at the interface metal-dilute KOH.—ζ-potentials for the three metals in contact with dilute KOH solutions are plotted in Fig. 8 as a function of the KOH concentration. The curves for gold and platinum are almost identical in both the magnitude of the maxima and the value of KOH concentration at which they occur. For the silver capillary the maximum was less pronounced, and was also shifted approximately one *p*H unit toward the lower KOH concentrations.

These maxima very likely result from a surface change similar to that proposed for the chloride solutions, with the exception that in this case the weakest binding for the adsorbing OH^- ion is presented by silver, with the result that silver shows the least change in ζ-potential. Since platinum and gold possess almost identical ζ-potentials in distilled water, it is reasonable to conclude that the metals should behave similarly toward the OH^- ion, which, insofar as adsorption at a surface is concerned, is not essentially different from the oxygen molecule. The marked similarity of the curves for platinum and gold in Fig. 8 was therefore not unexpected.

Future work in this investigation will be directed first of all to the measurement of ζ-potentials on metal surfaces from which the oxide layers have been removed. Afterwards, a method of measuring these potentials as a function of externally applied polarizing potentials will be sought.

Manuscript received September 21, 1955. This paper was prepared for delivery before the San Francisco Meeting, April 30 to May 3, 1956.

Any discussion of this paper will appear in a Discussion Section to be published in the December 1956 JOURNAL.

REFERENCES

1. R. M. HURD AND N. HACKERMAN, *This Journal*, **102**, 571 (1955).
2. W. EVERSOLE AND W. BOARDMAN, *J. Phys. Chem.*, **46**, 914 (1942).
3. S. M. NEALE AND R. H. PETERS, *Trans. Faraday Soc.*, **42**, 478 (1946).
4. A. S. BUCHANAN AND E. HEYMANN, *J. Colloid Sci.*, **4**, 157 (1946).
5. J. DE BOER AND E. J. VERWEY, *Rec. Trav. Chim.*, **55**, 675 (1936).
6. N. BACH AND N. BALASCHOWA, *Acta Physicochim., U.R.S.S.*, **3**, 79 (1935).

Galvanic Potentials of Grains and Grain Boundaries in Copper Alloys

R. Bakish and W. D. Robertson

Hammond Metallurgical Laboratory, Yale University, New Haven, Connecticut

ABSTRACT

Potentials of grains and grain boundaries were measured in pure copper, Cu_3Au, and in alpha brass; the three cases represent the structural grain boundary in a pure metal, an alloy in which only one component is oxidized, and an alloy in which both components are oxidized. Potentials were measured in ferric chloride and in aqueous ammonia, the former representing an electrolyte in which only Cu_3Au is susceptible to stress cracking and the latter representing conditions in which brass is susceptible to stress cracking. In general, it was found that the measured potentials could be correlated directly with observed structural changes and susceptibility to stress corrosion cracking.

Introduction

The measurement of electrochemical potential differences between grains and grain boundaries in aluminum alloys (1) has contributed greatly to an understanding of the electrochemical mechanism of stress corrosion cracking in age-hardening systems. The corresponding problem in homogeneous solid solutions has not been extensively studied. In fact, it appears that only one measurement of grain boundary potentials in brass is available (2).

There is no evidence that precipitates or impurities are responsible for intergranular stress corrosion cracking and intergranular corrosion of brass (3). On the other hand, it has been shown that the phenomenon is associated only with alloys and does not occur in pure metals (4).

Since pure metals are structurally similar to homogeneous alloys, it is necessary to measure and compare potentials as a function of composition in order to separate the effect of the structural grain boundary from the combined structural and compositional factors. Furthermore, stress corrosion cracking of copper base alloys is dependent on the environment and, accordingly, it is also desirable to obtain boundary potentials in several environments for correlation with the corresponding corrosion cracking susceptibility.

The following measurements were made to provide information necessary for an evaluation of the effects of alloy composition, structure and electrolyte.

1. Electrochemical potentials of grains and grain boundaries of pure copper were measured in 2% ferric chloride.
2. Galvanic potentials of polycrystalline copper-gold and copper-zinc alloys were measured as a function of alloy composition, including the pure components, in 2% ferric chloride and aqueous ammonia.
3. Potentials of grains and grain boundaries of a homogeneous copper-gold alloy (Cu_3Au) and alpha brass (copper-zinc) were measured in 2% ferric chloride as examples of two alloys of which only copper-gold is susceptible to cracking in the particular environment.
4. Potentials of grains and grain boundaries in alpha brass were measured in 2% ferric chloride and aqueous ammonia.

Structural observations of boundary corrosion of the various alloy and electrolyte combinations were also made for the purpose of correlation with electrochemical measurements.

Experimental Procedure

Materials.—All metals and alloys used in this investigation, Table I, were specially prepared for the purpose from materials of at least 99.99% purity or better, indicated by spectroscopic analysis, and they were annealed at a high temperature prior to preparation as electrodes.

Fine grained polycrystalline electrodes were made by conventional rolling and recrystallization techniques. Large grained copper specimens, for grain boundary measurements, were obtained by solidification in a single crystal furnace and the one-half inch cylindrical specimens were sectioned along the axis of the cylinder. Coarse grained copper-gold alloys were obtained by annealing at a high temperature. Large grained alpha brass was obtained by slow solidification and also by recrystallization; the latter specimens were kindly supplied by D. H. Thompson of the American Brass Co. and there is reason to believe that they are from the same lot of material used by Dix (2). Grain diameters in all coarse grained specimens for boundary measurements were about one centimeter.

Surface preparation.—After annealing, all polycrystalline electrodes in the form of sheet or more massive blocks were polished with levigated alumina and, finally, electropolished immediately before introduction in the measuring cell. Exposed areas were of the order of several square centimeters, and all edges and electrical connections were masked with an organic resin (Epon 100).

Grain boundaries were isolated from the adjacent grains, as far as possible, by masking the grains with the above resin and leaving the grain boundary exposed in an area about 0.03 mm wide. This operation was accomplished under a microscope at 100× by placing a drop of resin on the grain and moving it toward the grain boundary by means of a nylon tip attached to a micromanipulator. Obviously the exposed width is much greater than that associated with a grain boundary, but it appears that the

TABLE I. *Atomic per cent*

Alloy	Copper	Gold	Zinc
Copper	99.99+	—	—
Gold	—	99.99+	—
Zinc	—	—	99.99+
Cu_3Au	75	25	—
Cu Au	50	50	—
Brass	89.8	—	10.2
Brass	79.5	—	20.5
Brass	74.4	—	25.6
Brass	69.2	—	30.8

contribution of the boundary to the galvanic potential is sufficiently large so that its polarity and change of potential with time can be measured reproducibly; the absolute values, of course, have no significance. Potential measurements of the individual crystals in a polycrystalline aggregate were obtained by masking the grain boundaries with resin.

Measuring cell and standard electrode.—All potentials were measured with respect to the normal silver-silver chloride electrode. A silver wire, anodized in 10% hydrochloric acid, was inserted into a glass tube containing 1*N* potassium chloride; the tube was closed by an agar-agar diaphragm. Potential differences between a number of standard electrodes were less than 0.01 mv.

The standard electrode and the metallic electrodes were placed in a glass cell covered with a rubber stopper through which all electrical connections were passed. The cell was immersed in a water thermostat controlled to 0.005°C. Generally, polycrystalline electrodes, grain boundary, and matrix electrodes of the same composition were placed in the cell at one time, except in the case of zinc which could not be combined with copper electrodes. Most of the grain boundary and matrix potential measurements were repeated four times with a new surface preparation between each individual run. All potentials were measured over prolonged periods of time with a precision potentiometer.

Experimental Results

Pure copper.—Fig. 1 shows the results obtained on polycrystalline copper, copper grain boundaries and grains in 2% ferric chloride. Four independent runs were made and the variation between results was greatest in the case of the isolated grains in which the potentials at the maximum, for example, varied within ±0.005 v. Grain boundary potentials, on the other hand, were surprisingly reproducible to about ±0.001 v and values for the polycrystalline electrodes were within ±0.0002 v.

Since copper is readily oxidized by ferric chloride, the effect of cupric ion in the electrolyte was investigated to determine whether the changes of potential in time were associated with electrolyte composition. After reaching stable values, the copper ion concentration of the electrolyte was increased by adding cupric chloride. No permanent effect due to cupric ion concentration was observed.

Observed potential differences between grains and grain boundaries of pure copper are in complete accord with metallographic observations on copper specimens immersed in ferric chloride for periods of many weeks. Starting with a flat surface, a groove forms at the junction of the boundary and the surface, similar to boundary grooves characteristic of thermal etching; after establishment of a stable groove, copper continues to be removed uniformly from the surface, maintaining the equilibrium boundary angle. In terms of potentials, the grain boundary is initially more active than the grain, with an increasing potential difference in time; after a period of several hours the potential difference diminishes and finally goes to zero at about 10 hr and remains at zero for the duration of the experiment, which was prolonged to 50 hr. These results are also in accord with the fact that stress corrosion cracking and intergranular corrosion, beyond superficial grain boundary grooves, are not observed in pure copper.

Composition dependence of galvanic potential in copper-gold alloys.—Galvanic potentials of polycrystalline pure copper, copper-gold alloys and pure gold in ferric chloride are shown in Fig. 2. To compare potentials in terms of composition, steady-state values at 20 hr are plotted in Fig. 3 as a function of gold content and an average curve is drawn to emphasize the change in potential as a function of composition.

Grain and grain boundary potentials in Cu_3Au.—One of four sets of potential values for grains and grain boundaries of Cu_3Au in ferric chloride is shown in Fig. 4 as a function of time. In all four independent experiments, grain boundaries were invariably more active than the grains; furthermore, the observed potential difference of 0.005–0.006 v was constant in time to 50 hr. The evidence of a continuous

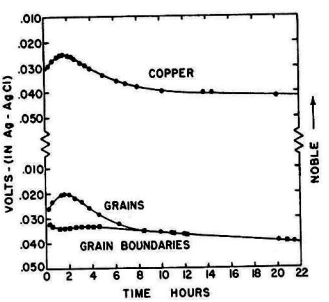

FIG. 1. Potentials of copper electrodes consisting of grains, grain boundaries, or a polycrystalline aggregate measured in ferric chloride.

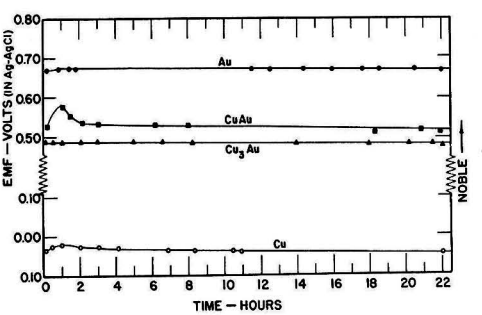

FIG. 2. Galvanic potentials of copper-gold alloys in ferric chloride as a function of time.

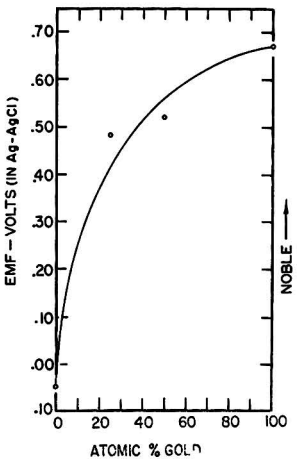

FIG. 3. Galvanic potentials of copper-gold alloys as a function of composition.

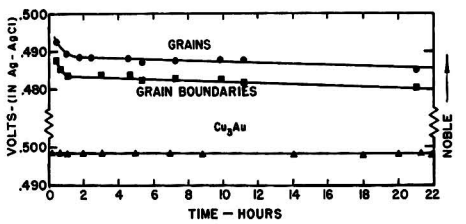

FIG. 4. Potentials of Cu_3Au electrodes consisting of grains, grain boundaries, or polycrystalline aggregates in ferric chloride.

driving force is in agreement with the observed structures and is in sharp contrast with the behavior of pure copper.

It has already been established (5) by prolonged immersion of Cu_3Au in ferric chloride that copper alone is removed from the alloy; at least, spectroscopic analysis of the solution shows no trace of gold. Furthermore, the reaction is preferentially concentrated at grain boundaries where penetration continues through the specimen, leaving a gold sponge in the vicinity of the boundary; reaction also proceeds normal to the outer surface and to the plane of the grain boundary, although at a comparatively slow rate, with the resulting structural pattern of attack shown schematically in Fig. 5. It seems that boundary activity is responsible for the nucleation of reaction at this location and, subsequently, the large potential difference between this alloy and residual gold, about 0.2 v, from Fig. 3, causes rapid and continuing penetration down the plane of the boundary.

The potential of the polycrystalline aggregate is nearly that observed for the grains. When individual grain and grain boundary electrodes are short circuited outside the cell, after reaching steady state, the potential of the combined electrodes is almost identical with that observed for the polycrystalline electrode; when the circuit between the two electrodes is opened, the individual potentials are re-established almost immediately.

Composition dependence of potentials in the copper-zinc system in $FeCl_3$.—Potentials of copper-zinc polycrystalline alloys in the alpha solid solution range, and pure zinc, were determined in ferric chloride with results shown in Fig. 6. Again, for comparative purposes, the values at 20 hr are shown in Fig. 7 as a function of composition.

In this case, a steady state evidently is not reached. Zinc becomes progressively more noble, presumably due to the formation of hydrated oxides, while the copper-zinc alloys become more active. The scale should be emphasized in Fig. 6 where the potential difference between zinc and the most active copper alloy is large, about 0.9 v at 20 hr.

Potentials of grains and grain boundaries of brass in ferric chloride.—Results of typical measurements of grain, grain boundary, and polycrystalline alpha brass (70%Cu-30%Zn) are presented in Fig. 8. Reproducibility was ade-

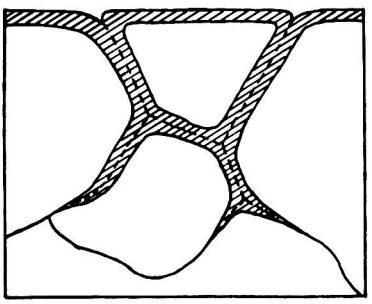

FIG. 5. Schematic drawing showing the preferential removal of copper from grain boundaries in Cu_3Au by ferric chloride and the relatively slow penetration of grains normal to the outer surface and to the boundary planes.

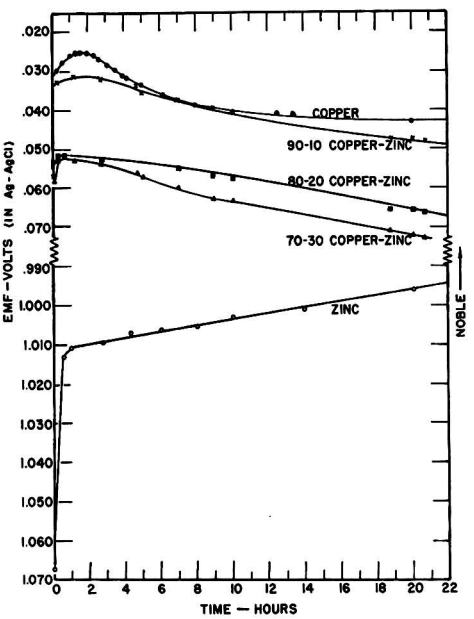

FIG. 6. Galvanic potentials of copper-zinc alloys in ferric chloride as a function of time.

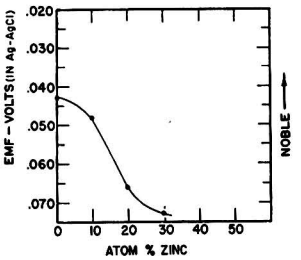

FIG. 7. Galvanic potentials of copper-zinc alloys in ferric chloride as a function of zinc concentration.

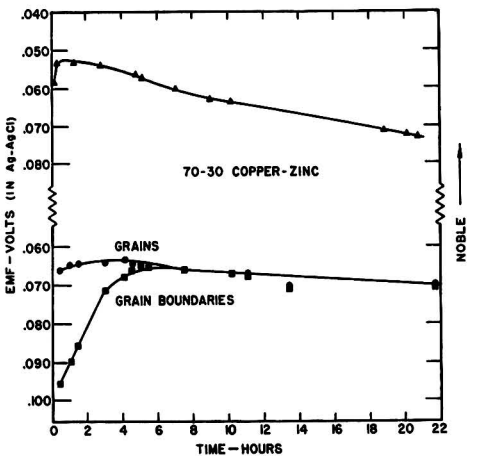

FIG. 8. Potentials of alpha brass (70% Cu–30% Zn) electrodes consisting of grains, grain boundaries, or a polycrystalline aggregate in ferric chloride.

quate for the purpose; for example, in four runs between which the specimens were completely repolished, the potential value at the maximum of the curve for the grains was -0.065 ± 0.004 v and similar deviation from the average of four was observed in polycrystalline electrodes.

Like pure copper, the potential difference between grains and grain boundaries goes to zero after about 8 hr and continues at zero thereafter. Again, this is in accord with structural observations. Immersion of annealed specimens in ferric chloride for prolonged periods results in dezincification and the formation of equilibrium grooves at the intersection of boundaries with the surface; continuous penetration of the boundary, characteristic of susceptibility to stress corrosion cracking, does not occur in conformity with the observed absence of cracking of brass in ferric chloride.

Composition dependence of potential of copper-zinc alloys in aqueous ammonia.—Present results in ammonia should be compared with corresponding results obtained in ferric chloride, the former constituting a combination in which brass is susceptible to cracking and the latter in which there exists little or no such susceptibility.

Data on copper, 70–30 copper-zinc, and pure zinc in 2% aqueous ammonia are presented in Fig. 9. It is clear that, in spite of the ammonia complex formed by copper, zinc and copper-zinc alloys remain active relative to copper in ammonia solutions. With respect to the ammonia electrolyte, however, the additional factor of oxygen concentration must be considered because, unlike ferric chloride, no oxidizing agent is present other than oxygen.

Grain and grain boundary potentials of brass in ammonia.—Except Dix (2), other investigators (6, 7) who have measured grain and grain boundary potentials of brass in ammonia have found invariably the grain boundaries to be more noble than the grains.

In the present case, six different experiments involving three runs with cast and homogenized 70/30 brass, two runs with recrystallized 70/30 brass, the latter specimens probably from the same piece as that used by Dix (2), and one run with 75/25 cast brass all confirmed the results of other investigators in that the boundary was invariably cathodic to the adjacent grains. Results for 75/25 brass are presented in Fig. 10. By comparison with previously

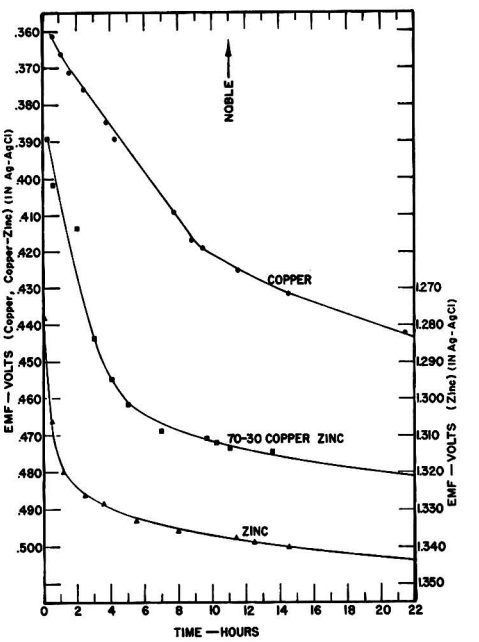

FIG. 9. Galvanic potentials of copper-zinc alloys in aqueous ammonia in a closed system without the addition of oxygen.

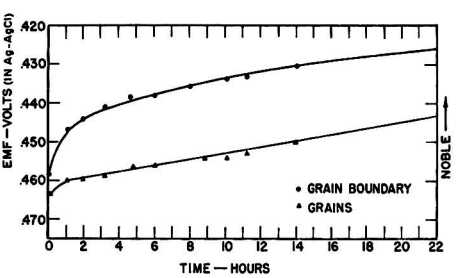

FIG. 10. Potentials of alpha brass electrodes (75% Cu–25% Zn) consisting of grains or grain boundaries in aqueous ammonia without oxygen additions.

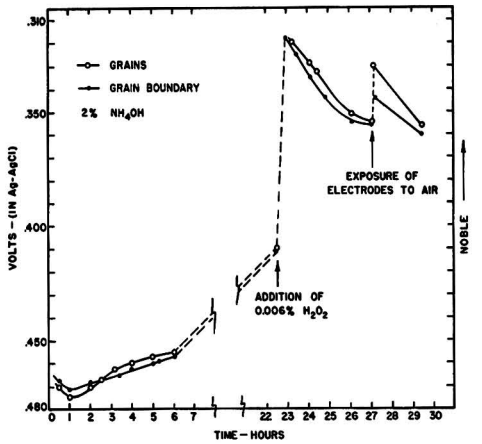

FIG. 11. Effect of oxygen on the potentials of grains and grain boundaries of alpha brass (75% Cu-25% Zn) in aqueous ammonia.

described experiments in different electrolytes, reproducibility of absolute values in ammonia was poor; however, the polarity was always that shown in Fig. 10 and exactly the inverse of what might be expected. Also, the observed difference in potential remained essentially constant in time up to 24 hr.

After considering that all measurements were conducted in a cell two-thirds filled with aqueous ammonia and closed with a rubber stopper, and that stress corrosion cracking is dependent on oxygen concentration (8), it was concluded that the above results in ammonia might be associated with a limited supply of oxygen.

Numerous trial runs in which hydrogen peroxide was added to the electrolyte generally confirmed the conclusion that previous results were associated with the relative absence of an oxidizing agent in the solution. However, the presence of hydrogen peroxide resulted in excessive gas evolution and erratic readings. Accordingly, a set of measurements was made with the cell open to the air with results shown in Fig. 11. Initially the grain boundaries were cathodic, as before, but in 2.5 hr the potential difference decreased to zero, subsequently reversed, and finally stabilized at a difference of about 1.5 mv with the grain boundaries active, a condition which was maintained for about 18 hr. At this time, a very small quantity of hydrogen peroxide was added to the cell which caused a large shift in both potentials in a noble direction; the potential difference between grains and boundaries first increased and finally decreased again while the absolute magnitude shifted back to more negative values, presumably due to the decomposition of the small quantity of hydrogen peroxide. As a further demonstration of the large effect of oxygen, the electrodes were removed from the cell and momentarily exposed to air before replacing in the same position. Again, all potentials shifted in a noble direction and, significantly, the potential difference between grains and boundaries increased to 14 mv; the potential difference subsequently diminished to about 4 mv, presumably as a result of oxygen consumption. Thus, while additional quantitative data are necessary, the general qualitative effects appear to be quite consistent and in harmony with observed stress corrosion cracking phenomena.

DISCUSSION OF RESULTS

The results indicate that there exists a direct, empirical relation between measured grain boundary potentials in copper alloys and observed structural reactions and stress corrosion cracking susceptibility. Such a correlation already exists for age hardening aluminum base alloys in which compositional changes associated with precipitation clearly account for the observed galvanic potentials between grains and their boundaries. The corresponding mechanism in homogeneous copper solid solutions is not so clear.

With respect to pure copper, it appears from the data in Fig. 1 that the initial active potential measured at the boundary is directly related to the reaction at the non-equilibrium grain corner, where the plane of a boundary meets the plane of the surface. However, when an equilibrium configuration is established, further reaction occurs without regard to structure and, in particular, continued preferential penetration at the grain boundary does not occur, as shown by metallographic examination and indicated by the subsequent equality of potentials in Fig. 1. It seems possible to conclude, therefore, that the structural boundary itself does not produce a galvanic potential, measurable with present methods.

In copper-gold alloys, crystallographically similar to pure copper, the situation is quite otherwise. Measurement of boundary potentials, Fig. 4, shows that a constant potential difference exists between grains and their boundaries, and metallographic examination shows that penetration proceeds preferentially down the boundary until a specimen is completely penetrated.

A potential difference of about 200 mv in ferric chloride exists between gold and a Cu_3Au alloy. Evidently, if a reaction removing copper is able to start at some preferred site, the large galvanic potential between the remaining gold and the copper alloy will result in further, and continuous, removal of copper. However, that both a preferred structural path and composition are involved in the mechanism is indicated by two facts: (*a*) the path of penetration down grain boundaries in Cu_3Au is enormously more rapid than through the grains, and (*b*) the characteristic penetration does not occur at all in pure copper or in a copper-gold alloy.

It appears, therefore, that the nucleating reaction is most probably the same one that occurs in pure copper at a boundary with the removal of copper at the grain edge; however, in the Cu_3Au alloy the resulting galvanic potential between the remaining gold sponge and the alloy increases greatly with the removal of copper and produces the observed continuous penetration. In the CuAu alloy, in which the potential differences are of the same magnitude and, therefore, electrochemically comparable, copper is surrounded by more gold atoms and the removal of additional copper, after the first superficial attack, apparently is limited by the remaining coherent layer of gold which renders the underlying copper inaccessible to the electrolyte (9).

Similar phenomena in copper-zinc alloys are complicated by the fact that both components of the alloy are chemically active. Since galvanic potential differences are evidently involved it is apparent that the relative activity of reactive components must be considered with regard to the electrolyte. Thus, the potential difference between grains and boundaries in copper-zinc alloys in ferric chloride goes to zero, after initial boundary activity, Fig. 8, in exactly the same manner as pure copper. Again it appears that this is primarily a structural phenomenon associated with the establishment of an equilibrium configuration at grain corners. However, it remains to explain why, in this alloy, penetration ceases after the formation of an initial groove at the boundary.

In the latter connection, it is instructive to compare Fig. 3 and 7 from which it is apparent that the change of potential with composition, measured in ferric chloride, is much greater in copper-gold alloys than in copper-zinc alloys, specifically about 22 mv/atom % gold as compared with approximately 1 mv/atom % zinc; furthermore, in zinc alloys the potential changes in the active direction with increasing zinc concentration. It seems, therefore, that the removal of zinc at boundaries by ferric chloride may result in diminishing the active potential of boundary areas with respect to adjacent grains, so that continued boundary penetration ceases.

It has been shown, qualitatively, that the polarity of grains and grain boundaries in alpha brass in ammonia is dependent on oxygen concentration, and that, in the presence of sufficient oxygen, the boundaries are active with respect to the grains. While this result is in complete accord with observations on intergranular corrosion and stress corrosion cracking, the detailed mechanism involving oxygen is not clear.

It is even more difficult to explain why the grain boundaries are reproducibly *cathodic* to the grains, Fig. 10, under conditions where oxygen is limited. Obviously, a quantitative study using various proportions of oxygen and gaseous ammonia is indicated and no general conclusions regarding the mechanism can be drawn without such data. It is also apparent that no consistent results are obtainable without quantitative control over this variable.

Conclusions

1. It has been shown that the measured potentials of grains and grain boundaries in pure copper and two different homogeneous copper alloys in two electrolytes are in complete conformity with corresponding intergranular corrosion and stress corrosion cracking observations.

2. In pure copper, the grain corners where the plane of the boundary meets the external surface is the site of a nucleating reaction. In copper and brass in ferric chloride, preferential reaction at the boundary ceases after an equilibrium configuration is established and potential differences between grains and grain boundaries go to zero; in copper-gold alloys penetration in the plane of the boundary continues, apparently as a result of the large potential difference created between the alloy and gold remaining after the oxidation of copper at the boundary.

3. The structural grain boundary, in itself, is not a source of galvanic potential measurable with the present technique after the initial reaction at the unstable corner where the plane of the boundary meets the outer surface. The boundary does, however, provide a preferential path for reaction when the necessary driving force is produced by the removal of one component of an alloy.

4. The polarity of grains and grain boundaries of brass in aqueous ammonia is dependent on oxygen concentration and, at low oxygen concentrations, boundaries are cathodic to the grains while, at higher oxygen concentrations, grain boundaries are anodic, in conformity with observed susceptibility to stress corrosion cracking and intergranular corrosion.

Acknowledgment

The authors are indebted to Handy and Harman, particularly to Mr. Ernest Chamer and Mr. John L. Christie for assistance rendered in preparation of the gold alloys. They are also indebted to the Office of Naval Research for financial support of this work and, accordingly, reproduction in whole or in part is permitted for any purpose of the United States Government.

Manuscript received November 7, 1955. This paper was prepared for delivery before the Pittsburgh Meeting, October 9 to 13, 1955, and was abstracted from a dissertation presented by R. Bakish to the School of Engineering, Yale University, in partial fulfillment of the requirements for the degree of Doctor of Engineering.

Any discussion of this paper will appear in a Discussion Section to be published in the December 1956 Journal.

References

1. R. B. Mears, R. H. Brown, and E. H. Dix, Jr., Symposium on Stress-Corrosion Cracking of Metals, A.S.T.M.—A.I.M.E., p. 323 (1944).
2. E. H. Dix, Jr., *Proc. Am. Soc. Testing Materials*, **41**, 928 (1941).
3. T. C. Wilson, G. Edmunds, E. A. Anderson, and W. M. Peirce, Symposium on Stress-Corrosion Cracking of Metals, A.S.T.M.—A.I.M.E., p. 173 (1944).
4. D. H. Thompson and A. W. Tracy, *J. Metals*, **1**, 100 (1949).
5. R. Bakish and W. D. Robertson, submitted to *J. Metals*; W. D. Robertson, "Impurities and Imperfections," p. 170, A.S.M., Cleveland (1955).
6. E. C. W. Perryman, Private communication relative to beta brass.
7. Hugh L. Logan, Private communication relative to alpha brass.
8. R. G. Johnston, *Sheet Metal Ind.*, **14**, 1197 (1940).
9. L. Graf, *Z. Metallkunde*, **40**, 275 (1949).

High Pressure Oxidation of Niobium

DONALD W. BRIDGES AND W. MARTIN FASSELL, JR.[1]

Department of Metallurgical Engineering, University of Utah, Salt Lake City, Utah

ABSTRACT

Niobium oxidizes according to the linear rate law from 400°–800°C (14.7–605 psia O_2). The oxidation rate is extremely pressure sensitive above 550°C. Theoretical considerations indicate that an equilibrium adsorption process occurs prior to the rate-determining step. It was necessary to include a term in the rate equation for the interaction between the adsorbed molecules to interpret results above 650°C. The interaction energy is influenced by the initial orientation of the metal surface. The activation energy for the oxidation process is approximately 9 to 10 kcal (500°–800°C).

INTRODUCTION

Oxidation data for niobium or columbium are not extensive. Gulbransen (1–3) found the metal to obey the parabolic rate law (200°–375°C). It has been stated (4) that the oxide formed at 200°C in air is adherent, preventing further oxidation unless the temperature is increased. McAdams and Geil (5) reported some data on relatively impure niobium. Inouye (6) published a survey of the scaling of niobium in dry air and in air containing water vapor (400°–1200°C). The metal oxidized according to the linear rate law (400°–1200°C) although irregular behavior occurred in dry air at 400°C, and in air containing moisture at temperatures below 600°C. Both black and white oxides were formed and identified as Nb_2O_5; three modifications were found.

According to Brauer (7) the following oxides exist: NbO_2, NbO, and Nb_2O_5. Nb_2O_5 has three forms: the so-called "low form," stable to 900°C; "medium form," 1000°–1100°C; and "high form," stable at temperatures above 1100°C. Recent work (6, 8) questions the transition temperatures cited by Brauer. A mixture of NbO and Nb_2O_5 has been reported at 400°C (2). Seybolt (9) investigated the solubility of oxygen in niobium (800°–1100°C). Kubaschewski and Schneider (10) studied the oxidation of several alloy systems containing niobium.

The present paper concerns the behavior of niobium in pure oxygen (14.7–605 psia) from 400° to 800°C.

EXPERIMENTAL PROCEDURE

Equipment and general technique are discussed in detail in a recent publication (11). Weight change is measured by observing the deflection of a quartz spring. Each individual experimental determination was made at constant temperature and constant pressure. The niobium used was Fansteel Metallurgical Corp. commercial sheet. Spectrographic analysis of the metal revealed traces of the following elements: aluminum, copper, gold, silver, zirconium, osmium, and rhodium. Average sample size was 1.5 in. x 0.375 in. x 0.02 in., a geometric surface area of about 1.2 $in.^2$.

[1] Present address: Howe Sound Co., Salt Lake City, Utah.

EXPERIMENTAL RESULTS

Effect of Oxygen Pressure

In all experimental determinations, the oxidation behavior of niobium was best represented by a linear rate law, i.e., $\Delta W/\Delta t = K$. K is a function of pressure and temperature and is referred to as the observed rate. Considerable time was required at 400°C to establish linearity. At 400°C and 14.7 psia oxygen, nearly six hours were required before the rate was truly linear. In dry air (one-fifth the concentration of pure oxygen) Inouye (6) required 21 hr to reach linearity at 400°C. Table I summarizes the data at 400° and 450°C. Above 500°C linear oxidation was observed from first recorded time to completion. Some samples ignited at 800°C at oxygen pressures in excess of 200 psia.

Fig. 1 shows the effect of oxygen pressure on the oxidation rate of niobium from 400° to 800°C. Niobium follows the general oxidation pattern of tantalum (11). The essentially "pressure independent" linear oxidation region terminates most abruptly at 500°C. The pressure dependent zone has its maxima at 575°C, with minima in the isobars at 650°C. A similar shaped plot has been obtained by oxidizing niobium under conditions of a linear increase in temperature (12).

Effect of Prior History of Niobium Metal

Two separate lots of niobium metal designated as "A" and "B" were used in this study. Marked differences in the oxidation behavior were observed in the two lots. Fig. 2 compares two isotherms of metal "A" with two isotherms of metal "B" in the same temperature region. Spectrographic analysis revealed no difference in composition between the two lots. Likewise metallographic work showed no marked difference; the grain size of both lots was very small. X-ray diffraction patterns showed that the orientation of the niobium surface of metal "A" differed from that of metal "B". The exact orientation of neither lot was determined.

Additional evidence that a difference existed between the corrosion behavior of the two lots was gained by following the wet corrosion of samples of metal "A" and metal "B" with periodic x-ray diffraction studies of the corroded surfaces. A hot solution of potassium hydroxide and potassium ferrocyanide [44.5 g/l KOH and 305 g/l $K_4Fe(CN)_6$]

TABLE I. *Oxidation rate of niobium "A" in oxygen for temperatures below 500°C*

Temp, °C	Oxygen pressure (psia)	Observed rate ($mg \cdot cm^{-2} \cdot hr^{-1}$)	Elapsed observed time before $\Delta W/\Delta t$ = const.	Observed period during which $\Delta W/\Delta t$ = const*
			min	*min*
400	14.7	0.18	350	200
400	30	0.27	200	200
400	400	0.13	300	100
450	100	5.8	Nil	70
450	200	3.8	Nil	70
450	300	2.8	15	40

* Run was terminated at the end of this period.

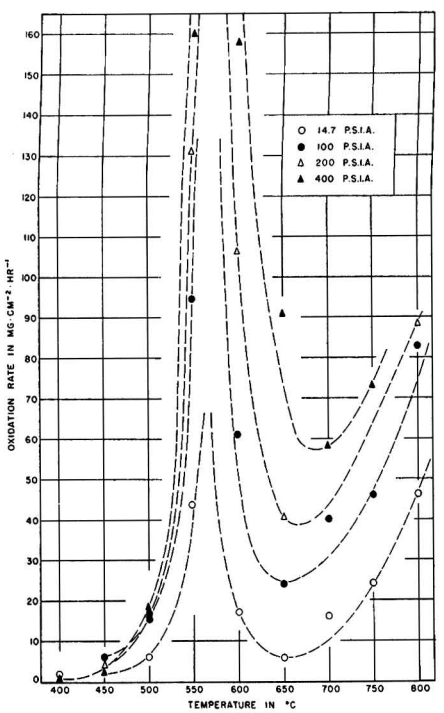

FIG. 1. Observed oxidation rate of niobium "A" in oxygen at various temperatures and pressures.

was employed as the corroding medium. Niobium samples of 20 mil thickness were corroded to an eventual thickness of 3–4 mils. A comparison of the relative intensities of the diffraction peaks as the surface was corroded revealed that corrosion occurred along different planes in the two lots.

The only data available for metal "B" are shown on Fig. 2. All other data reported are for metal "A". Repeated measurements under the same experimental conditions showed that the reproducibility of observed rates was most satisfactory.

X-ray Diffraction Results of Formed Oxides

Oxide coatings formed at various temperatures and pressures were examined by x-ray diffraction. Table II summarizes results and attempts a comparison with the available ASTM cards. Nb_2O_5 seems the most likely oxide present. Identification of the particular form of Nb_2O_5 is not attempted. The sample removed at the end of three hours' oxidation at 400°C and 14.7 psia was black in color, while the sample removed at the end of 25 hr was white. The oxides formed above 400°C were all white in color.

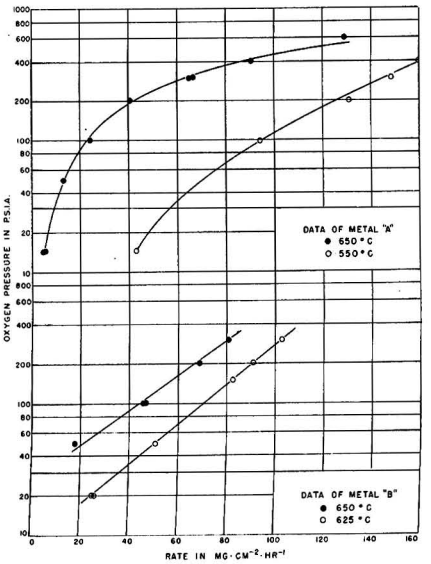

FIG. 2. Comparison of oxidation rates of metals "A" and "B" within "Dome" region (550°–650°C).

DISCUSSION OF EXPERIMENTAL RESULTS

No interpretation of the data below 500°C is attempted, as these rates were not initially linear. The observed rate of oxidation above 500°C is ideally linear, hence the rate-determining step is a phase boundary reaction (13). Recent work (14) suggests an underlying oxide as the zone of reaction in the linear oxidation of tungsten. Another possible interface for the reaction is the metal-metal oxide boundary. The basic assumption of the discussion to follow is that the adsorption of oxygen at the reaction boundary is much faster than the subsequent rate-controlling step and may be treated as an equilibrium process. A previous paper (11) develops concepts based on this assumption in detail and illustrates that application of the Theory of Absolute Reaction Rates (15) results in the following kinetic expression for an oxidation process governed by a boundary reaction,

$$\text{rate} = dm/dt = k_0 \cdot f(\theta) \cdot (kT/h) \cdot \exp(-\Delta F^*/RT) \quad (I)$$

k_0 is a proportionality constant with the dimensions of ML^{-2} and includes factors estimating the true surface area involved in the reaction. $f(\theta)$ is a function of θ, the fraction of the surface covered with adsorbed oxygen; expressions for this concentration term depend upon the nature of the adsorbed phase. $kT/h \cdot \exp(-\Delta F^*/RT)$ is the Eyring rate equation (15) with the transmission coefficient assumed to be unity.

TABLE II. *Comparison of interplanar spacings of the oxide scale formed on niobium metal*

Niobium metal		Diffraction data from this work					ASTM card information	
As determined this laboratory	ASTM Data card work of Meisel, and co-workers	400°C 14.7 psia 3 hr (oxide surface black)	400°C 30 psia 25 hr (oxide surface white)	575°C 100 psia (oxide surface white)	700°C 100 psia (oxide surface white)	750°C 100 psia (oxide surface white)	ASTM Card 5-03252 Niobium pentoxide ignited at 1000°C, work of Hahn, *JACS*, 73, 5091 (1951)	L.S. Iverm Westinghouse
7.369		7.248	7.248	5.242	5.181	5.211	5.241	4.04
2.336	2.336	3.966	3.914	3.931	3.931	3.931	4.329	3.17
1.652	1.65	3.151	3.140	3.463	3.463	3.463	3.931	2.48
1.348	1.35	2.378	2.434	3.162	3.151	3.151	3.484	1.97
1.168	1.17	1.679	2.120	3.097	3.097	3.097	3.140	1.81
1.166		1.362	1.959	2.736	2.728	2.728	2.855	1.67
0.044	1.04	1.182	1.819	2.460	2.460	2.453	2.728	1.65
0.041		1.059	1.652	2.116	2.434	2.421	2.590	1.57
		0.960	1.574	2.017	2.116	2.116	2.447	1.46
0.953	0.95	0.889	1.190	1.963	2.009	2.009	2.120	1.34
0.950				1.829	1.963	1.963	1.962	1.23
				1.792	1.829	1.829	1.908	1.18
0.882	0.88			1.660	1.789	1.789	1.825	1.14
				1.635	1.657	1.663	1.792	1.06
0.880				1.574	1.630	1.630	1.661	1.01
				1.460	1.572	1.572	1.571	1.00
0.825	0.83			1.336	1.541	1.541	1.543	0.94
				1.323	1.460	1.460	1.459	0.92
0.823				1.227	1.336	1.336	1.336	0.88
				1.195	1.323	1.323	1.322	0.86
				1.142	1.227	1.227	1.226	
						1.208	1.209	
						1.193	1.197	
							1.144	
							1.022	
							0.99	

Where interaction between the adsorbed molecules is negligible and the assumption of equilibrium allowable, the expression for $f(\theta)$ employed in the explanation of the linear oxidation of tantalum (11, 12) is suitable and equation (I) becomes,

$$\text{rate} = \theta \cdot K_0 = K_0 \frac{K_1[O_2]}{1 + K_1[O_2]} \qquad \text{(II)}$$

where K_0 equals $k_0(kT/h) \exp(-\Delta F^*/RT)$ and K_1 is the molar equilibrium constant for the adsorption of oxygen molecules. $[O_2] = P/RT$, and is the oxygen gas concentration provided the bulk gas phase obeys the perfect gas law (11, 12).

In order to satisfy equation (II) the following conditions must be satisfied.

Condition 1. Values of K_0 must be greater than any observed rate at the temperature in question. This would be expected as, limit $(\theta \rightarrow 1)$ $(dm/dt) = K_0$.

Condition 2. The slope of the plot, $\log_{10} K_0$ vs. 1/°K, must be negative in order that the activation energy for the process be positive.

Condition 3. The slope of the plot, $\log_{10} K_1$ vs. 1/°K, must be positive, since the heat of adsorption must be exothermic.

Condition 4. Values of K_1, the adsorption equilibrium constant, must be greater than unity since it is necessary that the adsorption free energy be negative or zero,

$\Delta F_{ads} \leq 0$, and

$$K_1 = \exp(-\Delta F_{ads}/RT) = \exp(-(\Delta H_{ads} - T \cdot \Delta S_{ads})/RT) \qquad \text{(III)}$$

TABLE III. *Comparison of observed oxidation rates of niobium "A" and trial and error fit of data by equation (II)*

Temp, °C	O_2 Pressure psia	Observed rate mg-cm^{-2}-hr^{-1}	Calc. rate mg-cm^{-2}-hr^{-1}	Constants	θ
550	14.7	43.4	43.4		0.26
	100	94.4	118.7	K_1, 23.3	0.70
	200	131	139.7		0.82
	300	148.4	148.3	K_0, 169.5	0.88
	400	159.9	153.2		0.91
600	14.7	17.2	13.1		0.06
	50	40	39.2		0.17
	100	61	67	K_1, 4.25	0.28
	200	106	105		0.44
	300	124	129	K_0, 238	0.54
	400	158	146		0.61
650	14.7	5.9	4.5		0.01
	50	13.6	14.8		0.05
	100	24.2	25.9	K_1, 1.1	0.08
	200	40.2	51.6		0.16
	300	66.7	71.9	K_0, 315	0.23
	400	91	88.9		0.28
	605	129	118		0.38

Trial and error fits, using equation (II), for the 550°, 600°, and 650°C isotherms for metal "A" are tabulated in Table III.

Fig. 3 illustrates the relationships found to exist between values of K_0, the absolute reaction rate constant, and reciprocal absolute temperature; as well as the relationship between the adsorption equilibrium constant, K_1, and

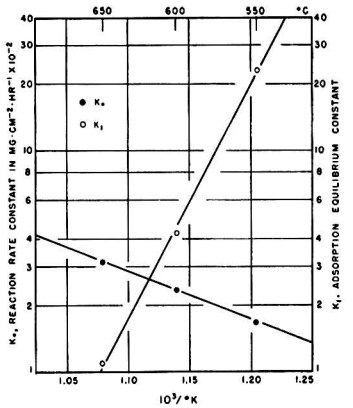

FIG. 3. Plot showing variation of the constants of Table III with temperature.

reciprocal absolute temperature. Slopes of the curves of Fig. 3 yield an activation energy, ΔH^*, of 9.9 kcal and an adsorption enthalpy, ΔH_{ads}, of -48.6 kcal/mole oxygen.

When adsorption occurs with appreciable interaction between the adsorbed molecules equation (II) is not applicable. The assumption of random distribution of the adsorbed molecules and interaction between the pairs of nearest neighbors lead to a varying adsorption enthalpy (16):

$$\Delta H_{ads} = \Delta H^0_{ads} + \theta z V, \qquad \text{(IV)}$$

where ΔH^0_{ads} is the enthalpy of adsorption for $\theta = 0$. zV is the product of the molar interaction energy, V, and the coordination number, z, i.e., the interaction energy of a pair of near neighbors multiplied by the number of such pairs. The adsorption entropy is assumed constant, thus the change in the adsorption potential, ΔF_{ads}, is identical with the change in ΔH_{ads}. Such behavior has been experimentally observed for the adsorption of hydrogen on tungsten (17).

A previous paper (18) has expanded these concepts into a suitable approximation for the rate of oxidation, viz.,

$$\text{rate} = \theta \cdot K_0 (4.6T/zV) K_0 [\log_{10} P + \log_{10} (K_1^0/RT)] \qquad \text{(V)}$$

TABLE IV. *Estimate of interaction energy, data of metal "A"*

Temp, °C	K_0	zV in cal	K_1^0
500	18	8,300	398
700	58	8,800	278
750	73	12,900	660
800	90	11,900	1470

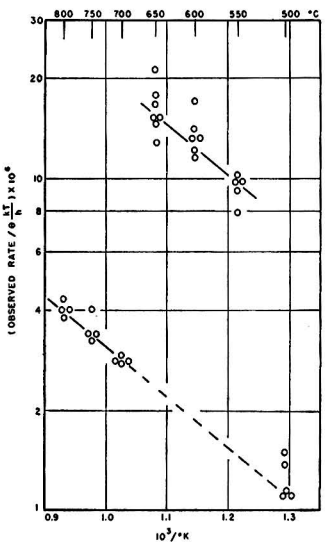

FIG. 5. Corrected Arrhenius plot. Each observed rate has been divided by the proper concentration term (θ).

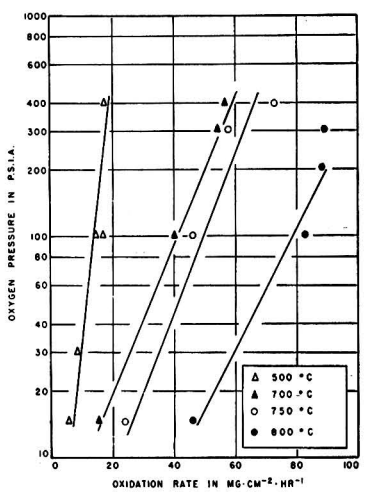

FIG. 4. Plot of niobium "A" isotherms showing correlation of data by application of equation (V).

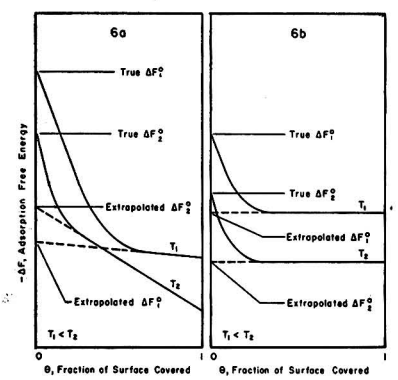

FIG. 6. Schematic diagrams of possible effects of surface coverage on the free energy of adsorption: (*a*) deviation of adsorption free energy from the linear behavior predicted by equation (IV) as $\theta \to 0$ results in extrapolated values of ΔF_{ads} differing from condition 3; (*b*) adsorption free energy, ΔF_{ads}, values result which are lower than the true values if the interaction energy is not negligible as $\theta \to 0$.

where K_0 is the absolute reaction rate constant as before and K_1^0 is the adsorption equilibrium constant for $\theta = 0$. The equilibrium constant is dependent on θ and is defined by

$$K_1 = K_1^0 \exp(-\theta zV/RT) \quad \text{(VI}a\text{)}$$

where

$$K_1^0 = \exp(-\Delta F^0_{ads}/RT) \quad \text{(VI}b\text{)}$$

Plots of observed rate vs. the logarithm of oxygen pressure for 500°, 700°, 750°, and 800°C are shown in Fig. 4. It is felt that the correlation of the data warrants application of equation (*V*). Estimation of zV is accomplished by selection of K_0 values in accordance with Conditions 1 and 2. These values are tabulated in Table IV. Plot of the logarithm of K_0 vs. reciprocal absolute temperature yields an enthalpy of activation, ΔH^*, of 8,750 cal.

Fig. 2 shows the 625° and 650°C isotherms for metal "B" plotted according to equation (V). It suggests that differences in surface orientation of metal "B" favor stronger interaction between the adsorbed oxygen molecules.

Fig. 5 represents the corrected Arrhenius plot. Each observed rate has been divided by the concentration term, θ, the fraction of the surface covered. The slope (and hence the activation energy) is essentially the same from 500° to 800°C, although the correlation of data by the two methods results in two parallel trends rather than a single straight line plot of absolute reaction rate constant vs. reciprocal temperature. Changes in the magnitude of the absolute reaction rate constant could be due to one or a combination of several factors: (*a*) difference in the entropy of activation, ΔS^*; (*b*) change in the number of active sites per unit area; or (*c*) change in surface roughness. A change in one of these quantities by a factor less than ten would correct the break (offset) in the plot.

The effect of surface coverage on adsorption free energy, demonstrated to apply in the investigated region of θ, may not be valid as the surface coverage, θ, approaches zero. The following evidence substantiates this conclusion: (*a*) the temperature dependence of K_1^0 (700°–800°C) is the reverse of the expected; (*b*) the adsorption free energies (550°–650°C) are extremely low. Fig. 6 shows a possible explanation. Neither the noninteraction nor linear enthalpy variation mechanism is obeyed for extremely low values of θ. The initial effect of interaction is much stronger than the variation over the investigated pressure range and causes a sharp descent in the adsorption potential in the region, $\theta \rightarrow 0$, followed by a linear dependence on θ, or, if zV is small, an essentially nonvarying enthalpy. Fig. 6*a* depicts the probable behavior of adsorption free energy as a function of surface coverage in the region of temperature 700°–800°C. Although the adsorption free energy always decreases as temperature increases, the actual nature of the deviation with respect to θ for the individual isotherms may result in an apparent violation of Condition 3, i.e., K_1^0, and hence free energy, increases with temperature. This violation would result if the initial abrupt descent in free energy places the straight line portions of Fig. 6*a* in such a position that the extrapolated lines intersect within the allowed θ values ($0 \leq \theta \leq 1$). Likewise Fig. 6*b* illustrates a case which would explain the low values of the free energy in the 550°–650°C region. It graphically expresses the belief that equation (II) results when the term θzV can be neglected in equation (IV).

Acknowledgments

The authors wish especially to thank Mrs. Gretta S. Baur who performed the diffraction analysis summarized in Table II. They also thank Mr. John P. Baur who interpreted the x-ray diffraction data gained in monitoring the wet corrosion phase of the investigation. They express their appreciation to the Office of Ordnance Research, U. S. Army, and their Watertown Arsenal Laboratory, for the funds that made the work possible, and to Dr. John R. Lewis, Head, Dept. of Metallurgy, University of Utah, for his support and interest in this work.

Manuscript received August 4, 1955. This paper was prepared for delivery before the Pittsburgh Meeting, October 9 to 13, 1955.

Any discussion of this paper will appear in a Discussion Section to be published in the December 1956 JOURNAL.

REFERENCES

1. E. A. GULBRANSEN AND K. F. ANDREWS, *J. (and Trans.) Electrochem. Soc.*, **96**, 364 (1949).
2. R. T. PHELPS, E. A. GULBRANSEN, AND J. W. HICKMAN, *Ind. Eng. Chem. Anal. Ed.*, **18**, 391 (1946).
3. E. A. GULBRANSEN AND K. F. ANDREWS, *J. Metals*, **2**, 586 (1950).
4. Technical Bulletin, Fansteel Metallurgical Corporation, Chicago (1945).
5. G. J. MCADAMS AND G. W. GEIL, *J. Research Nat. Bur. Standards*, **28**, 593 (1942).
6. H. INOUYE, ORNL-1565, Sept. 24, 1953; (Nuclear Science Abstracts, **7**, No. 22, 5933, Nov. 30, 1953).
7. G. BRAUER, *Z. anorg. u. allgem. Chem.*, **248**, 1 (1941).
8. A. V. LAPITSKII, *et al.*, *Zhur. Fiz. Khim.*, **26**, 56 (1952).
9. A. U. SEYBOLT, *J. Metals*, **6**, 774 (1954).
10. O. KUBASCHEWSKI AND A. SCHNEIDER, *J. Inst. Met.*, **75**, 403 (1949).
11. R. C. PETERSON, W. M. FASSELL, JR., AND M. E. WADSWORTH, *J. Metals*, **6**, 1038 (1954).
12. J. P. BAUR, D. W. BRIDGES, AND W. M. FASSELL, JR., *This Journal*, **102**, 490 (1955).
13. N. F. MOTT AND R. W. GURNEY, "Electronic Processes in Ionic Crystals," 2nd ed., p. 250, Oxford Press, New York (1948).
14. W. W. WEBB, J. T. NORTON, AND C. WAGNER, *This Journal*, **103**, 107 (1956).
15. S. GLASSTONE, K. LAIDLER, AND H. EYRING, "Theory of Rate Processes," McGraw Hill Book Co., New York (1941).
16. R. FOWLER AND E. A. GUGGENHEIM, "Statistical Thermodynamics," p. 429, Cambridge (1949).
17. J. K. ROBERTS, *Proc. Roy. Soc.* (London), **A152**, 445 (1935).
18. J. P. BAUR, D. W. BRIDGES, AND W. M. FASSELL, JR., *This Journal*, **103**, 266 (1956).

Inhibition of Iron Dissolution in Acid Solutions

CECIL V. KING AND ERIC RAU[1]

Department of Chemistry, New York University, New York, New York

ABSTRACT

The inhibition of iron dissolution from rotating cylinders has been studied in solutions of dilute hydrochloric or perchloric acid with excess nitrate as depolarizer. No better over-all oxidizing inhibitor than dichromate was found. Complexing and chelating agents greatly improve protection by dichromate in hydrochloric acid although they simultaneously shift the iron potential in the anodic direction. Iron is protected better by dichromate alone in perchloric acid; chelants tend to make the potential more cathodic, but shorten the time of protection.

Neocupferron, which forms insoluble chelate salts with iron ions, protects iron for many hours in these solutions. Carbon monoxide was studied as an adsorption inhibitor.

INTRODUCTION

Iron does not dissolve rapidly in dilute acids because hydrogen is not evolved freely on the pure metal. Maximum dissolution rates are attained with a suitable depolarizer; with excess nitrate present the dissolution rate can be that of convective-diffusive transport of acid to the metal surface (1). With 0.02M HCl, 0.06M KNO_3 as a representative corroding solution, addition of 0.01M $K_2Cr_2O_7$ reduces the weight loss in a 5-min run by 90% (2). Further addition of 0.01M sodium fluoride inhibits completely for 5 min, and various complexing and chelating agents aid in dichromate protection for a longer time (3). Eventually iron develops pits and corrodes rapidly in these solutions; zinc can be protected for a longer time.

The purpose of the present research was to investigate inhibition in solutions of this type (0.02M HCl, 0.06M KNO_3) in more detail. Inhibition is always due to some kind of protective film, which may be a comparatively thick layer of oxide or other insoluble compound, or a simple adsorbed film, monolayer or even less in coverage. In the solutions mentioned, any defection shows up quickly in terms of weight loss and pitting of the surface. Especial attention was given to a search for inorganic oxidizing inhibitors other than dichromate, to the role of chelating agents, to the effect of chloride ion, to weight gains as evidence of thick films, to the role of adsorption vs. insoluble compounds, and to the effect of some of the reagents on the potential of iron.

EXPERIMENTAL

Cylinders of SVEA Metal[2] 2.5 cm long and about 1.8 cm in diameter were mounted on a motor shaft with the ends protected. Rotation was adjusted with a calibrated stroboscope to give a peripheral speed of 15000 cm/min. Runs were made at room temperature, which varied from 20° to 30°C, but care was taken to run any comparable series at the same temperature ±1°C. Solution *p*H was measured, where mentioned, with a Beckman meter. Potentials were measured with a Student type potentiometer; contact to the rotating cylinder was made through the motor shaft with a carbon brush or a mercury cup. A commercial KCl-saturated calomel cell (S.C.E.) served as reference electrode. Corrosion was followed by weighing the cylinders to 0.1 mg.

The metal surface was prepared by polishing with progressively finer silicon carbide papers, ending with No. 600. The final surface was as free of flaws and pits (left from previous runs) as possible and was scanned carefully with a low-power microscope. Other polishing procedures are described later. In a series of runs in the same solution the cylinder was not repolished unless this is mentioned.

Oxidizing agents.—Several inorganic oxidizing agents were tried for comparison with dichromate, with iron and with zinc and cadmium cylinders of the same size. Table I gives results for the most effective concentrations which left the *p*H not above 2.

Permanganate left a loose film of oxide which was easily wiped off, leaving the metal stained. Arsenate and arsenite left a brown or black coating, probably elementary arsenic. Sodium fluoride did not improve inhibition except with dichromate.

Various combinations of arsenate, arsenite, and dichromate resulted in less than 1 mg weight loss in 5 min (for example, 0.004M Na_3AsO_4, 0.004M $K_2Cr_2O_7$, loss 0.5 mg). Longer runs led to rapid corrosion through pitting. The iron surface was examined under a low-power microscope and the number of pits per unit area (field of view, about 0.3 mm^2) counted. Before immersion an average of 3 spots which might be incipient pits was found. After a 5-min run an average of 67 pits was found in the field; this number did not increase as corrosion continued.

Complexing agents.—Attention was now turned to the effect of complexing and chelating agents with dichromate on iron. This is an extension of previous work (3); more care was taken to keep the *p*H near 2. Results are summarized in Table II. Weight gains are indicated as negative weight losses, and were checked with several runs. When such runs were continued for a longer time, weight losses usually continued at about the same rate for a while, then turned sharply upward as pitting became evident; or weight gains reached a maximum, then decreased with

[1] Present address: Bettis Plant, Westinghouse Electric Corp., Pittsburgh 30, Pa.

[2] Iron from Swedish Iron and Steel Co., stated to contain 0.02–0.05% C, less than 0.01% each of Mn, Si, and P, and less than 0.015% S.

TABLE I. *Effect of oxidizing agents in* 0.02M HCl, 0.06M KNO_3, 250 *ml solution, peripheral speed* 15000 *cm/min*

Oxidizing agent	Weight loss, mg in 5 min		
	Fe	Zn	Cd
None	65	75	123
0.01M $K_2Cr_2O_7$	5.7	5	7
0.01M $KClO_3$	67	84	73
0.007M NH_4VO_3	8	40	90
0.02M $KMnO_4$	3.7	2.3	4.9
0.01M Na_3AsO_4	1.7	29	40
0.01M $NaAsO_2$	1.1	33	29

TABLE II. *Inhibition of iron corrosion by dichromate and complexing agents*

0.02M HCl (except as specified), 0.06M KNO_3, 0.01M $K_2Cr_2O_7$, 250 ml, 15000 cm/min

Complexing agent	*p*H	Weight loss, mg in 5 min
None	1.8	5.7
0.01M glycine	2.0	0.7
0.005M nitrilotriacetic acid	1.8	2.4
0.01M nitrilotriacetic acid	1.8	−0.7
0.011M 1,10-o-phenanthroline	2.0	−0.9
0.008M Versen-ol*, 0.04M HCl‡	2.0	2.1
0.01M Quadrol†, 0.03M HCl‡	2.1	0.7
0.013M α,α' dipyridyl, 0.03M HCl‡	2.0	−0.3

* Trisodium *N*-hydroxyethylethylenediaminetriacetate Bersworth Chemical Co. (now Versenes Incorporated).

† *N,N,N',N'*-tetrakis (2-hydroxypropyl) ethylenediamine, Wyandotte Chemicals Corp.

‡ Part of the HCl is neutralized.

obvious pitting. It was necessary to abrade the cylinder enough to remove all pits between runs; otherwise early breakdown usually occurred.

The *o*-phenanthroline developed a yellowish film on the iron surface. After longer runs, a zone of interference colors was observed at each pit, widest at the pit and trailing out to a tip behind the pit. Evidently some ferrous ion is carried within the hydrodynamic boundary layer for a short distance before precipitating on the metal surface.

Table III gives details of two longer runs with dipyridyl. After pitting became pronounced in the first run the cylinder was repolished and immersed in the same solution (2nd run). It is evident that the surface condition, not solution depletion, is responsible for inhibition breakdown.

Pitting did not occur at random, but preferentially along certain abrasion marks. It was possible to photograph the same spot before and after a run as shown in Fig. 1; the area is about 0.4 x 0.6 mm. The behavior suggested that a smoother surface might result in better protection, and various procedures were tried as shown in Table IV. A high polish was obtained with rouge on a damp cloth, leaving only traces of the abrasion marks. The chemical etch was in 0.02M HCl, 0.06M KNO_3, and removed about 3 μ of iron.

It has been reported that even light abrasion of iron may result in a surface temperature as high as 900°C (4). In an attempt to avoid the resulting air oxidation the iron was electropolished in a perchloric acid-acetic anhydride solution (5) with an aluminum beaker as cathode. After several trials most of the cylinder came out well polished. On rinsing and starting to dry, flash oxidation of the surface often took place, interference colors spreading across the

TABLE III. *Inhibition breakdown in* 0.05M HCl, 0.06M KNO_3, 0.01M $K_2Cr_2O_7$, 0.032M *dipyridyl* 250 ml, 15000 cm/min, *p*H 2.05

Time, min	Weight loss, mg	
	1st run	2nd run
5	0	−0.5
10	0.1	−0.5
20	−0.1	−0.1
30	0.2	−0.2
60	0.2	−0.2
120	1.1 pitted	1.2 pitted

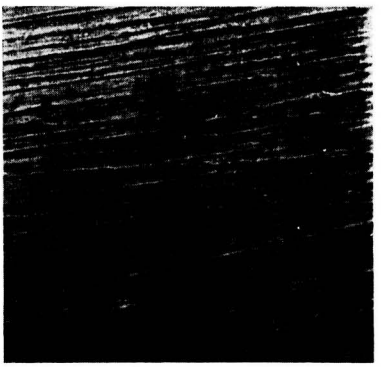

FIG. 1*a*. Abrasion marks on iron cylinder before immersion

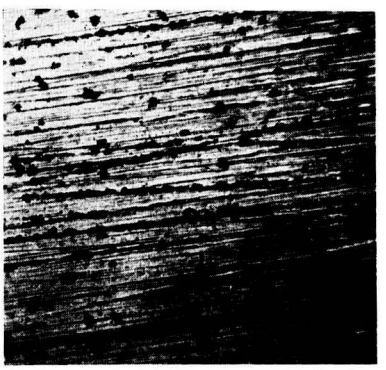

FIG. 1*b*. Preferential pitting along certain abrasion marks after 30 min in inhibited solution.

TABLE IV. *Effect of surface preparation in* 0.04M HCl, 0.06M KNO_3, 0.01M $K_2Cr_2O_7$, 0.012M *dipyridyl* 250 ml, 15000 cm/min, *p*H 2.0

Treatment	Weight loss, mg in 5 min	Time to appearance of pits, min
No. 600 SiC paper	0	240
Rouge polish	0.1	210
Chemical etch	0.1	270
Electropolish	16.7	—

TABLE V. *Effect of pH on iron inhibition* HCl, 0.06M KNO_3, 0.01M $K_2Cr_2O_7$, 0.013M dipyridyl, 250 ml, 15000 cm/min

pH	Weight loss, mg, 30 min	pH	Weight loss, mg, 30 min
5	0	2.1	−0.4
4	0.5	2.0	−0.4
2.9	1.4	1.9	9.1
2.5	2.0	1.8	11
2.2	0.5	1.5	25

TABLE VI. *Protection time with pH less than* 2, 0.06M KNO_3, 0.01M $K_2Cr_2O_7$, 15000 cm/min

Complexing agent	Breakdown time, min	
	HCl	$HClO_4$
None	Immediate	330
0.004M Versen-ol	120	210
0.01M glycine	240	240
0.013M dipyridyl	240	90

cylinder, with enough heat to produce bursts of steam. Eventually, after electropolishing, the cylinder was immersed in a Versene solution for an hour, washed, and dried without developing evident heat; no doubt this only results in a thinner oxide film. The electropolished iron was always much more active than other samples; the initial film is important in protection.

Although inhibition wih dichromate and dipyridyl does not depend on a visible compound on the iron surface, a precipitate formed throughout the solution 15–30 min after the start of each run, and was identified as the dichromate salt of the ferrous-dipyridyl complex. Neither dipyridyl nor the other complexing agents previously mentioned inhibited in the absence of dichromate. Dipyridyl was found to have a maximum effect at *p*H 2.0–2.1 as shown in Table V (the *p*H was adjusted with additions of concentrated acid).[3]

Perchloric acid.—Many experiments similar to the above were carried out with perchloric acid and potassium nitrate, with the addition of dichromate and various complexing agents. Dichromate alone proved to be the best inhibitor; there were weight gains up to 1.2 mg in the first 5 min and no weight loss for about 5 hr. The chelants all decreased the time at which pitting became pronounced and rapid corrosion set in. Table VI compares breakdown times in HCl and $HClO_4$.

Potentials.—All potential measurements were made in deaerated solutions. The rotating iron cylinder was immersed in 100 ml of solution contained in a square bottle with neck only slightly larger than the cylinder and the motor shaft sleeve. The bottle had two holes, one for a nitrogen tube, the other for a KNO_3-agar bridge. Nitrogen was passed over hot copper, through water, and through the reacting solution for 30 min before, and during, the run.

Potentials of iron vs. the S.C.E. in HCl solutions are shown in Fig. 2. In HCl-KNO_3 (curve A) the potential

[3] Actually, the effect of dipyridyl was not examined at the higher *p*H values. In the range 3–1.5, dichromate alone allows weight losses similar to those in Table I, or greater.

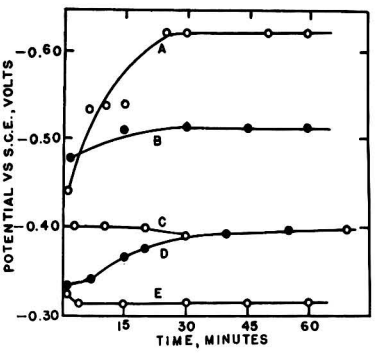

FIG. 2. Potential of iron as function of time. All solutions contain 0.02M HCl and the following additions: A, 0.06M KNO_3; B, acid alone; C, 0.06M KNO_3, 0.01M $K_2Cr_2O_7$, 0.01M dipyridyl; D, 0.06M KNO_3, 0.01M $K_2Cr_2O_7$, 0.01M glycine; E, 0.06M KNO_3, 0.01M $K_2Cr_2O_7$.

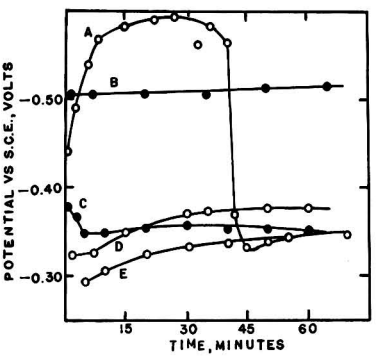

FIG. 3. Potential of iron as function of time. All solutions contain 0.02M $HClO_4$ and the following additions: A, 0.06M KNO_3; B, acid alone; C, 0.06M KNO_3, 0.01M $K_2Cr_2O_7$; D, 0.06M KNO_3, 0.01M $K_2Cr_2O_7$, 0.013M dipyridyl; E, 0.06M KNO_3, 0.01M $K_2Cr_2O_7$, 0.01M glycine.

rises rapidly in the anodic direction because of the rapid corrosion. In HCl alone (curve B) the anodic drift is slow, but when corrosion has proceeded to the same extent (after several hours) the potential is similar to that with the depolarizer. Dichromate makes the iron slightly noble with respect to a hydrogen electrode in the same solution. The chelants partly reverse this effect.

In perchloric acid (Fig. 3) there are two noteworthy features. In $HClO_4$-KNO_3 the potential changes 0.25 v in the cathodic direction when the *p*H reaches 4.5; and chelants make the initial potential more cathodic than dichromate alone, although this effect disappears in time.

In acid alone a greenish coating formed on the cylinder when the solution *p*H became 4–4.5; this was probably ferrous hydroxide since the solution gave no test for ferric ion. With nitrate present a brown coating appeared at about the same *p*H (but in much shorter time); this was no doubt hydrated ferric oxide, and the solution contained ferric ions. In HCl the coating was nonadherent and slow corrosion continued; in $HClO_4$ it was adherent and corrosion was arrested, small weight gains being noted. The

TABLE VII. *Inhibition by neocupferron in air-saturated solutions*
0.02M HCl, 0.06M KNO_3, 100 ml, 15000 cm/min

Neocup.	Time, min	Weight loss, mg	Neocup.	Time, min	Weight loss, mg
0.001M	5	36	0.01M	10	−6.6
0.001	5	−0.4		60	−7.9
	10	27		1170	−8.3
0.002	5	0		2700	−4.3
	16	−0.1		2960	4.5
	31	4.7		3000	12
	36	25	0.01*	5	−1.6
0.005	5	−1.0		100	−1.8
	15	−1.1		260	−0.7
	75	−0.7		500	1.8
	330	−0.8		555	4.4
	1170	27			

* Wiped with acetone at each weighing.

coating appeared at the same time as the large change in potential.

Neocupferron.—It was found previously (3) that cupferron (the ammonium salt of nitrosophenylhydroxylamine) protects iron with an insoluble film. The acid form of cupferron is not very stable. Neocupferron (the ammonium salt of nitrosonaphthylhydroxylamine) is more stable in acid solution and forms even less soluble chelated ferrous and ferric salts (6). Consequently it was investigated as an inhibitor.

The commercial salt was recrystallized twice by dissolving in water, filtering, and evaporating the solution to dryness under vacuum at room temperature. Solutions were made by dissolving weighed samples in potassium nitrate and adding the acid last. With 0.01M neocupferron this resulted in a small amount of white precipitate (the acid form), which soon dissolved when the run was started. The compound did not change the *p*H appreciably.

Table VII shows details of some runs. At low concentrations protection is uncertain and lasts only a short time. With 0.01M neocupferron protection was obtained up to 50 hr. Addition of glycine, dipyridyl, or fluoride had little, if any, effect. The neocupferron becomes oxidized eventually and too little is left for protection; by replacing the solution each 40 hr one run (actually with 0.01M dipyridyl, which was unnecessary) was kept going for 132 hr with a weight loss of 6 mg.

Yellow films, streaked with brown oxidation products, formed on the iron in these solutions. The films could be wiped off with acetone or benzene, leaving the iron bright and shiny. It was noted that the visible film contributed practically nothing to the weight gains, but, if dissolved off frequently, the time of protection was decreased. If a cylinder which had formed a film was run in the corroding solution without neocupferron, protection broke down in about an hour.

Since neocupferron is lost by air oxidation, further experiments were run in solutions deaerated with nitrogen. Some results are shown in Table VIII. Two observations stand out: protection was always for a shorter time than in air (10 hr compared to 50 hr), and the visible yellow film contributed most or all of the weight gain. On wiping with acetone or benzene there was usually a net weight loss, in contrast to the experiments in air, where such wiping did not decrease the weight as much as 0.1 mg.

The best protection by neocupferron required rotation of the cylinders. The following experiment is informative: a cylinder was immersed (0.01M neocupferron, air) for 30 min with no rotation. About 40% of the surface was covered with visible film, in wedges, apex up, and the cylinder had lost 5 mg. The cylinder was now rotated at 15000 cm/min for 5 min. The entire surface was covered with film, but areas previously covered were clearly visible, with more new film on the leading than on the trailing edges; the iron had gained 2 mg. On standing still in the solution for 24 hr, the trailing edges of the wedge-shaped areas were badly pitted. Net weight loss was 5 mg. Fig. 4 is a photograph of this cylinder and the lower third shows the typical appearance. The white portions are corroded; black spots are resinous oxidation products.

These experiments indicate that iron dissolves at anodic spots and the ferrous ion precipitates some distance away. As a further test an iron disk 1.8 cm in diameter was given a very smooth machine polish, and inhibited solution was forced in a fine stream onto the center of the smooth surface. Corrosion took place at the impact point and a film built up around it, getting thicker toward the edges.

Other possible inhibitors.— The ammonium salt of nitroso-

TABLE VIII. *Inhibition by neocupferron in deaerated solutions*
0.02M HCl, 0.06M KNO_3, 100 ml, 15000 cm/min

Neocup.	Time, min	Weight loss, mg	Neocup.	Time, min	Weight loss, mg
0.005M	10	−0.9	0.01M	15	−3.0
	60	−1.9		90	−5.8
	100	−2.3		290	−7.2
	300	−2.5		525	−11.6
	390	−2.3		585	−6.4
	Pitting			Pitting	

FIG. 4. Corrosion along trailing edge of initially protected area.

TABLE IX. *Inhibition of iron corrosion by carbon monoxide*
0.02M HCl, 0.06M KNO_3, 100 ml, 15000 cm/min

Time, min	Weight loss, mg				
	1	2	3	4	5
60	0.2	—	7.6	1.4	0.7
120	0.6	5.4	10.3	—	1.5
180	0.8	—	12.5	4.3	2.1
240	1.0	7.4	—	—	3.5
300	—	9.0	16	—	—
600	—	—	21	9.9	—

fluorenylhydroxylamine has been reported useful in analysis (7). A sample was prepared[4] and tested, but found ineffective, perhaps because the compound is only slightly soluble in water.

Stearato chromic chloride (8), tricresyl phosphate, heptacosafluorotributylamine, perfluorodecanoic acid (9) form water-repellent coatings on many materials. These were tried as corrosion solution additives (saturated solution with excess) and for surface treatment of iron, zinc, and cadmium cylinders before immersion. None was successful as an inhibitor.

Carbon monoxide.—It has been shown by Uhlig (10) that carbon monoxide is a good inhibitor for stainless steel, fair for mild steel, in moderately concentrated HCl with no depolarizer. Runs were now made in which carbon monoxide was bubbled through the corroding solution (0.02M HCl, 0.06M KNO_3) in which the iron cylinder was rotated. The commercial CO contained a little iron carbonyl, which was caught in a dry-ice trap. Some of the results are shown in Table IX.

No weight gains were ever noted. The exact amount of corrosion must depend on accidental factors. In run 5 the cylinder had a preliminary etch; in run 3 it was kept in CO gas 20 min before immersion. No other treatments were more effective. Pitting became evident in all runs but not at a reproducible stage of time or weight loss. The total dissolving capacity of these solutions is about 50 mg of iron, and without carbon monoxide this amount would dissolve in about 30 min, whether in air or nitrogen.

Discussion

It is evident that, in all the experiments with dichromate, protection is accompanied by the formation of comparatively thick oxide films. The electropolishing experiments emphasize the fact that iron, exposed to air, is always covered with an oxide film, formed with evolution of heat. Such air-formed films are not protective in acid solution; this has been ascribed to weak spots or flaws in the film. Most forms of Fe_2O_3 do not dissolve readily in acids, but, if in contact with iron, reductive dissolution may occur more rapidly. According to Pryor and Evans (11), ferric oxide is a sufficiently good electronic conductor to function as cathode in the cell $Fe/acid/Fe_2O_3$; the oxide is reduced simultaneously with iron dissolution at the anodes. For best protection the oxide film must be continuous and be replaced as fast as it dissolves. If unprotected pits are present and function as anodes, they will lead eventually to uncontrollable corrosion.

[4] Courtesy of T. Kaniecki, New York University.

The iron cylinders of 14 cm^2 area gained as much as 1.2 mg in weight in the first 5 min in $HClO_4$-KNO_3-$K_2Cr_2O_7$ solutions. This indicates a film of Fe_2O_3 about 5×10^{-5} cm thick if no ferrous or ferric ion escaped into solution. The weight gain persisted for several hours before pitting resulted in a net weight loss. Investigators of the Evans school believe that oxidizing inhibitors tend to repair flaws in the oxide film and at the same time thicken the good film as iron ions migrate through from the underlying metal. Unfortunately only a few oxidizing agents are effective. Chromate and dichromate are perhaps the best; oxygen can inhibit in neutral and alkaline solution if its concentration is high enough. Molybdate and tungstate are somewhat effective (12) but offer difficulties in acid solution (2). The reduction products of permanganate, arsenite, and arsenate offer only porous mechanical barriers.

A comparison of the experiments with hydrochloric and perchloric acids is significant. Complexing or chelating agents are essential to make dichromate an effective inhibitor with hydrochloric acid. It was suggested previously (3) that complexing agents dissolve loose precipitates or prevent their formation, allowing dichromate to reach the clean metal surface. Chloride ion apparently prevents the formation of large continuous crystals of oxide film, so that the cleaning process is necessary in its presence. The "peptizing" effect of chloride ion in such cases has been discussed by Gatty and Spooner (13).

In perchlorate solutions the dichromate can form much larger crystals or aggregates of "good" oxide film. Now complexing agents can dissolve "good" oxide as well as loose material, although at a slower rate. They limit the protective time before pits become pronounced to about the same value in both acids, by creating new weak spots or preventing really good coverage of old ones. In hydrochloric acid chelants make the iron more anodic while helping protect it (Fig. 2), which indicates more rapid ion exchange and electron flow through a film which still allows less dissolution than that formed by dichromate alone. Chelants tend to make the initial potential in perchloric acid more cathodic, which may indicate a slightly better initial film. This effect disappears as the breakdown time approaches (Fig. 3). It has been noted by Cohen (14) that in inhibited neutral or slightly alkaline solutions certain chelants make the iron potential more anodic and increase the corrosion rate.[5]

In acid alone the iron potential becomes more negative with time until ferrous hydroxide (or perhaps a ferrous-ferric mixture or compound) is formed on the surface. This occurs at a bulk *p*H of 4–4.5 and a ferrous ion concentration near 10^{-2}M. The potential is about −0.36 v on the hydrogen scale, and according to the potential-*p*H diagrams prepared by Pourbaix (15) for $Fe\text{-}Fe(OH)_2$ equilibrium at this potential the surface *p*H should be 6.5–7. It is not unlikely that a *p*H gradient exists through the film since slow corrosion continues.

With nitrate present, the potential changes sharply in the anodic direction since hydrogen evolution is eliminated

[5] Most chelants are more effective at higher *p*H; in acid solution the metal ion must compete with H^+ for the chelant K: HK (or HK^+) + $M^+ \rightleftharpoons MK + H^+$.

as the cathodic process and the local anodes are depolarized. Ferric hydroxide is formed when the bulk *p*H rises to 4 or 4.5. With chloride present there is no protective film, corrosion continues, and the potential remains far away from the $Fe\text{-}Fe(OH)_3$ equilibrium value. In perchloric acid the potential changes to a value which corresr onds to this equilibrium if the surface *p*H is about 6 (15). Small weight gains were noted at this point.

Dichromate converts the potentials to slightly noble values. The potential for reversible hydrogen evolution is −0.37 v at *p*H 2 and −0.49 v at *p*H 4 (vs. the S.C.E.). The reversible iron-ferrous ion potential is about −0.75 v with a low concentration of ferrous ion; the anodic process is very highly polarized in all the inhibited systems.

Neocupferron.—It has been suggested that chelants, molecules which have two or more points of attachment to metal ions, may be especially good adsorption inhibitors (16). Neocupferron forms very insoluble chelate salts with both ferrous and ferric ions, but does not inhibit by adsorption; iron must dissolve, then form the insoluble complex. If the neocupferron concentration is high enough the solubility is exceeded very near the iron surface, and it is probable that nucleation occurs more readily on the iron than in the solution.

The film formed in air-saturated solution consists of two layers, an outer yellow one which is very thin, since it does not contribute appreciably to the weight gain, and an inner invisible film which must consist at least partly of iron oxide formed by oxygen under the protection of the yellow film. This oxide may be quite porous and plugged by neocupferron compound, since the weight gain is large for oxide alone; but the appearance is that of shiny iron. In deaerated solution such oxidation cannot take place and the yellow film is thicker. If frequently removed and the cylinder re-immersed the film forms again, but not as heavily, until the neocupferron is exhausted.

Weight gains found in the deaerated solutions are plotted in Fig. 5 against the square root of time. While the data are meager, they seem to indicate an initial parabolic film growth law (17), with later deviations due to partial disintegration of the films.

Carbon monoxide.—This compound fulfils the requirements stated by Uhlig for an adsorption inhibtior (18). It is strongly chemisorbed on iron (19, 20) but reacts only very slowly to form carbonyl, which is probably not stable in the acid solutions (21). The carbon monoxide molecule most likely has a pair of electrons strongly directed away from the carbon-oxygen bond (22), which should facilitate adsorption on a metal with unfilled electron levels. Carbon monoxide is not adsorbed on zinc and does not inhibit zinc dissolution. It should be noted that neither the rather high heat of adsorption (20) nor the "Lewis base" electrons are necessary for adsorption or inhibition. Other gases with equal or greater adsorption enthalpy are not inhibitors, while substances adsorbed by electrostatic or van der Waals forces are (16). However, other molecules with "lone-pair" electrons such as nitric oxide NO are suggested as possible inhibitors.

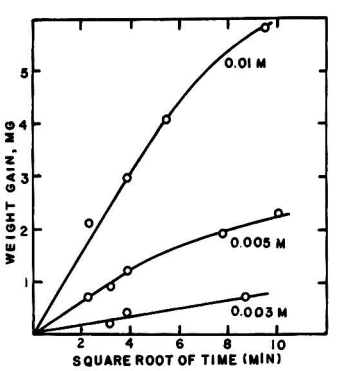

FIG. 5. Weight of film on iron with neocupferron concentrations as shown.

Carbon monoxide is not completely effective, i.e., there is no complete lack of weight loss for even short periods of time. This is generally true of pure adsorption inhibitors. It is not known whether this is due to insufficient solubility of CO at atmospheric pressure, or to inability to be adsorbed on and protect certain areas (which show up as pits and are anodic in nature). The latter is probably the correct reason.

It has been shown by Cartledge (22) that pertechnetate ion is an exceptionally good inhibitor for steel in water, as little as 5×10^{-5}M $KTcO_4$ stopping corrosion in aerated distilled water. With such low concentrations the protection has to be due to adsorption or coverage of only a few active spots, but it was shown that less than 1% of a monolayer is actually adsorbed or deposited. Probably no prediction can be made as to inhibition by the pertechnetate ion in the acid solutions of the present research.

Manuscript received October 21, 1955. This paper was prepared for delivery before the San Francisco Meeting, April 29 to May 3, 1956, and taken from a Ph.D. thesis submitted by Eric Rau to the Graduate Faculty of New York University. Work done under Office of Ordnance Research Contract No. DA-30-069-ORD-1113.

Any discussion of this paper will appear in a Discussion Section to be published in the December 1956 JOURNAL.

REFERENCES

1. M. B. ABRAMSON AND C. V. KING, *J. Am. Chem. Soc.*, **61**, 2290 (1939).
2. C. V. KING, E. GOLDSCHMIDT, AND N. MAYER, *This Journal*, **99**, 423 (1952).
3. C. V. KING AND E. HILLNER, *ibid.*, **101**, 79 (1954).
4. R. P. AGARWALA AND H. WILMAN, *Proc. Phys. Soc. (London)*, **66B**, 717 (1953).
5. G. KEHL, "The Principle of Metallographic Practice," McGraw-Hill Book Co., New York (1949).
6. G. F. SMITH, "Cupferron and Neocupferron," G. Frederick Smith Chemical Co., Columbus, Ohio (1938).
7. R. E. OESPER AND R. E. FULNER, *Anal. Chem.*, **25**, 908 (1953).
8. R. K. ILER, *Ind. Eng. Chem.*, **46**, 766 (1954).
9. F. SCHULMAN AND W. A. ZISMAN, *J. Am. Chem. Soc.*, **74**, 2123 (1952).
10. H. H. UHLIG, *Ind. Eng. Chem.*, **32**, 1490 (1940).
11. M. J. PRYOR AND U. R. EVANS, *J. Chem. Soc.*, **1950**, 1259.
12. W. D. ROBERTSON, *This Journal*, **98**, 94 (1951).
13. O. GATTY AND E. SPOONER, "Electrode Potentials of Corroding Metals," Oxford Press (1938).
14. M. COHEN, Paper presented at Pittsburgh Meeting of The Electrochemical Society, October, 1955.
15. M. J. N. POURBAIS, "Thermodynamics of Dilute

Aqueous Solutions," Edward Arnold and Co., London (1949).
16. N. Hackerman and A. C. Makrides, *Ind. Eng. Chem.*, **46**, 523 (1954).
17. H. H. Uhlig (Editor), "Corrosion Handbook," John Wiley & Sons, Inc., New York (1948).
18. H. H. Uhlig, *Ann. N. Y. Acad. Sci.*, **58**, 843 (1954).
19. P. H. Emmett and S. Brunauer, *J. Am. Chem. Soc.*, **59**, 310 (1937).
20. J. Bagg and F. C. Tompkins, *Trans. Faraday Soc.*, **51**, 1071 (1955).
21. J. R. Partington, "General and Inorganic Chemistry," p. 876, Macmillan and Co., London (1949).
22. C. A. Coulson, "Valence," Oxford Press, New York (1932).
23. G. H. Cartledge, *J. Am. Chem. Soc.*, **77**, 2659 (1955); *Corrosion*, **11**, 335t (1955); *J. Phys. Chem.*, **59**, 979 (1955).

Electrical Conductivity of Carbon Black-Reinforced Elastomers

Gerard Kraus

Research Division, Phillips Petroleum Company, Bartlesville, Oklahoma

and

J. F. Svetlik

Rubber Chemicals Division, Phillips Chemical Company, Akron, Ohio

ABSTRACT

Electrical conductivity of carbon black-reinforced elastomers at fixed loading is a function of the particle size and aggregation habit of the carbon black, its intrinsic conductivity, and the ability of the black to adsorb certain ionic impurities. These factors vary greatly in their relative importance, depending on the filler concentration. The mechanism of conduction is primarily one of carbon black chain formation. Experimental evidence suggests the existence of a small number of highly conductive paths consisting of rather large black aggregates in contact in addition to a fine network of carbon black chains formed by otherwise well-dispersed black. Electrical conductivity data supporting the above conclusions are presented for nine carbon blacks in GR-S, natural, and butyl rubbers.

Introduction

One of the many interesting characteristics of carbon black-reinforced elastomeric compounds is their unique electrical behavior which makes it possible to vary their electrical conductivity over a 10^{12}-fold range while maintaining their useful mechanical properties. This enormous change in conductivity is brought about simply by the choice of the type and volume loading of carbon black.

It is generally accepted that the electric current is carried by continuous chains of contacting carbon black particles and, indeed, all published experimental evidence is consistent with this view (1–6). There are, however, a number of effects associated with the conductivity behavior of rubber vulcanizates which are still far from being completely understood. These include a rather surprising increase in resistivity accompanying the addition of the first small amount of carbon black to the rubber compound, the existence of a well-defined threshold loading for incipient conductivity, dependence of conductivity on the dimensions of the test specimen, and the role of the intrinsic conductivity of the carbon black. The present investigation was undertaken with the objective of contributing toward a better understanding of some of these phenomena.

Experimental

The GR-S, natural rubber, and butyl rubber compounds included in this investigation were formulated according to the following basic recipes. The black level was varied while all other ingredients in each formulation were held constant:

GR-S-101	100	—	—
Hevea (No. 1 Smoked sheet)	—	100	—
GR-I-17	—	—	100
Carbon black	Variable	Variable	Variable
Zinc oxide	3	4	5
Stearic acid	—	3	1
Sulfur	1.75	2	2
Santocure[a]	1.10	0.5	—
Tuads[b]	—	—	1
Captax[c]	—	—	1

[a] *N*-cyclohexyl-2-benzothiazyl sulfenamide; [b] Tetramethylthiouram disulfide; [c] Mercaptobenzothiazole.

GR-S-101 is a 75/25 copolymer of butadiene and styrene of 48 Mooney viscosity, polymerized in a sugar-free recipe

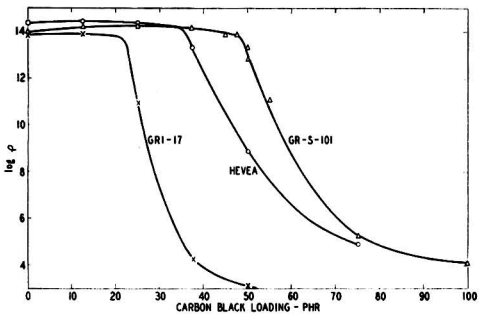

FIG. 1. Electrical resistivity as a function of filler loading FEF black (Philblack A).

at 5°C. GR-I-17 is a standard butyl rubber of 1.5% unsaturation. The carbon blacks investigated represent a fairly complete cross section of commercial rubber-grade carbons. They are identified by the standard carbon black type symbols: FT—fine thermal, SRF—semireinforcing furnace, FEF—fast extrusion furnace, HAF—high abrasion furnace, EPC—easy processing channel, SAF—super abrasion furnace. For convenience their trade names have been listed in parentheses. Graphon from Godfrey L. Cabot, Inc., is a carbon derived from graphitization of channel black by heating for 2 hrs at 2700°-3000°C; it is not a commercial rubber black. For a summary of physical and chemical properties of these blacks see reference (7).

All rubber compounds were mixed on a 6 x 12-in. roll mill with a friction ratio of 1.4 to 1. Experimental 6 x 6 x 0.075-in. slabs were vulcanized for 45 min at 153°C.

The electrical resistivities reported in this paper are all for direct current. The apparatus employed in the determination of the resistivity utilized an electrode with a guard ring of the type recommended in standard procedures for measuring dielectric constant (8). All of the highly resistant stocks were tested at an impressed voltage of 45 volts using a feedback microammeter arrangement similar to the one described by Roberts (9) to measure current flow from which the specific resistivity was calculated. The resistivity of more conductive stocks was determined with a direct reading ohmmeter (VOMAX, Model 900).

To decrease contact resistance the surfaces of the slabs were painted with a dilute graphite (Aquadag) paint. The entire surface on one side was covered; on the other side only an area corresponding to the size of the test electrode was painted with the Aquadag. Testing was conducted under a load of 1.75 psi to insure good contact between the electrode and rubber specimen. Two test electrodes were used having areas of 5 and 20 cm^2, respectively. The small electrode was used only in the experiments concerned with resistivity fluctuations over the face of a test slab.

Sections of rubber stocks for microscopic examination were prepared by embedding small slivers of rubber in an 80/20 mixture of *n*-butyl and methyl methacrylates, polymerized *in situ* using 2,4-dichlorobenzoyl peroxide as initiator. Polymerization time was usually about 8 hr to produce a hard resin suitable for cutting on a Minot Ultra Thin Sectioning microtome employing a glass knife. Sections were cut one micron thick, straightened by floating on water, and transferred to the microscope slides.

Magnetic susceptibilities of carbon blacks were determined by the Gouy method (10).

RESULTS AND DISCUSSIONS

A set of typical resistivity vs. carbon black-loading curves is shown in Fig. 1. At small black loadings the resistivity is of the same order of magnitude as for the gum vulcanizates. Beyond a certain point the resistivity begins to change abruptly, falling several decades on addition of only a small increment of carbon black. This threshold loading is different for each rubber; it will be seen that it is also characteristic of the carbon black. Resistivity-loading curves eventually level out to values determined to a considerable extent by the carbon black. It is convenient to divide the conductivity curve into three distinct sections: (*a*) the range between zero loading and the threshold loading, covering all electrically insulating stocks; (*b*) a transition range extending over the large resistivity drop in the vicinity of the threshold loading; and (*c*) the conductive range.

Insulation Range

Table I shows resistivity data for several carbon black-natural rubber combinations below the threshold loading. Similar results are obtained with synthetics. It is apparent that the observed behavior is hardly that expected for a mixture of a conductor and a nonconductor. The electrical conductivity, k, of a random dispersion at low concentration of the disperse phase is given by the classical Maxwell equation:

$$k = k_1 \frac{k_2 + 2k_1 - 2v_2(k_1 - k_2)}{k_2 + 2k_1 + v_2(k_1 - k_2)} \qquad (I)$$

TABLE I. *Electrical resistivity of insulating stocks (Hevea Rubber)*

Carbon black	Specific surface area (m^2/g)		Loading	Resistivity × 10^{14}
	Nitrogen adsorption[a]	Electron microscope		
			phr[b]	*ohm-cm*
None	—	—	—	2.35
FT (P-33[c])	13.7	17	12.5	2.28
			25	2.22
			37.5	2.11
			50	2.26
SRF (Gastex[d])	27.6	35	12.5	2.55
			25	2.23
			37.5	1.98
FEF (Philblack[e] A)	45.6	65	12.5	2.65
			25	2.34
HAF (Philblack[e] O)	75.1	94	12.5	2.83
			25	2.34
EPC (Wyex[f])	114.2	89	12.5	2.50
			25	2.05
Acetylene	58.0	65	12.5	2.72
SAF (Philblack[e] E)	142.6	138	12.5	2.79

[a] Method of Brunauer, Emmett and Teller; *J. Am. Chem. Soc.*, **60**, 309 (1938).
[b] Parts (by weight) per 100 parts of rubber.
[c] From Thermatomic Carbon Co.
[d] From General Atlas Carbon Co.
[e] From Phillips Chemical Co.
[f] From J. M. Huber Corp.

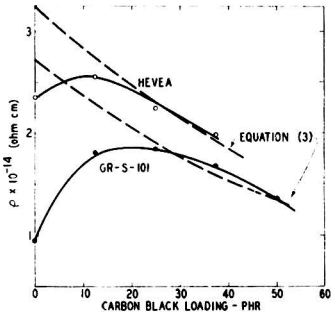

FIG. 2. Resistivity of rubber vulcanizates below the threshold loading SRF black (Gastex).

where k_1 is the conductivity of the continuous phase, k_2 that of the disperse phase, and v_2 the volume fraction of the disperse phase. A recent treatment by Baron (11) which extends the validity of Maxwell's theory to high-volume loadings gives

$$\frac{k - k_2}{k_1 - k_2} = (1 - v_2)\left(\frac{k}{k_1}\right)^{1/3}. \qquad \text{(II)}$$

When $k_2 \gg k_1$, as in the case of carbon black and rubber, equation (II) leads to

$$\rho = \rho_1(1 - v_2)^3 \qquad \text{(III)}$$

where ρ is the resistivity of the mixture and ρ_1 that of the continuous phase.

In almost every instance the resistivity increases initially and then falls (Fig. 2) at a rate roughly of the order predicted by equation (III). The only plausible explanation for such an effect appears to be that carbon black exerts an influence on the resistivity of the rubber matrix itself, possibly through immobilization of trace ionic impurities by adsorption. This view has also been advanced in a recent paper by Kickstein (12). In any event, it seems clear that there can be no continuous conductive paths *extending through the entire sample* at these loadings, for, in this instance, a far more drastic drop in resistivity than predicted by equation (III) would be expected. It also appears that those ionic impurities which are immobilized by the carbon black must be present in minute quantities so that the peak in resistivity is reached at low loadings and is relatively insensitive to the specific surface area of carbon black. Fig. 3 shows that at a loading of 12.5 phr of carbon black the rise in resistivity is related to the specific surface area of the black but levels out at 60 square meters/gram.

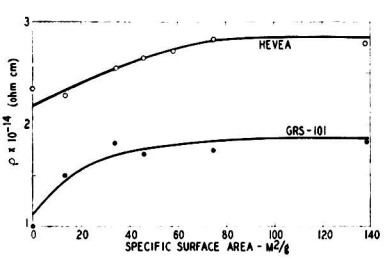

FIG. 3. Resistivity of natural and synthetic rubber stocks containing 12.5 phr of various carbon blacks as a function of specific surface area of the black.

Transition Range

The extremely sharp drop in resistivity at the threshold loading suggests that continuous conductive paths are formed suddenly in great abundance on incorporation of only a small amount of additional black. This sudden formation of a conductive network can only be visualized if the elements of the network are present even below the threshold loading as structures requiring only a relatively small quantity of black to weld them into a continuous maze of carbon chains.

Many carbon blacks show a definite tendency toward forming chain-like aggregates (13). This effect is usually referred to as "structure" (a more appropriate term would be "aggregate structure") and can be estimated by an oil absorption test. The test consists of adding linseed oil slowly to a weighed sample of black until a single ball of stiff paste is obtained. At this point the oil completely fills the space in the interstices between particles. Defining a packing factor γ such that

$$\gamma \equiv Nd^3 \qquad \text{(IV)}$$

where N is the number of particles per unit volume and d their average diameter, it can be shown that

$$\gamma = 6/\pi(1 + A\delta) \qquad \text{(V)}$$

where δ is the density of the black and A is the oil absorption in ml/g. A sort of coordination number (Z) for the black particles can be estimated by calculating γ's for several regular lattices and using the resulting curve to read off the Z-values.

Lattice	Z	γ
Face-centered cubic	12	1.41
Body-centered cubic	8	1.29
Simple cubic	6	1.00
Diamond	4	0.650

The data of Table II were compiled in this manner. Assuming that the coordination of particles is at least *qualitatively similar* in rubber and in oil, it follows that the over-all tendency for chain formation can be expressed as a function of the ratio of the specific surface area to the coordination number. This is so because the total number of particles capable of forming chains increases at a fixed

TABLE II. *Aggregation habit of carbon blacks from oil absorption test*

Carbon black	Oil absorption	γ	Z
	ml/g		
FT (P-33)	0.55	0.940	5.7
SRF (Gastex)	0.81	0.766	4.6
EPC (Wyex)	1.13	0.628	4.0
HAF (Philblack O)	1.14	0.620	3.9
FEF (Philblack A)	1.17	0.613	3.8
SAF (Philblack E)	1.28	0.585	3.6
FEF (Sterling SO)	1.38	0.546	3.4
Acetylene	2.40	0.355	2.2

TABLE III. *Threshold black loadings for incipient electrical conductivity*

Carbon black	S/Z[a]	Approximate threshold loading (phr)		
		GR-S-101	Hevea	GR-I-17
FT (P-33)	3.0	85	72	44
SRF (Gastex)	7.6	75	50	—
FEF (Philblack A)	17.1	49	35	22
FEF (Sterling SO)	19.1	47	30	20
EPC (Wyex)	22.3	30	32	17
HAF (Philblack O)	24.0	37	36	14
Acetylene black	29.6	25	18	5
SAF (Philblack E)	38.4	21	24	12

[a] S = electron microscope surface area.

loading with the specific surface area, and because the size of the aggregates increases with lower coordination number by virtue of their smaller density.

A test of these hypotheses is shown in Table III where the threshold loadings are compared with the ratio of electron microscope surface area to coordination number (S/Z). In general, the threshold loadings tend to vary inversely as the ratio S/Z. Thus, the behavior is consistent with the idea of the merging of black aggregates which are already present below the threshold loading but not in continuous paths through the sample.

Two questions arise: (*a*) can these aggregates be detected by microscopic examination; and (*b*) what is the order of magnitude of the conductivity contributed by one single path (or bundle of paths) formed on contact of these aggregates. The first of these questions may safely be answered in the affirmative. Even stocks of 10^{14} ohm-cm resistivity showed some visual evidence of flocculates under the optical microscope. The second question poses considerably more difficulty. If the average resistance of a continuous path is r and the number of paths per unit area is n, the resistivity of the slab is

$$\rho = r/n \qquad \text{(VI)}$$

as long as the resistivity of the matrix is much larger than r. If n is still relatively small near the threshold loading, one would expect to find considerable fluctuations in the conductivity of small areas tested randomly over the surface of a test slab. On the other hand, the conductivity should not vary greatly with position, both below and above the threshold loading. Table IV shows that at least qualitatively the behavior is as expected. Conductivity measured at different positions of a test slab varies most drastically near the threshold loading. However, even at 80 phr loading of FEF black the spread is appreciable, much more than can be accounted for by a random distribution of paths. Judging by the rather high conductivity at 80 phr loading the number of effective paths must be considerable, if indeed one may still speak of individual paths at all.

It may be shown that a completely random occurrence of paths would lead to the distribution (*see* Appendix)

$$p(x) = \bar{x}^x e^{-\bar{x}}/x! \qquad \text{(VII)}$$

where p is the probability of finding exactly x paths in the electrode area, and $\bar{x}$ is the mean number of paths for an area of the size of the electrode. The standard deviation of this distribution is $\bar{x}^{\frac{1}{2}}$, which means that the relative deviation is $\bar{x}^{-\frac{1}{2}}$. For an $\bar{x}$ of as little as 10 the relative deviation would be only 31.8% which would be reasonable for the spread in conductivities observed with FEF black at 80 phr, but here $\bar{x}$ is undoubtedly much larger than 10. The explanation must lie in the fact that the individual paths vary tremendously in their conductivity, which in turn implies that they must be formed by aggregates of widely different sizes, including some very large ones. In all probability only these largest flocculates are visible under the optical microscope.

It is somewhat peculiar that in the rubber reinforced with 50 phr of FEF black the conductivities deviating most from the mean value are *low*, indicating a deficiency of conductive paths at a relatively few locations. One might be tempted to interpret this as being due to flexing of the slab which might rupture the conductive chains at these points. Although mechanical deformation is known to affect resistivity (1), the effect is not nearly large enough to account for the 600-fold difference observed here (6), particularly since considerable care was taken in handling the slabs to insure freedom from flexing. Local contact resistance likewise appears to be an unlikely cause for the fluctuations in conductivity over the surface of the slab. Contact resistances necessary to account for the observed results appear prohibitively large, and there is no reason to expect extremely large contact resistance to occur locally and only at certain black loadings. It is also apparent from Table IV that in the regions of highest and lowest conductivity the fluctuations hardly exceed the experimental error as required by the theory.

TABLE IV. *Electrical conductivity as a function of position over test slab*

Loading (phr)	m	Conductivity (mho-cm^{-1}) $\times 10^m$											
		Readings at individual positions										Mean	Std. Dev.
FEF black (Philblack A) in GR-S-101; threshold loading—49 phr													
12.5	14	1.31	1.26	1.48	1.30	1.39	1.35	1.09	1.20	1.22	1.11	1.27	0.11
50	11	0.35	2.51	7.80	3.60	8.40	0.051	0.014	0.065	3.76	4.71	3.13	2.99
80	7	3.06	3.92	5.25	4.85	3.94	1.91	2.08	3.36	2.90	2.22	3.35	1.08
SAF black (Philblack E) in GR-I-17; threshold loading—12 phr													
12.5	12	4.00	12.5	0.19	1.26	1.20	3.02	—	—	—	—	3.70	4.13
50	3	1.31	1.49	1.81	1.65	1.63	1.30	1.67	1.88	1.56	—	1.59	0.19

Another point of interest is the rather systematic variation of the threshold loading with the type of rubber. In almost all instances the order of decreasing threshold loading is

$$\text{GR-S-101} > \text{Hevea} > \text{GR-I-17}$$

This behavior suggests an increasing tendency toward chain formation of all blacks in butyl rubber as compared to Hevea and, in particular, GR-S. Evidently the coordination number Z is different for each rubber, which is hardly surprising. It must be remembered that the numerical values of Z given in this paper are for linseed oil and can therefore only serve to compare trends between blacks. They allow no comparison between different media.

Conductive Range

As the carbon black loading is raised to higher levels and the number of conductive paths becomes very large, the intrinsic conductivity of the carbon black exerts a noticeable influence on the conductivity of the rubber compound. At the same time particle size and aggregation habit are still important variables. The inability to control these last two variables completely makes it extremely difficult to demonstrate the intrinsic conductivity effect clearly. One example in which a comparison is possible is that of channel and furnace blacks. EPC and HAF blacks have nearly the same threshold loadings and S/Z ratios (Table III). Nevertheless they yield greatly different resistivities in rubber at high (and equal) loadings (Table V).

The relatively high resistivity of the EPC black stock is readily explained by the fact that channel blacks contain appreciable amounts of combined noncarbon constituents, particularly hydrogen and oxygen, the presence of which may be expected to tie up electrons and decrease the intrinsic conductivity (14, 15). Another example of the intrinsic conductivity effect is observed on graphitization of carbon black. Graphon, a carbon produced from channel black by exhaustive graphitization, yields rubber vulcanizates of extremely high conductivity.

In general, high conductivity of a rubber compound at fixed black loading may be brought about by a combination of the three factors already mentioned: small particle size (large surface area), high "structure," and high intrinsic conductivity. Of these only the estimation of intrinsic conductivity poses any real difficulty. However, it is found (16) that the diamagnetic susceptibility of a carbon black furnishes an excellent index of its intrinsic conductivity. The susceptibility increases both with the desorption of chemisorbed oxygen and hydrogen and with increasing degree of graphitization as inferred from x-ray analysis (17–19). These changes are in accord with theoretical considerations on the electronic structure of carbon blacks and graphites (20). For the examples of Table V, the magnetic susceptibilities are:

TABLE V. *Electrical resistivity at 50 phr loading*

	Resistivity, ohm-cm		
	GR-S-101	Hevea	GR-I-17
EPC (Wyex)	2.6×10^{9}	1.6×10^{8}	6.6×10^{5}
HAF (Philblack O)	1.2×10^{7}	3.7×10^{4}	1.2×10^{3}
Graphon	6.0×10^{2}	3.2×10^{3}	5.2×10^{2}

	Mass susceptibility
EPC (Wyex)	-0.59×10^{-6}
HAF (Philblack O)	-0.79×10^{-6}
Graphon	-2.78×10^{-6}

Conclusions

The experimental evidence indicates that electrical conductivity in carbon black-reinforced rubbers is due to conductive chains formed by carbon black particles. Below the critical threshold loading for conductivity these chains do not extend continuously throughout the rubber sample and hence do not cause conductivity, the resistivity of random dispersion being independent of particle size and shape [equation (III)]. High surface-area blacks appear to adsorb ionic impurities to produce an increase in resistivity at low loadings which is not offset by the conductivity of the carbon blacks themselves. Because high surface area blacks also contain the largest number of particles per unit volume, the very blacks which produce the most highly resistant stocks at small loadings also yield the most conductive rubbers at high black contents. Particle aggregation habit contributes strongly in determining the conductivity of rubber stocks at intermediate and high black loadings, but the intrinsic conductivity of the carbon black exerts a noticeable influence only at high black concentrations.

Manuscript received August 8, 1955. This paper was prepared for delivery before the Cincinnati Meeting, May 1 to 5, 1955.

Any discussion of this paper will appear in a Discussion Section to be published in the December 1956 Journal.

REFERENCES

1. B. B. S. T. Boonstra and E. M. Dannenberg, *Ind. Eng. Chem.*, **46**, 218 (1954).
2. L. H. Cohan and J. F. Mackey, *ibid.*, **35**, 806 (1943).
3. P. E. Wack, R. L. Anthony, and E. Guth, *J. Appl. Phys.*, **18**, 456 (1947).
4. D. Bulgin, *Trans. Inst. Rubber Ind.*, **21**, 188 (1945).
5. B. Dogadkin, K. Pechkovskaya, and M. Dashevskii, *Kolloid Zhur.*, **10**, 357 (1948).
6. L. R. Sperberg, G. E. Popp, and C. C. Biard, *Rubber Age*, **67**, 561 (1950).
7. G. Kraus, *J. Phys. Chem.*, **59**, 343 (1955).
8. A.S.T.M. Standards on Rubber Products, Test Designation D150-47T, American Society for Testing Materials, Philadelphia, Pa. (1947).
9. S. Roberts, *Rev. Sci. Instr.*, **10**, 181 (1939).
10. L. G. Gouy, *Compt. rend.*, **109**, 935 (1889).
11. T. Baron, unpublished work; cf. R. E. De La Rue and C. W. Tobias, "Conductivities of Random Dispersions", paper presented at 107th meeting of The Electrochemical Society, Cincinnati, May 1 to 5, 1955.
12. G. Kickstein, *Kautschuk and Gummi*, **7**, 50 (1954); *Rubber Chem. Tech.*, **27**, 940 (1954).
13. C. W. Sweitzer and W. C. Goodrich, *Rubber Age*, **55**, 469 (1944).
14. M. L. Studebaker, *Kautschuk and Gummi*, **6**, 193 (1953).
15. M. L. Studebaker, *India Rubber World*, **129**, 485 (1954).
16. G. Kraus, to be published.
17. C. R. Houska and B. E. Warren, *J. Appl. Phys.*, **25**, 1503 (1954).

18. J. Biscoe and B. E. Warren, *J. Appl. Phys.*, **13**, 364 (1942).
19. W. D. Schaeffer, W. R. Smith, and M. H. Polley, *Ind. Eng. Chem.*, **45**, 1721 (1953).
20. S. Mrozowski, *Phys. Rev.*, **85**, 609 (1952).

APPENDIX

Area Distribution of Conductive Paths

The problem is to calculate the probability of finding exactly x paths in the area A of the test electrode. For this purpose one may divide the area A into n subareas large enough to accommodate no more than one path. If p is the probability of finding a path in a subarea, the desired probability is

$$p(x) = \frac{n!\, p^x(1-p)^{n-x}}{x!(n-x)!} \tag{I}$$

The probability p is given by

$$p = \bar{x}/n \tag{II}$$

where $\bar{x}$ is the mean number of paths for an area the size of the electrode. Then

$$p(x) = \frac{n!\, \bar{x}^x \left(1 - \frac{\bar{x}}{n}\right)^{n-x}}{x!(n-x)!\, n^x} \tag{III}$$

and on applying Stirling's approximation to the factorials involving n (since $n \gg x$), one arrives at

$$p(x) = \frac{e^{-x}\bar{x}^x}{x!} \cdot \left(\frac{n-x}{n-\bar{x}}\right)^x \cdot \left(\frac{n-\bar{x}}{n-x}\right)^n \cdot \left(\frac{n}{n-x}\right)^{\frac{1}{2}} \tag{IV}$$

Also, because $n \gg x$, we may neglect x against n except where the result is raised to the power n, so that

$$p(x) = \frac{e^{-x}\bar{x}^x}{x!} \cdot \left(\frac{n-\bar{x}}{n-x}\right)^n \tag{V}$$

Furthermore, for large n

$$\left(\frac{n-\bar{x}}{n-x}\right)^n \cong e^{-\bar{x}}/e^{-x}$$

and

$$p(x) = \frac{e^{-\bar{x}}\bar{x}^x}{x!} \tag{VI}$$

The standard deviation, σ, of this distribution is obtained as follows. One has

$$\sigma^2 = x^2 - \bar{x}^2 \tag{VII}$$

so that it is only necessary to evaluate x^2:

$$x^2 = e^{-\bar{x}} \sum \frac{x^2 \bar{x}^x}{x!} = e^{-\bar{x}}\bar{x}^2 \sum \frac{x^2 \bar{x}^{x-2}}{x!} \tag{VIII}$$

The summation yields

$$0 + \bar{x}^{-1} + 2 + 3\bar{x}/2! + 4\bar{x}^2/3! \cdots + m\bar{x}^{m-2}/(m-1)! \cdots$$

which is recognized as

$$e^{\bar{x}} + \frac{1}{\bar{x}}\, e^{\bar{x}}$$

Hence,

$$x^2 = \bar{x}^2 + \bar{x} \tag{IX}$$

and

$$\sigma = \sqrt{\bar{x}} \tag{X}$$

Activator Systems in Zinc Sulfide Phosphors

J. S. Prener and F. E. Williams

Research Laboratory, General Electric Company, Schenectady, New York

ABSTRACT

Zinc sulfide containing copper at random zinc sites was prepared by radioactive decay of Zn^{65}. Measurements indicate that the isolated copper impurities do not contribute to luminescent emission. Using a covalent model of zinc sulfide, and recognizing the acceptor-donor nature of activators and coactivators, association of these impurities is found and the luminescent center is identified as second or third nearest neighbor associated activator-coactivator pairs. The nearest neighbor pairs are transparent to 3650Å radiation and have many of the characteristics necessary to account for edge emission.

Introduction to Zinc Sulfide Phosphors

In many ways zinc sulfide phosphors form a unique class of luminescent solids. The most effective activators and coactivators, both of which are apparently necessary for luminescence, lie in columns of the periodic table on either side of zinc and sulfur. Thus, elements which have been recognized as activators are copper, silver, and gold in group I B, and phosphorus (1) and arsenic (2) in group V B; those elements most effective as coactivators are chlorine, bromine, and iodine in group VII B, and aluminum, gallium, and indium (3) in group III B. Activation by manganese has been recognized to be of quite a different nature than the activation by the elements described above (4).

Zinc sulfide is essentially a covalent crystal as indicated by the directional tetrahedral bonds in the structure and

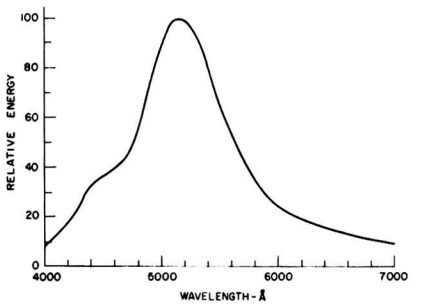

FIG. 1. Emission spectrum of $Zn^{65}S$:Cu:Cl under 3650Å excitation.

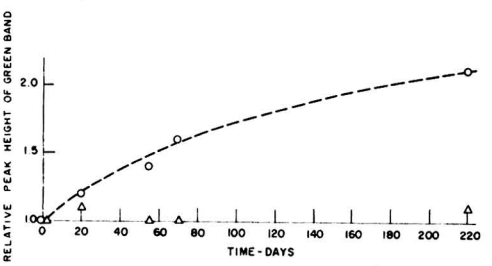

FIG. 2. Change in intensity of the green Cu peak as a function of time. O, calculated from data of Urbach; △, experimental points.

is, therefore, quite different in nature from the ionic phosphor systems on which most theoretical work has been done.

The nature of the activator and coactivator systems in zinc sulfide phosphors has been the subject of a great deal of discussion in the literature. The most recent work on this subject has been done by Klasens (5) who, using an ionic model of zinc sulfide, concluded that the activators copper, silver, and gold are present in zinc sulfide as unipositive ions at zinc sites. The localized negative charge in the neighborhood of the activator perturbs the levels of $S^=$ ions immediately surrounding it, providing a localized filled level above the valence band. It is this perturbed $S^=$ ion which constitutes the luminescent center. The local excess positive charge in the neighborhood of the coactivator is capable of acting as an electron trap. Aside from the inappropriate use of an ionic model for zinc sulfide, the activation of zinc sulfide by such elements as phosphorus or arsenic is less satisfactorily accounted for by the ionic model. If one assumes that the group V B elements substitute in zinc sulfide as trinegative ions at sulfide sites, the sulfide ions whose levels would be perturbed would be those in the next nearest neighbor positions. The effect of the excess negative charge would be expected to be smaller than if the sulfide ions were nearest neighbors as in the case of copper, silver, or gold. Yet the yellow and orange emissions in these phosphors would indicate a larger effect.

Formation of Substitutional Activator by Radioactive Decay

In order to learn more about the activator systems in zinc sulfide phosphors at low activator concentrations, a method was devised for preparing zinc sulfide containing copper impurities unambiguously located at random substitutional zinc sites. A study of the luminescent properties of this material was expected to aid in elucidating the nature of the activator systems in zinc sulfide phosphors prepared by conventional methods.

The zinc sulfide was prepared with the radioisotope Zn^{65} by first sealing 1.25 grams of Johnson, Mathey and Company high-purity zinc oxide in a quartz ampule and irradiating for twelve days in the Materials Testing Reactor at Idaho Falls. The sample was placed in a region of the reactor where the neutron flux was 1.7×10^{14} neutrons/cm²/sec. The natural isotope Zn^{64} was converted to Zn^{65} and the final activity of the sample was calculated to be 350 millicuries corresponding to a Zn^{65} concentration of 0.0034%. Zn^{65} decays to stable Cu^{65} with a half-life of 250 days by K-electron capture and the emission of a 1.12 mev gamma ray. A recoil energy of 10.3 ev is imparted to the nucleus by the emission of the gamma ray.

The radioactive zinc oxide was then converted to zinc sulfide by heating for 45 min at 900°C in a stream of dry hydrogen sulfide containing about 2% hydrogen chloride. The initial copper content due to the decay of the Zn^{65} during irradiation and in the time before the zinc sulfide was prepared amounted to 0.00025% by weight of the zinc sulfide. This copper, together with the hydrogen chloride used in the preparation, gave rise to the emission spectrum shown in Fig. 1. Under 3650Å excitation, the luminescent emission consisted of the green "copper" band at 5160Å and the blue "self-activated" band at 4500Å. Similar preparations of zinc sulfide from an unirradiated sample of the same zinc oxide had only the blue emission band. Additional emission spectra were taken over a period of 220 days during which time the copper content rose to 0.0015%, a sixfold increase. What was sought was an increase in the intensity of the green band.[1] Experimental results are given in Fig. 2, in which the height of the green band relative to its initial value is plotted as a function of time. During the period of the experiment, no change in the emission spectrum was detected. Assuming the copper impurities formed by the decay of the Zn^{65} could give rise to those centers responsible for the green emission in zinc sulfide, then the data of Urbach (6) and the control experiments in the present work could be used to indicate the expected change in the intensity of the green band with time. Urbach's data are also plotted in Fig. 2, and indicate that a change should have been observed if indeed the copper impurities could give rise to luminescent centers.

The question of the effect of the 10 ev recoil energy acquired by the copper nucleus due to the emission of the 1.12 mev gamma ray was examined. Electron bombard-

[1] The ratio of the blue to green band was used as a measure of any changes in the intensity of the green band. The sample, the exciting source, and the spectrometer were positioned in as much the same manner for each measurement of the emission spectrum as was possible considering the difficulties of handling samples having activities near 300 millicuries. As far as could be noticed, there was no change in the relative intensity of the green to blue band, in the absolute intensity of the green band itself, or in the over-all efficiency of the phosphor.

ment experiments on germanium (7), which has the same structure as cubic zinc sulfide, indicated that, in order to produce vacancies and interstitials in these solids, recoil energies of the order of 30 ev are required. An approximate calculation based on an ionic model of zinc sulfide indicated that at least one-half of the copper impurities formed by the decay process would remain at substitutional zinc sites. One would expect that the covalency would increase the fractions remaining at substitutional sites.

It is evident, therefore, that an appreciable fraction of the copper impurities remained at zinc sites. Since no detectable increase in concentration of activator systems occurs during the transmutation, the conclusion that isolated copper impurities at substitutional zinc sites do not give rise to a luminescent center in zinc sulfide is inescapable.

Covalent Model for Zinc Sulfide Phosphors

In order to account for these results and to explain in a consistent manner the unique features of the zinc sulfide class of phosphors discussed in the first part of this paper, we propose an acceptor-donor model of the activator and coactivator, respectively, together forming the luminescent center and each located at substitutional sites.

Both zinc and sulfur in zinc sulfide can be considered to have a hybrid sp^3 configuration (8). Thus, both zinc and sulfur can form the four tetrahedral bonds to neighboring atoms. The formation of zinc sulfide can then be written as

$$\mathrm{Zn}\,(\cdots 3d^{10}4s^2) + \mathrm{S}\,(\cdots 3s^23p^4) \rightarrow \mathrm{Zn}^{=}\,(\cdots 3d^{10}4s4p^3) + \mathrm{S}^{++}\,(\cdots 3s3p^3) \quad \text{(I)}$$

Incidentally, the electron distributions in the bonds will be strongly enhanced in the region of the S^{++}. This is equivalent to an ionic contribution to the electronic structure. Therefore, the ionic species $Zn^{=}$ and S^{++} are merely a convenient basis for the description of the covalent model.

The structure of zinc sulfide is shown pictorially in Fig. 3*a*. In Fig. 3*b* the corresponding energy band scheme of zinc sulfide is indicated schematically. The electronic states of the valence band are those of the least tightly bound electrons in the system, namely, the electrons in the zinc to sulfur bonds. The band gap of 3.7 ev is the minimum

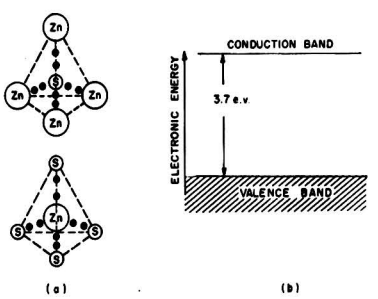

Fig. 3. (*a*) Representation of the electronic structure of zinc sulfide, indicating the four covalent bonds each containing two electrons in localized orbitals; (*b*) corresponding energy band scheme of zinc sulfide showing the separation between the highest lying filled band and empty conduction band.

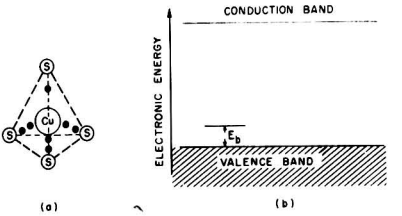

Fig. 4. (*a*) Representation of the local electronic structure around a single copper impurity in zinc sulfide indicating a missing electron in the copper-sulfur bonds; (*b*) corresponding energy band scheme. The empty localized level corresponds to a trapped hole. E_b is the energy required to remove an electron from a zinc sulfur bond and place it in the incomplete copper-sulfur bond.

energy required to remove an electron from a bond and free it in the crystal maintaining the atomic configuration of the perfect lattice. Consider the situation if an element of group I B is placed at a zinc site without making any other changes in the lattice. This is what occurs, for example, in the decay of zinc^{65} to copper^{65}. These elements have the configuration $(\cdots nd^{10}(n+1)s)$ where $n = 3$, 4, or 5 for copper, silver, or gold. The replacement reaction may be visualized as

$$\mathrm{M}[\cdots nd^{10}(n+1)s] + \mathrm{Zn}^{=}(\cdots 3d^{10}4s4p^3) \rightarrow \mathrm{M}^{=}[\cdots nd^{10}(n+1)s(n+1)p^2] + \mathrm{Zn}(\cdots 3d^{10}4s^2) \quad \text{(II)}$$

Thus, copper, silver, or gold can only form three good bonds to neighboring sulfur atoms with the fourth bond being incomplete. In other words, because Zn in group II B is replaced by an element of group I B, an electron must be missing from the system in order to maintain electrical neutrality and the missing electron will be one of the least tightly bound ones, that is, an electron in the covalent bond. Again, the situation can be illustrated as in Fig. 4*a* and give the corresponding energy band scheme in Fig. 4*b*. The incomplete bond gives rise to a localized level above the valence band. The energy E_b is the energy required to remove an electron from a zinc to sulfur bond and place it in the incomplete bond between the impurity and the four surrounding sulfurs. Thus, while copper at a substitutional zinc site gives rise to a localized level above the valence band, the level is unfilled and cannot give rise to luminescence when excited by 3650Å radiation. A similar scheme can, of course, be used to indicate the origin of a localized level when an element of group V B, such as phosphorus or arsenic, replaces sulfur.

$$X(\cdots ns^2np^3) + \mathrm{S}^{++}(\cdots 3s3p^3) \rightarrow X^{++}(nsnp^2) + \mathrm{S}(\cdots 3s^23p^4) \quad \text{(III)}$$

Again the activator can only form three good bonds, the fourth being incomplete, with this incomplete bond giving rise to an empty localized level above the valence band.

Consider now an impurity such as chlorine at a sulfur site. The elements of group VII B have the configuration $\cdots ns^2np^5$ and the replacement reaction can again be written as

$$X(\cdots ns^2np^5) + \mathrm{S}^{++}(\cdots 3s3p^3) \rightarrow X^{+++}(\cdots nsnp^3) + e^{-} + \mathrm{S}(\cdots 3s^23p^4) \quad \text{(IV)}$$

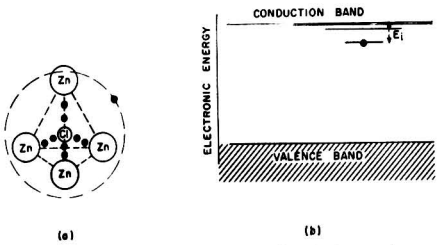

FIG. 5. (*a*) Representation of the local electronic structure around a single chlorine impurity in zinc sulfide indicating the four complete covalent bonds and the extra electron moving in a bound hydrogen-like orbit around the excess positive charge; (*b*) corresponding energy band scheme. The trapped electron lies in a localized level near the conduction band. E_i is the energy required to ionize this electron into the crystal. Some of the excited, more diffuse, coulombically bound states are also indicated.

The elements of group VII A can, therefore, form four tetrahedral bonds to neighboring zincs with the extra electron trapped in the coulomb field of the local excess positive charge. The case here is illustrated in Fig. 5*a* with the corresponding energy band scheme given in Fig. 5*b*. There is a filled localized level below the conduction band and the energy E_i is the energy required to ionize the trapped electron into the crystal. In addition, there are a series of excited hydrogen-like levels below the conduction band. E_i is of the order of the ionization energy of a hydrogen atom in a medium whose dielectric constant is that of zinc sulfide.

A similar scheme applies to coactivators of group III B at zinc sites. These have a configuration $(\cdots ns^2np)$ and the replacement reaction can be written as

$$\mathrm{M}(\cdots ns^2np) + \mathrm{Zn}^{=}(\cdots 3d^{10}4s4p^3) \rightarrow \mathrm{M}^{-}(\cdots nsnp^3) + e^{-} + \mathrm{Zn}(\cdots 3d^{10}4s^2) \quad \text{(V)}$$

In an actual phosphor the activator and coactivator are both needed to produce luminescence. At equilibrium the electron trapped in the field of the coactivator will be transferred to the low-lying empty level due to the presence of the activator. The activator and coactivator then each form four complete tetrahedral bonds. The energy of the system is thereby reduced by approximately the energy required to ionize an electron from a covalent bond. This accounts for the increased solubility of copper in zinc sulfide in the presence of aluminum coactivator as found by Froelich (9).

To summarize, the localized level above the filled valence band arises from the fact that the periodic potential of the zinc sulfide lattice in which the valence electrons move is perturbed locally in the vicinity of the activator impurity. The more negative potential in this vicinity is less binding and raises the energy of the localized states of the electrons in the vicinity of the impurity. The extent to which the localized level is raised above the filled band will depend on the electron density in the region where the perturbing potential due to the activator is largest. It has been indicated that the electron density in bonds is enhanced in the region of the sulfur sites. The localized level arising from a phosphorus or arsenic impurity at a sulfur site would be expected to lie higher above the valence band than the localized level arising from a copper, silver, or gold impurity at a zinc site. The emission at longer wave lengths of phosphors activated by group V B elements as compared to those activated by group I B elements can thus be understood qualitatively when a covalent model of the zinc sulfide phosphors is used.

Associated Activator-Coactivator System

Since an activator impurity and a coactivator impurity each forming four covalent bonds constitute locally an excess negative and positive charge, respectively, there is an electrostatic attraction between the two. At the firing temperatures of zinc sulfide phosphors where diffusion is rapid, this attraction must lead to deviations from a random distribution of the two impurities. The activator and coactivator tend to be close together and it is possible to make some estimates of the deviations from a random distribution due to electrostatic interactions, using the mass action law and free energy considerations. Defining α_i as the fraction of copper impurities having a chlorine impurity in the i^{th} shell of sulfur sites around the copper, then (10)

$$\frac{\alpha_i}{(\alpha_1 + \alpha_2 - 1)^2} = cz_i e^{-E_i/kT} \quad \text{(VI)}$$

Where z_i is the number of available sites in the i^{th} shell of sulfurs around the copper, E_i is the interaction energy between the copper and the chlorine, and c is the concentration of copper or chlorine in gram atoms per mole of zinc sulfide. The interaction energy between activator and coactivator will be taken as

$$E_i = -e^2/\kappa r_i \quad \text{(VII)}$$

where κ is the static dielectric constant of zinc sulfide and r_i is the distance between the copper and the chlorine. Using a concentration of 10^{-4} and a temperature of 1000°K, $\alpha_1 = 0.60$ and $\alpha_2 = 0.03$. Other activator-coactivator systems will also obviously be associated, although some, such as copper-aluminum, cannot form nearest neighbor pairs.

For the nearest neighbor associated activator-coactivator system, the localized states of the separated activator and coactivator vanish because of overlap. The perturbation is no longer that of a charge but that of a dipole. Based on Handler's calculation (11) of an electron interacting with a dipole, weakly bound states are found very

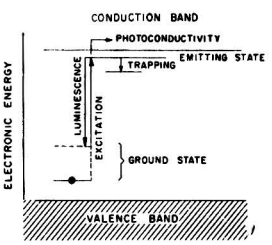

FIG. 6. The luminescent center in ZnS phosphors. The filled localized level near the valence band which constitutes the ground state of the luminescent center and the empty localized level near the conduction band which constitutes the emitting state are shown. The trapping state is also indicated.

close to the conduction and valence bands. The nearest neighbor pairs are, therefore, quite transparent to 3650Å radiation. Many characteristics of "edge emission" are, however, in accord with the nearest neighbor associated activator-coactivator system (10).

It is known from the interpretation of the nonlinear characteristics of zinc sulfide phosphors that the luminescent center excited by 3650Å has a large probability of ionization compared to emission (12). Consequently, these experimental results using radioactive Zn^{65} indicate that the copper formed by the decay of zinc must differ from copper centers in ordinary zinc sulfide phosphors in other than the occupancy of the localized state in the unexcited crystal. This difference can be explained on the basis of the above discussion of association of activators and coactivators since copper formed by the decay of Zn^{65} would have a negligible probability of having a chlorine at a second nearest neighboring sulfur site. There is other evidence to indicate association of activator and coactivator in zinc sulfide phosphors, since it has been found that the line emissions of praseodymium (3) and samarium (13) when used as group III coactivators are markedly different in the presence of different coactivators.

It is probable that the second nearest-neighbor associated coactivator provides a localized emitting state of the luminescent centers in zinc sulfide phosphors. Emission could occur by transitions between the excited hydrogen-like states associated with the coactivator and the localized state associated with the activator. These excited states have large orbits and overlap the low lying state associated with the activator thus facilitating transitions between the two. They are more nearly coulombically bound than the lowest lying state of the coactivator, which can be identified with the trapping states in these phosphors. Thus, the emission spectra will be independent of the nature of the coactivator, whereas trap depths will depend on the specific coactivator used (14).

In summary, we consider the luminescent center in zinc sulfide phosphors to consist of an activator impurity and an associated (but not nearest neighbor) coactivator impurity. Excitation by 3650Å results in a transition between the localized state associated with the activator and one of the coulombically bound states associated with the coactivator (Fig. 6). The reverse transition, after atomic rearrangement which perturbs the localized state associated with the activator upward, results in luminescence. The electron may, however, also be trapped in the lowest localized state associated with the coactivator or be thermally excited to the conduction band resulting in photoconductivity.

Manuscript received August 10, 1955. This paper was prepared for delivery before the Cincinnati Meeting, May 1 to 5, 1955.

Any discussion of this paper will appear in a Discussion Section to be published in the December 1956 JOURNAL.

REFERENCES

1. A. H. McKeag and P. W. Ranby, *J. (and Trans.) Electrochem. Soc.*, **96,** 85 (1949).
2. J. S. Prener, *This Journal*, **98,** 406 (1951).
3. F. A. Kröger and J. Dickhoff, *Physica*, **16,** [3], 297 (1950).
4. F. E. Williams, *Brit. J. Appl. Phys., Supplement No.* **4,** 597 (1954).
5. H. A. Klasens, *This Journal*, **100,** 72 (1953).
6. D. Pearlman, N. R. Nail, and F. Urbach, "Preparation and Characteristics of Solid Luminescent Materials," p. 365, John Wiley and Sons, Inc., New York (1948).
7. K. Lark-Horovitz, "Semi-conducting Materials," p. 64, Academic Press, Inc., New York (1951).
8. C. A. Coulson, "Valence," p. 263 Oxford University Press, London (1952).
9. H. C. Froelich, *This Journal*, **100,** 280 (1953).
10. J. S. Prener and F. E. Williams, *Phys. Rev.*, **101,** 1427 (1956). J. S. Prener and F. E. Williams, Paris Luminescence Symposium (1956).
11. G. S. Handler, *J. Chem. Phys.*, **23,** 1977 (1955).
12. S. Roberts and F. E. Williams, *J. Opt. Soc. Amer.*, **40,** 516 (1950).
13. Z. A. Trapeznikova, *Zhur. Eksptl. i. Teoret. Fiz.*, **21,** 283 (1951).
14. W. Hoogenstraaten, *This Journal*, **100,** 356 (1953).

Ductile Chromium

W. H. Smith and A. U. Seybolt

Research Laboratory, General Electric Company, Schenectady, New York

ABSTRACT

The effects of certain impurities on the room temperature ductility of chromium have been investigated. Results indicate that nitrogen in amounts <0.01% raises the bend transition temperature of annealed material above room temperature. No effect of oxygen on the ductility in amounts <0.3% was found. Sulfur in amounts as great as 0.1% does not appear to affect adversely the bend ductility of as-cast material. It appears that carbon in amounts greater than 0.02% cannot be tolerated. Preliminary work on the development of chromium-base alloys containing more than 90% chromium developed many unsolved problems. The beneficial effects of adding rare earths to tie up harmful impurities in chromium are discussed. Results of mechanical tests on chromium-cerium alloys are presented.

Introduction

Parke and Bens (1) in 1946 and Havekotte, Greenidge, and Cross (2) in 1950 studied the high temperature strength and creep properties of chromium-base alloys. While some of their compositions showed promise, none of their alloys showed any ductility at or near room temperature; these were all cast materials.

Blocher and associates (3) succeeded in fabricating sheet in small quantities from pure metal prepared from the iodide. While much of their material was cold bendable, it exhibited little or no tensile ductility near room temperature. They felt that carbon and sulfur could not be tolerated for cold ductility if the sum of these two were greater than 0.015 wt%. They also found that over 0.2% nickel was very detrimental. Oxygen up to 0.3% had no effect, nor did nitrogen in quantities up to about 0.03%.

Johansen and Asai (4) describe the successful preparation of room temperature ductile chromium at the Bureau of Mines Laboratory at Albany, Oregon. This procedure is essentially the purification of electrolytic chromium by an elevated temperature treatment in pure hydrogen, followed by consumable electrode arc-melting to a 2-in. diameter ingot which is then fabricated to sheet. Much of the sheet is cold bendable, and wire has also been prepared which is not only bendable, but which exhibits considerable reduction in area during a tensile test.

Wain and Henderson (5) reported on high-purity electrolytic chromium made by arc melting and hot-rolling at 900°C in mild steel, which was ultimately etched away. Even as-recrystallized, this material was cold bendable. No detectable metallic impurities could be found, and the nonmetallic impurities were 0.06% oxygen, < 0.001% nitrogen, and < 0.005% carbon. More recent work by Wain and Henderson (6, 7) is in agreement with many of the findings reported here.

Sully and co-workers (8) reported on an extensive investigation into the metallurgy of chromium, which dealt with the properties and fabrication of pure chromium and some chromium alloys. Sully's main findings were that metallic additions could not be tolerated in the sense that everything he added rapidly raised the bend transition temperature. He had no success in achieving any measure of cold ductility. Most of his specimens were prepared by powder metallurgical techniques.

To summarize the previously existing knowledge, there was evidence that sufficiently pure chromium was room temperature ductile, but aside from the information cited above there was almost none on what impurity or combination of impurities was most critical.

The immediate objectives of this work were to determine the most critical impurities, to find the level of concentration needed to cause trouble, to find means of eliminating this difficulty, and to establish a practical procedure for the preparation of room temperature ductile metal and to prepare such metal in sufficient quantity for various mechanical property tests.

Properties of Electrolytic Chromium

Electrolytic chromium appears to be the only practicable starting material for the production of chromium and chromium alloys at present.

To test the possibility that mere spheroidization of the oxide inclusions might be enough to cause some improvement in ductility, a sample of electrolytic chromium containing 0.003% nitrogen and 0.50% oxygen was heated in argon to 1400°C for 6½ hr. Although spheroidization was practically complete, the sample was brittle at room temperature and failed with the customary transgranular fracture. The hardness of this sample was 119 VHN, about as low a hardness as has been observed on any samples of chromium examined during this investigation, including samples of ductile chromium. A careful determination of the bend transition temperature, however, revealed that the temperature was lowered from >500°C for the as-deposited material to 150° to 200°C for the annealed material.

Purification of Electrolytic Chromium

The Bureau of Mines group considered oxygen the most objectionable impurity. They removed it by hydrogen reduction at 1200°C or higher, using a recirculating system with ZrH_2 as a source of hydrogen.

There is reason to believe that the reason for their success in making ductile chromium was the use of this hydrogen system, and possibly more important the fact that the furnace tube containing the chromium also contained zirconium turnings as a getter. While their 1200°C hydrogen treatment lowers the oxygen content to about 0.01%, it also appears to lower the nitrogen content even more, to the neighborhood of 0.001%.

The material thus produced showed some room temperature ductility, at least in the as-rolled or work hardened condition. When it was vacuum annealed or otherwise recrystallized, apparently without atmosphere contamination, it generally became brittle.

Hydrogen Reduction Technique

Hydrogen treatment was employed in the present work to eliminate oxygen from electrolytic chromium. However, since there was no critical temperature limitation, much higher temperatures were used to speed up oxygen removal and to reduce the oxygen content still further. At about 1400°C and with soaking times of approximately 20 hr, the oxygen content was reduced to about 0.001%. Hydrogen was first passed through a palladium catalyst and an activated alumina dryer to remove oxygen and water, respectively. From this it was passed through a tube furnace containing an iron pipe at 600°C charged with metallic calcium to pick up nitrogen, since it was noted early in the work that the chromium tended to show nitride needles in the microstructure.

Since there was evidence that, in spite of the precautions noted above, the chromium was still being contaminated with nitrogen, some turnings of a 50-50 zirconium-titanium alloy were placed at either end of the molybdenum boat containing the chromium. At the conclusion of the 20-hr 1400°C run it was noted that the turnings at the gas entrance opening had largely turned yellow, indicative of titanium or zirconium nitride. On the other hand, the turnings at the exit end were still clean and bright.

It has been observed in many cases where the zirconium-titanium alloy has been used close to the sample to be treated that the sample which previously had been brittle was now ductile. Evidently some impurity had been removed from the chromium which had caused brittleness.

While the hydrogen treatment at 1400°C was originally used only to reduce the oxygen content to very low levels, it has been shown that, properly conducted, it can also lower the nitrogen content to about 0.001% or lower. The hydrogen content is also reduced so much that it cannot be measured by vacuum fusion analysis.

Vacuum Heat Treatment

The nitrogen pressure over the chromium-nitrogen solid solution (at temperatures over 1200°C) is the order of millimeters (9), and it was clear that vacuum degassing of the chromium should be possible. Accordingly, some brittle hydrogen-treated electrolytic flake was given a 24-hr heat treatment in a vacuum furnace at 1150°C. At the conclusion of this test, the chromium could be bent cold if the rate of bending was slow. Analysis[1] showed 0.002% nitrogen, while after a similar heat treatment on some

[1] Analytical accuracy is about 0.002%.

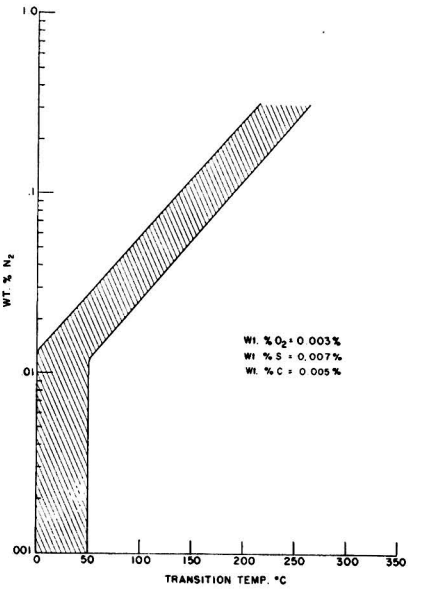

FIG. 1. Effect of N_2 content on the slow bend transition temperature of chromium.

chromium which had originally a somewhat higher nitrogen content, the nitrogen content was 0.003%, but this material was brittle. These experiments and others of a similar nature suggest that (*a*) nitrogen is at least one source of brittleness, and (*b*) the critical nitrogen content may be around 0.002–0.003% or even less. This statement cannot be made unequivocally because it is known that the amount of damage done by nitrogen is a function of the cooling rate. A fast cooling rate from an elevated temperature tends to keep nitrogen in solution and to raise the transition temperature, while a very slow cooling rate allows more complete nitrogen precipitation, in which form it is not so harmful. In addition, the brittleness of any sample depends upon factors such as the amount of cold work it has had, possibly grain size, surface smoothness, and similar variables.

Addition of Controlled Impurities

Nitrogen.—In order to know how much impurity is needed to cause embrittlement, some quantitative relationship had to be established such as per cent impurity vs. transition temperature in slow bending or in impact bending. For this work, arc cast samples $\frac{1}{8}$-in. thick by $\frac{3}{8}$-in. wide by $1\frac{1}{4}$ in. long with a 1-in. gauge length, were slowly bent around a $\frac{1}{16}$-in. radius. Some rolled specimens were also tested in the form of sheet of varying dimensions and gauge length. While a few impact tests were made, the slow bend test using an Instron testing machine with a strain rate of 0.1 in./min was customary.

An attempt was made to prepare chromium samples of similar composition and structure but with varying amounts of nitrogen. This was done by heating as-cast samples of chromium containing 0.029% N_2, 0.003% O_2, 0.007% S, and 0.005% C either in vacuum to lower the

nitrogen content, or in a nitrogen atmosphere to raise the nitrogen content. Fig. 1 shows the transition temperature-percent nitrogen plot obtained on samples prepared from one lot of arc-melted chromium. These results should be regarded as preliminary, since adequate control over the nitrogen content at low levels was difficult to obtain, and similar tests on wrought material would probably show much less scatter. As mentioned earlier, the specific effect of nitrogen depends upon the mechanical and thermal history.

The experiments of Wain and co-workers (7) show conclusively that nitrogen contents of about 0.001% can cause brittleness in recrystallized chromium.

To establish the effect of cooling rate on the bend transition temperature samples of chromium containing 0.029% N_2 were heated to 1200°C in H_2, followed by either water quenching or slow cooling. The transition temperature for the water-quenched sample was 150°–200°C, while for the furnace cooled sample it was about 50°C. These results indicate that nitrogen in solution is more harmful to ductility than is precipitated chromium nitride.

Tests were made to determine if grain orientation in cast, rolled, or recrystallized material influenced the transition temperature. In none of these experiments was it found that the transition temperature changed by an amount greater than the suggested accuracy of the results ±25°C.

A great deal has been written concerning the effect of surface preparation on the ductility of chromium. It has been stated that cold-rolled material exhibits ductility only after the rolled surface is removed by polishing or etching. This effect has been attributed to such factors as oxygen, nitrogen, and notch sensitivity. In this laboratory cold-rolled sheet has been produced which exhibits room temperature ductility without any surface preparation after rolling. Samples of annealed chromium severely vacuum etched had the same transition temperature as similar samples polished through 3-0 paper. In general etching or polishing the surface helped restore ductility only when there was some indication that nitride contamination of the surface had occurred. These results are in agreement with those of Wain and co-workers (7).

Oxygen.—So far, no data have been obtained which clearly suggest that oxygen has an appreciable effect upon the ductility of chromium. Experiments can be cited which make it appear likely that the oxygen content is of no consequence.

It was found that oxygen up to 0.34% has no appreciable effect on the brittle-to-ductile transition temperature of as-cast chromium. For material in the cold-worked or recrystallized condition, chromium with oxygen contents as high as 0.04% had the same transition temperature as material with 0.001% oxygen. Higher oxygen contents were not examined for cold-worked or recrystallized material. Specimens containing 0.04% oxygen and <0.002% nitrogen had the same transition temperature regardless of whether they were rapidly or slowly cooled from the recrystallization temperature.

In another set of experiments, bend tests of the type already described were made on cast ingots containing 0.3% oxygen and 0.005% nitrogen. From Fig. 1 a transition temperature at about 30°C is expected for this much nitrogen if the oxygen content were simply ignored. The measured transition temperature was 75° ± 25°C, showing that, in this case at least, oxygen appeared to have an insignificant effect.

Finally, the results of Wain and co-workers (7) appear to indicate quite clearly that oxygen is an insignificant factor in cold ductility.

Carbon and sulfur.—Slow bend tests have been performed on as-cast chromium samples containing 0.02%, 0.08%, and 0.12% carbon. The oxygen, nitrogen, and sulfur contents were all less than 0.005%. These tests indicated that 0.02% carbon is not detrimental to room temperature ductility. Alloys of higher carbon content showed considerably higher transition temperatures, the value increasing as the carbon content increased. Attempts to prepare test bars without cracks from alloys containing more than 0.50% carbon were not successful. Examination of the fracture after bending revealed an increasing amount of intercrystalline failure as the carbon content increased. At a composition of 0.12% carbon the fracture was completely intercrystalline.

Slow bend tests on cast samples containing 0.1% sulfur indicated the transition temperature to be less than 100°C. This is in the range expected for material of the base composition used, without sulfur. The sulfur was observed to be present both by chemical analysis and by the microstructure.

Metallic additions.—The discouraging results found by Sully and co-workers (5) for all metallic additions have already been mentioned, as has the equally deleterious effect of nickel observed by Blocher and co-workers (3).

The observations made here on the effects of metallic additions have thus far been very incomplete, and have not always been under good control. Many of the observations, for example, have been made before the marked deleterious effect of nitrogen was realized. Certain additions such as copper, silver, and gold in amounts of a few per cent seem to have comparatively little effect on the hardness of chromium (and hence, presumably, upon the strength), although there appears to be some solubility of copper or silver in solid chromium.

Some elements like silicon, titanium, tantalum, nickel, beryllium, iron, tungsten, and aluminum are very potent hardeners, and make chromium even more brittle. This effect is so marked that it is often difficult to arc-cast these alloys without getting cracks in the ingot, particularly in small buttons of around 100 grams or less which cool very rapidly in the water-cooled hearth.

Addition of Scavenging Elements

The prior work of the Bureau of Mines group included the preparation of a number of alloys with the primary intention of tying up oxygen as more stable oxides such as Al_2O_3, Ta_2O_5, ZrO_2, etc. Formation of stable compounds is of course an appropriate expedient for removing effectively any undesirable element, such as carbon, oxygen, nitrogen, sulfur, etc. The Bureau of Mines' efforts to secure room temperature ductility in chromium by this means were not successful. It is not entirely clear why this method does not work better; similar experiments here have been dis-

appointing, although partial success was achieved by the addition of cerium.

Cerium was added to scavenge oxygen, nitrogen, or sulfur since it is known that very stable compounds of these three impurities and the rare earths are formed. The results of such additions on the bend transition temperature for as-cast specimens are shown in Fig. 2. It will be noted that at about 2 per cent of cerium the transition temperature reaches an approximate minimum value. Fig. 3 shows the effect of cerium on the Vickers hardness number for as-cast alloys. Here again, little is gained by adding more than about 2%. It is considered at present that the major effect of the rare earth addition is in tying up the nitrogen content as CeN.

Unfortunately, the cerium addition does not prevent or nullify further nitrogen contamination, presumably be-

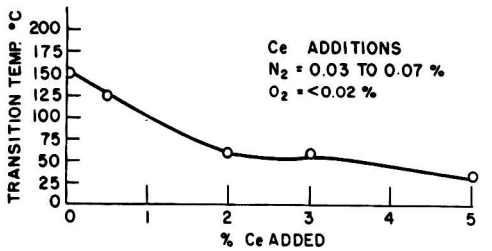

FIG. 2. Effect of cerium additions on the slow bend transition temperature of as-cast chromium containing approximately 0.03–0.07% N_2. Oxygen content < .02%.

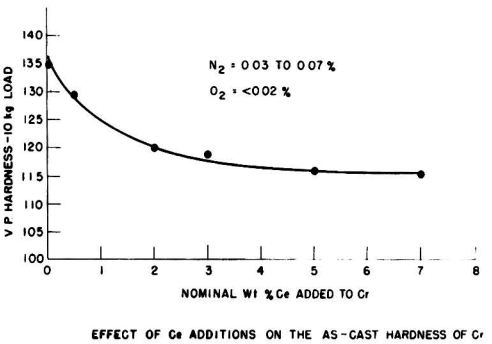

FIG. 3. Effect of Ce additions on the as-cast hardness of Cr.

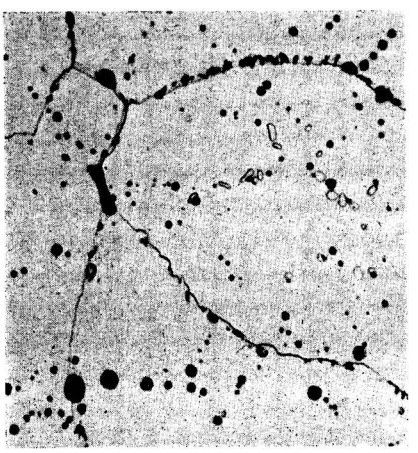

FIG. 4. 98% Cr + 2% Ce heated at 800°C in a N_2 atmosphere. Blak inclusions are Ce, light inclusions within grains ande at grain boundaries are nitrides. (500×).

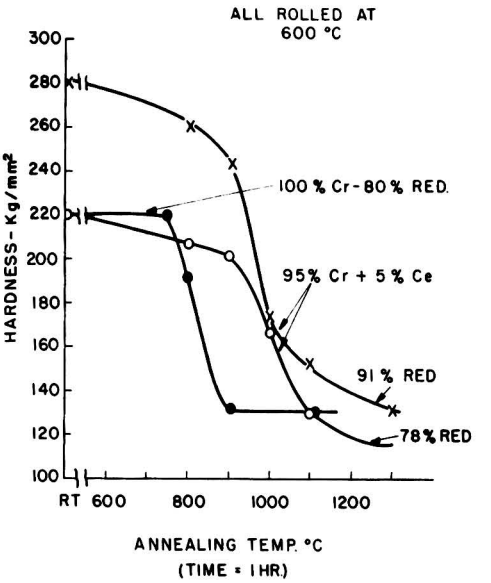

FIG. 5. Effect of annealing temperature on the hardness of rolled Cr and Cr + 5% Ce alloys.

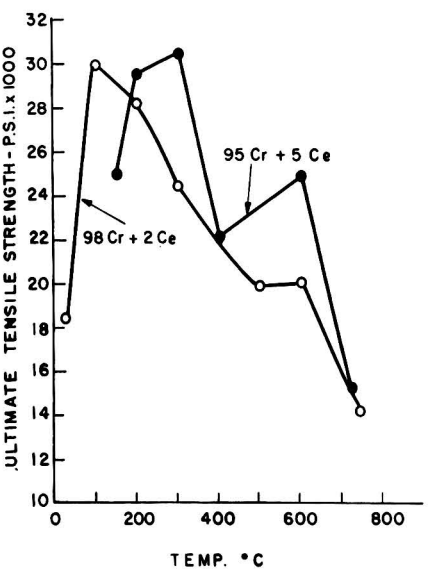

FIG. 6. Ultimate tensile strength of as-cast Cr-Ce alloys as a function of testing temperature.

cause cerium is present mainly as an insoluble second phase of very limited solubility in solid chromium. Fig. 4 shows the microstructure of a 2% cerium alloy which was heated in a nitrogen atmosphere. The dark areas are globules of cerium while the light-etching, almost white, inclusions are the nitride Cr_2N. The fact that these can coexist in this manner means that the previously existing islands of cerium are relatively ineffective in gettering the nitrogen as it diffuses into the chromium.

The recrystallization temperature behavior for a chromium-5% cerium alloy reduced 91% and 78% at 600°C is shown in Fig. 5, together with some nominally pure chromium with an 80% reduction at the same temperature. Cerium appears to exert an appreciable resistance to recrystallization.

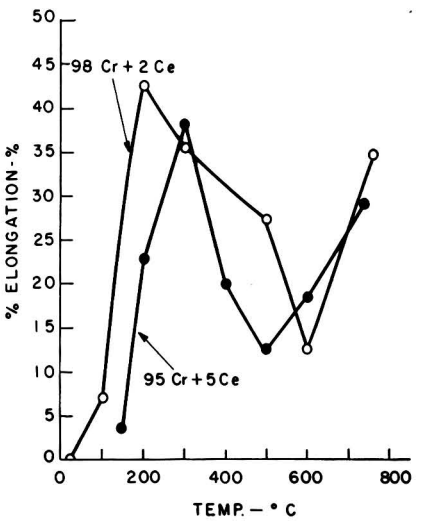

FIG. 7. Ductility of as-cast Cr + Ce alloys as a function of testing temperature.

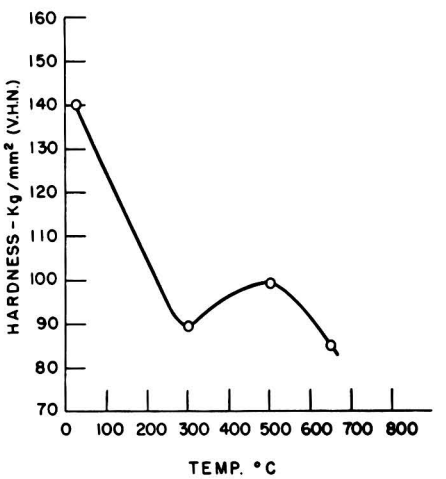

FIG. 8. Hot-hardness of chromium

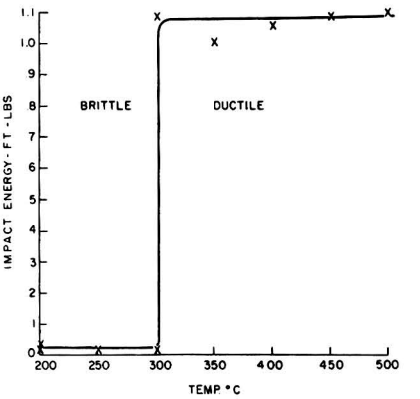

FIG. 9. The transition temperature of as-cast Cr + 2% Ce alloy as measured in impact on unnotched miniature Charpy bars.

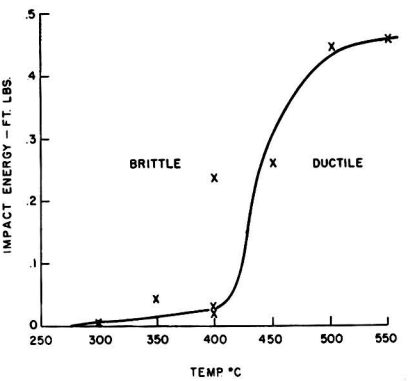

FIG. 10. Transition temperature of as-cast Cr + 2% Ce alloy as measured in impact on notched miniature Charpy bars.

MECHANICAL PROPERTIES OF CAST CHROMIUM-CERIUM ALLOYS

Results of some short-time tensile tests on cast chromium-cerium alloys are shown in Fig. 6 and 7. The pronounced minimum at 500°–600°C in per cent elongation (1-in. gauge length) may be associated with some precipitation phenomena. This might be due to the same agent which causes the maximum in hot hardness at this temperature (10) (see Fig. 8). The maximum in ductility near 200°C was unexpected. The tensile-test results in Fig. 6 and 7 require additional work for confirmation. It is expected that similar tests on cold-worked material will be performed.

Impact transition temperature data as measured on as-cast unnotched 2% cerium samples are plotted in Fig. 9. A much higher temperature, with considerably more scatter, was found for the same material tested as notched specimens (Fig. 10).

SUMMARY

While there is no question that small amounts of nitrogen impurity in the range around 0.001% to 0.005% (by

weight) has a marked deleterious effect on the ductility of annealed chromium, Wain and co-workers (7) claim that as much as 0.02% N_2 has little adverse effect upon the ductility of cold-worked chromium.

There is some rather convincing evidence that oxygen is probably not an important impurity, particularly after a nominal clean-up by a high temperature hydrogen anneal. Carbon when present in amounts greater than 0.02% forms a brittle grain boundry film which raises the transition temperature well above room temperature. Sulfur in amounts up to 0.10% does not appear to be harmful to low temperature ductility.

Much larger additions of metallic alloying metals are required to obtain embrittlement, i.e., 1% or more, as contrasted to the great sensitivity of chromium to nitrogen. The sensitivity, however, of chromium to small percentages of many alloying additions does cause some concern about the problem of chromium-rich alloy development. Fortunately, there is some evidence that chromium-base alloys containing rather large amounts of alloying metals (for example around 30–40% iron or nickel) are not as sensitive as alloys much richer in chromium. However, a 1% titanium and 5% tungsten alloy in the rolled condition showed some cold ductility (6).

It is not possible at present to explain some of the vagaries of ductility as a function of amount of cold work or of heat treatment. For example, it has been noted that chromium which has been "cold" rolled at 700°C to 0.021-in. thick had a transition temperature between room temperature and 50°C after a total reduction of 90%. The same sheet after further reduction, which brought the total to 94%, and the sheet thickness to 0.015 in., had a transition temperature of −25°C. This same sheet, if recrystallized by a vacuum anneal without apparent change in composition, has a transition temperature of 150°–200°C.

On the other hand, ductile chromium has been prepared in the as-recrystallized condition, so that a cold-worked structure is not a prerequisite for cold ductility. However, there is evidence that the chromium which exhibits ductility only in the cold-worked state is somewhat less pure than the chromium which is ductile in the recrystallized condition. These ideas are in agreement with Wain and co-workers (7).

It has also been found that by the addition of cerium it is possible to lower markedly the brittle to ductile transition temperature of chromium containing nitrogen. Evidence now available indicates this improvement in ductility is due to the removal of nitrogen from the chromium matrix by the formation of a stable insoluble nitride and to the extremely limited solid solubility of cerium in chromium.

Manuscript received July 22, 1955.

Any discussion of this paper will appear in a Discussion Section to be published in the December 1956 JOURNAL.

REFERENCES

1. R. M. PARKE AND F. B. BENS, ASTM Symposium, "Gas Turbines" (1946).
2. W. L. HAVEKOTTE, C. T. GREENIDGE, AND H. C. CROSS, *Am. Soc. Testing Materials, Proc.*, **50**, 1101 (1950).
3. J. M. BLOCHER, JR., I. E. CAMPBELL, D. J. MAYKUTH, R. I. JAFFEE, AND H. B. GOODWIN, "The Development of Chromium-Base Heat Resistant Alloys", WADC Tech. Rept. 53-470 (1954).
4. J. JOHANSEN AND G. ASAI, *This Journal*, **101**, 604 (1954).
5. H. L. WAIN AND F. HENDERSON, *Proc. Phys. Soc.*, **B66**, 515 (1953).
6. F. HENDERSON, S. T. QUAASS, AND H. L. WAIN, *J. Inst. Metals*, **83**, 126 (1954).
7. H. L. WAIN, F. HENDERSON, AND S. F. M. JOHNSTONE, *ibid.*, **83**, 133 (1954).
8. A. H. SULLY, "Metallurgy of the Rarer Metals: Chromium," Academic Press, New York (1954).
9. A. U. SEYBOLT, To be published.
10. J. WESTBROOK, Private communication.

Technical Feature

Electric Smelting Furnaces

MARVIN J. UDY

546 Portage Road, Niagara Falls, New York

ABSTRACT

Design and operation of electric smelting furnaces go hand in hand. The kilowatt per cubic foot of molten material is an important factor in operation, and constancy of the peripheral ohms factor, for slag forming or smelting operations, is another. Both factors are basically important, and must be properly coordinated with operation to get the best results. In recent work, it is shown that the peripheral ohms factor is a very useful criterion where slags of very high resistance are encountered. An even more useful factor is the kilowatt per square inch of electrode, or of electrode periphery, in contact with the slag.

INTRODUCTION

In the design of smothered arc smelting furnaces the kilowatt per cubic foot of molten material produces the highest energy efficiency. This is in accord with Stansfield's opinion.[1] However, enlarging the smelting zone by high heating rates is more a factor of operation than design. The highest efficiency would be obtained when operating at sufficiently high kilowatt per cubic foot of molten material so that continuous tapping was attained. Under such conditions a definite and constant size of smelting zone would result and there would be no corrosion of the side walls.

Most operations are of the intermittent type wherein the highest heating rate is attained directly after tapping, with a constantly lowered heating rate during the period between taps. Heating rates can be lowered too much and the material will freeze on the bottom of the furnace if the periods between taps are too long.

Thus, to meet the conditions laid down by Stansfield, tapping must be done on a regular basis, e.g., every hour, and becomes more of an operating condition than a factor of design.

Andreae (2) showed that the peripheral ohms factor[1] is a constant for any particular operation where slag is produced. This factor must be determined by experiment. The author has found the peripheral ohms factor to be very useful in the design of the electric smelting furnace. In dealing with the electric furnace, one should know the conditions necessary at the tip of the electrode to produce a given result with the lowest energy cost and greatest recovery. The conditions are temperature, nature of slag (acid or basic), resistance, and the maximum kilowatts per cubic foot that can be put through the particular type of slag. All are important to the proper design of the electric smelting furnace. Other factors of importance are electrode spacing, electrode size, and physical characteristics of the material to be smelted, as well as the time of tapping which controls the kilowatts per cubic foot of molten material. The peripheral ohms factor provides a means of determining these conditions and, thus, a way to design the proper furnace.

To obtain the right conditions of temperature in the electric furnace, full arc heating, arc bath resistance heating, and full bath resistance heating may be used. Proper use and coordination of these factors makes it possible to produce almost any temperature desired, and, when coupled with the proper rate of feed, maintain that temperature within close limits.

The usual furnace design is based on the standard commercial electrodes available, their current carrying capacity, transformer limitations, and bus. Results are not always satisfactory because of the necessary limitations.

TABLE I. *Average data for 100-kw furnace*

Kw total	110
Power factor	95
Voltage (phase)	240
Amp	460
Electrode diameter	4 in.
Resistance at tip	0.248 ohm
Peripheral ohms	3.0

In some recent work on high resistance slags predominating in silica and other acid materials, the author has found that data are needed regarding what takes place at the tip of the electrode in the area where most of the heat is developed in the full open arc, and the point where most of the heat is developed in the slag just short of full bath resistance heating.

The peripheral ohms factor is a good guide in most cases, but it is not always enough. In one operation using a small 100-kw furnace, the peripheral ohms factor was determined for the best results, both operational and economic. Operation under these particular conditions was highly successful as to metallurgical results, electrode consumption, and workability of the furnace, as well as kilowatt hour per ton of product. Results were not entirely satisfactory since a comparatively high voltage was needed for a small energy input. The voltage required was 240 for about 100 kw input with two 4-in. electrodes and an electrode spacing of approximately 12 in. between centers.

[1] Resistance between electrode tip and furnace bottom × electrode circumference.

TABLE II. *Calculated relationships for one electrode of a 3300-kw furnace*
Power factor (P.F.) = 95%

Phase, volts	Effective volts†	Tip volts*	Electrode		Amp in peri.‡	In. in peri.	Electrode		Amp in.²	Res. at tip, ohms
			kw	Amp			Dia.	Area		
200	190	110	1042	9500	36.7	260	82.5	5350	1.78	0.0116
220	208	120	1042	8700	40.0	217	66.5	3900	2.22	0.0137
240	228	132	1042	7900	44.0	179	57.0	2660	2.97	0.0167
260	246	142	1042	7350	47.5	155	49.0	1880	3.88	0.0193
280	265	153	1042	6825	51.0	134	42.5	1420	4.80	0.0224
300	286	165	1042	6320	53.2	119	38.0	1130	5.57	0.0260
320	303	175	1042	5950	57.2	104	33.0	852	6.95	0.0294
340	322	185	1042	5650	61.5	92	29.2	667	8.50	0.0328
360	341	197	1042	5300	66.7	79	25.0	492	10.75	0.0371
380	360	208	1042	5000	69.2	72	23.0	415	12.00	0.0416
400	380	220	1042	4750	73.0	65	20.6	332	14.30	0.0463
480	455	263	1042	3970	87.7	45	14.3	160	24.80	0.0660

* Effective volts ÷ $\sqrt{3}$ = tip volts.
† Phase volts × P.F. = effective volts.
‡ Amp in peri. = volts ÷ 3 (the peripheral ohms).

TABLE III. *Voltage-current relations with electrodes submerged in slag*

Volts	Electrode on surface of slag		Electrodes 1 in. submergence in slag		Electrodes 2 in. submergence in slag	
	Amp	kw	Amp	kw	Amp	kw
200	200	40	490	98	820	164
220	365	80	840	185	975	215
240	460	110	910	218	Reached limit	
260	500	130	760	198	of circuit	
280	580	160	850	238	breaker	
300	530	159				
320	520	167				

Translating these figures to a 3-phase 3300-kva furnace, and maintaining a peripheral ohms factor of 3.0, conditions shown in Table II result.

From Table II it is obvious that conditions desired, as shown in Table I, could not be met at 200–260 v. Electrodes would be excessively large and current densities extremely low for practical operation. In the range of 280–320 v, conditions could be met with a reasonable electrode size and low resistance, but current densities would still be extremely low. At 340–480 v, electrode sizes are more reasonable, but current densities are low, except at 480 v. The only possible range of operation would be at 480 v o

TABLE IV. *Calculations for submerged electrodes*

Phase volts	4 in. Electrode, 12.57 in.² on surface of slag					4 in. Electrode, 25.50 in.²; submerged 1 in. in slag						4 in. Electrode, 38.4 in.²; submerged 2 in. in slag					
	Amp	C.D. amp/in.²	Peri. ohms	Kw/electrode	Kw/in.²	Amp	C.D. amp/in.²	Peri. ohms	Kw/electrode	Kw/in.² in peri.	Kw/in.² in electrode	Amp	C.D. amp/in.²	Peri. ohms	Kw/electrode	Kw/in.² in peri.	Kw/in.² in electrode
200	200	16	5.97	20.0	1.60	490	19	2.44	48	3.81	1.88	820	21.6	1.46	84	6.70	2.22
220	365	29	3.60	40.0	3.18	840	33	1.56	92	7.30	3.60	975	25.6	1.39	107	8.50	2.81
240	460	36	3.10	55.5	4.20	910	35	1.57	109	8.65	4.27			——			——
260	500	39	3.10	65.0	5.17	760	29	2.22	96	7.62	3.76			1.42 avg.			2.51 avg.
280	580	46	2.88	81.0	6.45	850	33	1.96	114	9.12	4.46						
300	530	42	3.47	79.5	6.30			——			——						
320	520	41	3.65	83.5	6.65			1.95 avg.			3.59 avg.						
			——		——						4.00 avg. of last 4 readings						
			3.67 avg.		4.79 avg.												

Note: Area of 4 in. electrode—12.57 in.²; circumference—12.57 in.

TABLE V. *Effect of electrode size on total power input*

Diam. in.	Area, in.²	Circumference, in.	Area 1 in. submergence	Total kw at 4 kw in.²
10	78.5	31.42	109.92	439.6
14	153.9	43.98	197.88	791.5
16	201.1	50.26	251.36	1055.4
20	314.2	62.83	377.03	1508.1

The data on a 24-hr basis averaged as shown in Table I with the tips of the electrodes just on the surface of the slag; much higher voltages were required for operation with a full arc.

TABLE VI. *3300 Kva furnace based on 4 kw/in.² effective electrode area*

Volts	P.F.	Eff. v	Tip v	Kw/elect.	Amp/elect.	Electrode 16 in. effect. area 1 in. submergence	C.D. amp/in.²	Res. at tip
200	95	195	110	1042	9500	251.3	37.8	0.0116
220	95	208	120	1042	8700	251.3	34.6	0.0137
240	95	228	132	1042	7900	251.3	31.4	0.0167
260	95	246	142	1042	7350	251.3	29.3	0.0193
280	95	265	153	1042	6825	251.3	27.0	0.0224
300	95	284	164	1042	6320	251.3	25.0	0.0260
320	95	303	175	1042	5920	251.3	23.6	0.0294

higher. At any lower voltage there would be excessive surface oxidation of the electrodes, resulting in high electrode consumption due primarily to the low current densities.

In order to get within reasonable voltages for safe operation, the region of submergence of the electrode in the slag was explored. The same 100-kw furnace was used and the same type slag. In 3-phase furnaces there is a limit to submergence of the electrodes in any particular slag, beyond which the arc-bath-resistance type of heating is lost and true bath resistance heating takes place with loss of automatic control of the electrode position in the slag. This can result in burned out furnace bottoms and generally poor operation. The results of these tests are shown in Table III, using the same two-electrode furnace and 4 in. diameter electrodes.

Using the above data, Table IV shows the results of calculating amperes per square inch of effective electrode area, peripheral ohms factor, and the kilowatts per square inch of effective electrode area. From these results the kilowatt per square inch of effective electrode area appears to be about as constant as the peripheral ohms factor, within the limits of accuracy of the readings. Power factor is taken as 95.

Calculation of Furnace Design

With these data it becomes quite easy to design a furnace with the electrodes at the surface of the slag bath or with 1 in. or 2 in. submergence that will give reasonably safe working voltages. Thus, to design a 3300 kva 3-phase furnace at 4 kw/in.^{2} of effective electrode area, 1 in. submergence, and to operate at a reasonable and safe voltage, calculations for various electrode sizes are made as shown in Table V.

Since a 3300 kva furnace at 95 P.F. requires 1042 kw/electrode, it is obvious from Table V that a 16 in. electrode is needed at 4 kw/in.^{2} effective electrode area. Calculations on this basis for a 3300 kva furnace are shown in Table VI.

Operating at 2 in. submergence with a 16 in. electrode, the current density would be 31.6 amp/ft^2 for 200 v and 29 amp/ft^2 for 220 v. The resistance would remain the same.

It is plain that a 16 in. diameter carbon electrode with 1 in. submergence of the tip in the slag gives reasonable voltages and current densities within the range of standard practice for carbon electrodes. Much smaller graphite electrodes could, of course, be used; the kilowatt per square inch of effective electrode area would be higher.

Electrode Spacing

Once having determined the voltage range and size of electrode, the next important problem is that of electrode spacing. In smelting furnaces making metal and a slag, matte and a slag, or spiess and a slag, the electrode spacing should be such that the resistance in the slag from electrode to electrode is less than the resistance through the slag to the metal, matte, or spiess in the bottom. Slag composition and characteristics become very important. In high-resistant slags and close electrode spacing, metals like antimony, which melts at 630.5°C, can be frozen on the bottom when the slag reaches much more than 7 in. Spiess, which melts in the 1200°C range, can also be frozen on the bottom when the slag reaches much more than 7 in. in depth. Likewise, pig iron, steel, and ferroalloys will freeze on the bottom if the electrode spacing and slag depth have unsuitable values.

If the electrode spacing is too large and too much of the power goes to the bottom and through the metal, the metal becomes hot and the slag freezes on top.

There is a correct electrode spacing for every type of smelting operation, but it is not always easy to meet the conditions of electrode spacing mechanically. However, in recent years much has been done to improve the design of electrode clamps so that it is now possible to get electrode spacings as low as 18 in. between faces for large 35 in. electrodes. For the most part, the electrode spacing from electrode face to electrode face should be from one-half the diameter of the electrode for very high-resistance slags to one and one-half times the diameter for the more conductive slags. In general, a spacing of one diameter between the electrode faces will satisfy most conditions.

Manuscript received December 27, 1954. This paper was prepared for delivery before the Cincinnati Meeting, May 1 to 5, 1955.

Any discussion of this paper will appear in a Discussion Section to be published in the December 1956 Journal.

REFERENCES

1. A. Stansfield, "The Electric Furnace," 2nd ed., p. 126, McGraw Hill Book Co., New York, (1914).
2. F. V. Andreae, *Trans. Electrochem. Soc.*, **67**, 168 (1935).

Discussion Section

HIGH TEMPERATURE OXIDATION OF TWO ZIRCONIUM-TIN ALLOYS

M. W. Mallett and W. M. Albrecht (pp. 407–414)

DAVID A. VERMILYEA[1]: The oxygen consumed is used up in two processes: (*a*) solution in the metal, and (*b*) formation of an oxide film. Have the authors any estimate, either experimental or from diffusion calculations, of the amount used in each process?

M. W. MALLETT AND W. M. ALBRECHT: Calculations based upon diffusion data indicate that about 0.5–1.5% of the total amount of oxygen consumed by a reacted specimen was used up in the diffusion process. Normal variations in rate data are greater than this. In the proposed mechanism, solution of oxygen must occur. However, not all of the dissolved oxygen diffuses into the metal core since much of it is incorporated into the advancing oxide film by further oxidation.

APPLICATION OF BACKSIDE LUGGIN CAPILLARIES IN THE MEASUREMENT OF NONUNIFORM POLARIZATION

M. Eisenberg, C. W. Tobias, and C. R. Wilke (pp. 415–419)

ROBERTO PIONTELLI[2]: This valuable paper points out some problems of general interest. The main problem in electrochemical kinetics is actually that of the methods for measuring overvoltages at different electrodes, in the very wide range of conditions covered by: plating, refining, finishing, corrosion of metals and alloys. The fear of the systematic errors involved by the so-called "direct" methods, in which the overvoltages are measured during current flow, has given incentive to other techniques (commutator, thyratron potentiometer, alternate current, limit current, etc.).

Although these methods give useful information on some particular aspects of the problems, they are less general and exhaustive than the "direct methods," whose results are moreover exempt from the more or less explicit hypothesis involved by the other ones. For making the direct methods correspond to the requirements of precision measurements, in addition to the general precautions concerning: purity of materials, control of the surface conditions of electrodes, form of current supply, quick and complete recording of voltages (easy at present, thanks to electronics), a satisfactory solution of the problem of the choice of the electrolysis cell, and of the "tensiometric element," formed by coupling the studied electrode to a reference electrode through a probe (so-called capillary), was however urgently required.

The electrolysis cells must grant the uniformity of the current distribution on electrodes[3] and a reasonable control of the conditions of diffusion or convection.

The tensiometric element must avoid the inclusion in the measured overvoltages of parasitic ohmic drops, or, on the contrary, of shielding effects. In this respect the backside capillary[4] presents the advantage that the systematic error is in any case in the same direction, and one may evaluate it with a reasonable approximation. We are therefore in agreement with the authors in believing that this device can find satisfactory application when any interference with hydrodynamic conditions at the solution-electrolyte interface has to be avoided. However, this point is essential, in our opinion, only when conditions of nonturbulent flow are to be investigated.

In our cells[5] a perfect symmetry of geometric conditions is realized such as to permit carrying out experiments in conditions of very regular diffusion.

On the other hand it is also possible, in the aim of minimizing the concentration changes at the electrode surface, to obtain a very efficient stirring by rapid circulation of the solution, which enters and leaves the cell very near to the electrode surface.

The presence of a frontal capillary of our type [represented in Fig. 1(b) of the discussed paper] not only respects the geometric symmetry but does not lower appreciably the local efficiency of the convection due to the turbulent flow of the solution. As a matter of fact, in our cells distribution of current (controlled, for instance, by means of the distribution of the cathodic deposit or of the anodic attack) is perfectly uniform on the electrode to be investigated both in the presence and absence of stirring. These properties are not shown by the capillaries of the classic Luggin type. We succeeded in improving the backside capillary so as to eliminate the systematic error involved by this probe.[6]

For minimizing the sources of systematic errors involved by direct methods, one must in fact apply the following rule: the uniformity of distribution of the current on the electrode to be investigated must be granted by a suitable design of the electrolysis cell and not perturbed by the presence of the capillary of tensiometric element, which must incorporate only the limiting bound-

This Discussion Section includes discussion of papers appearing in the JOURNAL of The Electrochemical Society, **102**, No. 7–12 (July–December 1955). Discussion not available for this issue will appear in the Discussion Section of the December 1956 JOURNAL.

[1] Research Lab., General Electric Co., Schenectady, N. Y.

[2] Lab. of Electrochemistry, Polytechnic Institute of Milan, Milan, Italy.

[3] The experiments of Eisenberg, Tobias, and Wilke confirm once more the dependence of the values of the measured overvoltage on the position of the capillary, when the current distribution is nonuniform on the electrode. The cells sometimes used for measuring hydrogen overvoltages [J. O'M. BOCKRIS, *This Journal*, **98**, 153*C* (1951)], in which a tip electrode is utilized, are therefore, in our opinion, unsuitable also from this point of view.

[4] Perhaps utilized in a quite rough form of realization by other authors before the Piontelli-Poli experiments mentioned in the discussed paper.

[5] R. PIONTELLI, U. BERTOCCI, G. BIANCHI, C. GUERCI, AND G. POLI, *Z. Elektrochem.*, **58**, 86 (1954).

[6] R. PIONTELLI, *Gazz. chim. ital.*, **83**, 357, 370 (1953); *Z. Elektrochem.*, In press; R. PIONTELLI, G. BIANCHI, U. BERTOCCI, C. GUERCI, AND B. RIVOLTA, *ibid.*, **58**, 54 (1954).

ary layer of the electrode solution, avoiding also any current leakage in the rest of the element itself.

For making the backside capillary correspond to these requirements, it is sufficient to introduce a nearly complete obstruction of the capillary by means of a piece of insulating material, protruding in the solution for a length of the order of the capillary diameter. In this manner the current on the studied electrode is uniform, while any inlet of current lines in the probe is avoided, without hindering the convection obtainable by an efficient stirring, or a regular diffusion in absence of stirring.

We seize this opportunity for pointing out once more the advantages of the frontal capillary of the type represented in Fig. 1(b) of the discussed paper,[7] for experiments concerning: single crystals and, generally, electrodes not allowing the application of a backside capillary; conditions requiring special care for avoiding any contamination source; and some others. The application of the rule above led us also to some satisfactory solutions of the problem of the overvoltage measurements in fused salts.[8]

Recently progress has been made with the elaboration of a new type of probes called "electrode probes." As to the arrangement of these probes, they also obey the general rule mentioned above. In the new type the reference electrode may be arranged for instance in such a manner as to be in direct contact with a solution layer very near to the electrode surface. The properties and possible applications of these devices are discussed elsewhere.[9]

CHARLES W. TOBIAS AND MORRIS EISENBERG: We were very interested in the valuable comments made by Professor Piontelli. For some time we have been sharing with him, and a few other workers in this field, a serious concern about the direct methods for measurements of potentials of polarized electrodes.

It has been recognized for some time that, while achievement of uniform *primary* current distribution is possible by proper design of cell geometry, the *actual, secondary* current distribution is rarely uniform throughout the surface of the polarized electrode. Theoretically, the only cases in which the secondary current distribution is uniform are: (*a*) when a pure unidirectional (normal to electrode surface) diffusion of the potential determining species takes place, (*b*) in case of perfect homogeneous turbulence resulting in a mass transfer boundary layer of uniform thickness on the electrode surface.

It must be pointed out, however, that the realization of these two ideal conditions in laboratory practice is quite difficult. For instance, the commonly used mechanical stirring or the bubbling of a gas in the vicinity of the electrode certainly cannot be expected to produce uniform turbulence and cannot be subjected to a rigorous hydrodynamic analysis. On the other hand, the case of pure diffusion can be realized (in case of a metal deposition system) by placing the cathode at the top end of a vertical cell and eliminating possible thermal gradients. In this case, the use of a perpendicular capillary pressing against the electrode, as suggested by Piontelli, is quite acceptable and free of error. We wish to emphasize these points because very frequently one finds polarization data taken on the assumption that pure diffusion was operative and ignoring the large contribution of free convection.

In principle, it is not possible to provide a uniform boundary layer, by stirring or by flow of the electrolyte or when natural convection takes place, in the vicinity of limiting walls or protrusions on a plane surface. Although this principle has been well known to us, we performed some simple experiments, in which a Lucite (insulator) rod of 2 mm diameter was fitted into a hole of exactly the same diameter in the electrode surface. The electrode was placed in a vertical position, so that the Lucite rod was horizontal. Current distribution due to geometry was perfect, since the anode was parallel to cathode, and all edges were connected by parallel insulating planes. Copper was deposited at current densities well below the limiting, under the following conditions: (*a*) no stirring, (*b*) stirring by 2 glass propellers placed on two sides of rod, (*c*) flow of electrolyte parallel to cathode surface.

Following each experiment, the Lucite rod was removed, and the deposit adjacent to the hole observed by means of photomicrographs. In each case, the deposit thickness was appreciably smaller in the direction of flow, e.g., where the rod "shielded" the flow. In case (*a*), in which natural convection was operative, a well-defined groove formed in an exactly vertical direction above the hole.

We cannot accept the idea that proper measurements of concentration polarization can be made by a junction piece which interferes with the flow at the electrode surface. The error will be particularly large if such a capillary tube touches the surface.

However, if mass transfer is not controlling (e.g., polarization due to concentration changes in the electrolyte is negligible compared to activation polarization), frontal capillary arrangements can be used satisfactorily.

In selecting the method for coupling the polarized electrode with a reference electrode, it is necessary to choose carefully the type of capillary best justified under the existing conditions. Piontelli's work in this field is of great value and has certainly contributed to a better awareness of the errors involved in the traditional use of frontal Luggin capillaries at some distance from the electrode surface. The realization of the importance of hydrodynamic factors affecting these problems has, in recent years, added to a better understanding of the relative advantages and disadvantages of the various methods, and, since there is no one single, perfect method applicable to all cases, it is hoped that workers in this field will examine their experimental techniques in the light of the present discussion.

ROBERTO PIONTELLI: The stimulating reply of the authors makes some supplementary information opportune

[7] We regret that one of the few presentations of this device in the English language [J. O'M. BOCKRIS, "Modern Aspects of Electrochemistry," p. 265, Fig. 10, Academic Press, New York (1954)] is unfortunate insofar as the probe is represented (Fig. 10 of Bockris' work) placed at some distance from the electrode surface, while, for an efficient shielding of the covered part of the electrode surface, this probe must be pressed against the electrode.

[8] R. PIONTELLI AND G. MONTANELLI, *J. Chem. Phys.*, **22**, 1781 (1954); R. PIONTELLI AND G. STERNHEIM, *ibid.*, **23**, 1358 (1955); R. PIONTELLI, B. RIVOLTA, AND G. MONTANELLI, *Z. Elektrochem.*, **58**, 64 (1954).

[9] R. PIONTELLI, *Rend. ist. lombardo sci.*, **85**, 665 (1955).

on our technique,[10] which takes into account the difficulties pointed out by the authors.

The main goal of our experiments is that of measuring "activation overvoltages" in conditions in which concentration changes at electrodes are minimized. We are in agreement with the authors in believing that stirring obtained by means of propellers or bubbling of gases in the cells may result unsatisfactory, while a liquid flow parallel to the electrode surface may be shielded by an obstacle.

For these reasons, in our cells the active area of electrodes (in the shape of a quite narrow annulus) is uniformly swept by a rapid circular flow of solution entering from two tangential inlets.[11] The cells are designed for working with their axis either horizontal or vertical, but in our present practice this second arrangement is preferred (the electrode surface being thus horizontal), also when stirring is applied. The electrodes are, moreover, subject only to short current pulses.

These precautions, suitable for minimizing composition changes at the electrode surface, also make secondary current distribution very satisfactory, likewise in immediate proximity to the probe. Clear evidence on this point is given in a paper in preparation. Our cells are designed for working in absence of stirring too, but keeping their axis vertical; the known effects, due to natural convection on vertical electrodes in presence of obstacles, recalled by the experiments quoted in the authors' reply, are absent, because the material flow is normal to the electrode surface and unperturbed by the probe. Of course, the realization of conditions of pure diffusion control is by no means easy.

Concluding, I share with the authors of this valuable paper the hope that the problems pointed out by this discussion will find due consideration finally by workers in experimental electrochemistry.

ELECTRODEPOSITION OF MOLYBDENUM ALLOYS FROM AQUEOUS SOLUTIONS

D. W. Ernst, R. F. Amlie, and M. L. Holt
(pp. 461–469)

STANLEY J. KLIMA[12]: How stressed are the nickel-molybdenum deposits?

M. L. HOLT: No measurements were made of the stress in the alloy deposits; however, I would guess that some of the deposits were rather highly stressed.

PERIODIC CURRENT REVERSAL IN PLATING COPPER-LEAD ALLOYS

Nelson W. Hovey, John L. Griffin, and Albertine Krohn
(pp. 470–473)

ABNER BRENNER[13]: The method of obtaining current reversals in different ratios to the direct current developed by the authors is quite ingenious. I would like to suggest a simplification of the apparatus. Instead of using commutator segments and shorting screws, simply 2 metal disks, each of which consists of 2 insulated halves or sectors, could be used. Each sector of one disk is connected by a single flexible lead to the corresponding sector of the other disk. The two brushes for each disk are 180° apart, that is, at opposite ends of a diameter.

Two methods of obtaining reversal of the current may be used. The simplest would be to have the brushes for one disk fixed in position. The brushes for the other disk are set in a frame so that the diameter-line drawn between the brushes can be set at any desired angle to that of the first set of brushes. One set of brushes serves as the input, the other as the output. By simply changing the angle between the diameter-lines of the two sets of brushes, any ratio of direct to reverse current may be obtained. The other method would be to have all four brushes fixed in a frame and to simply rotate one disk to a fixed position relative to the other, such that the diameters along which the half circles are insulated are at an angle to each other.

ALBERTINE KROHN: The authors appreciate Dr. Brenner's evaluation of this paper and his suggestions for the simplification of the apparatus described.

FORMATION OF MANGANESE(II) ION IN THE DISCHARGE OF THE MANGANESE DIOXIDE ELECTRODE

A. M. Chreitzberg, Jr., D. R. Allenson, and W. C. Vosburgh
(pp. 557–561)

J. BRENET[14]: With the assumptions put forward by the authors on the formation of Mn^{2+}, at the time of the discharge of the electrode of MnO_2, it is considered that the reduction product of MnO_2 during the discharge of the cell is, in fact, MnOOH. We have just proved with our collaborators[15, 16] that during the discharge the nature of the active dioxide used has a certain influence, as we have been able to show clearly in the discharged cathodes either the structure of manganite, MnOOH, or the one of γMn_2O_3 isostructural of Mn_3O_4. Besides, in the experimental method utilized by Vosburgh and his collaborators, the deposited dioxide on the carbon is obtained by anodic oxidation. Very certainly it would be easy to verify that γMnO_2 is thus formed. In this case we have shown[15, 16] that γMnO_2 during the discharge evolves toward γMn_2O_3 and not toward MnOOH. Of course, even in the case of γMn_2O_3 it could be considered the ion Mn^{2+} is formed in solution. It would also be interesting for the same authors to examine the case in which utilized dioxide is formed with αMnO_2, as well as with βMnO_2 (pyrolusite), although the activity for the latter one is very weak. Considered from the fundamental mechanisms viewpoint, these studies should be extremely important.

I should add that the reduction of MnO_2 during the discharge is not entirely influenced by the presence of carbon in the cathodes, as we have just shown, when effecting discharges on cathodes entirely free from carbon, therefore composed entirely of MnO_2.

All these researches are extremely important, but, in my opinion, have not yet really allowed the working out

[10] R. PIONTELLI, *Z. Elektrochem.*, **58**, 86 (1954); *ibid.*, **59**, 778 (1955).

[11] Dr. U. Bertocci has given very valuable cooperation in realizing this device in which the liquid flow is derived by argon or nitrogen.

[12] Sperry Gyroscope Co., Great Neck, N. Y.

[13] National Bureau of Standards, Washington 25, D. C.

[14] 9 Rue d'Artois, Paris, 8a, France.

[15] J. BRENET AND A. M. MOUSSARD, Proceedings of the International Symposium on the Reactivity of Solids, Gothenborg 1952, Part II, p. 593, Elanders Boktryckeri Aktiebolag, Gothenborg (1954).

[16] J. BRENET, A. M. MOUSSARD, AND A. GRUND, *Compt. rend.*, **236**, 615 (1953).

of an energetic balance in the Leclanché cells founded on purely chemical mechanisms. Furthermore, none of the theories put forward takes into account the more or less high activities of various dioxides. A complete and satisfactory theory of depolarizing, in my opinion, will have to allow at the same time an energetic balance and a factor characterizing the dioxide activity. Those are points that I have been attempting to develop for several years and which it would be desirable to have investigated further by others.

W. C. Vosburgh: Our experiments and our conclusions are independent of the exact nature of the lower oxide formed. We have often called the reduction product merely lower oxide in order to avoid naming a particular compound that was not identified in our experiments. When writing equations it is necessary to use a definite formula and we have used MnOOH to represent reduction to the trivalent state and Mn_3O_4 to represent further reduction. It should be noted that the lower oxide is assumed to be formed on the surface, and in this state it may not have the same form as the lower oxide found in the discharged electrode.

THE NATURE OF ALUMINUM AS A CATHODE

M. J. Pryor and D. S. Keir (pp. 605–607)

H. K. Farmery[17]: Dr. Pryor and Dr. Keir's Technical Note is extremely interesting to those studying the corrosion behavior of aluminum, although the title is perhaps a little misleading since it is the oxide that is really being considered.

When the surface film on the metal is essentially aluminum oxide, then not only will the weak spots be the most likely places for electrons to migrate through the film but also the metal cations. In other words, the anodic and cathodic regions will be in close proximity. If, however, the oxide film contains other metal ions apart from aluminum, e.g., copper or iron, it becomes more conductive and, consequently, electrons can migrate through thicker films; in this way the anodic and cathodic reactions can be spatially separated.

Such mixed oxide films are more likely to occur on clean metal surfaces exposed to the air at room temperature than at high temperatures, since the oxide will be formed from the metal atoms at the surface in the first case, whereas, at high temperatures, with greater diffusion rates, preferential oxidation can occur.

This may account partially for the greater reactivity of etched aluminum surfaces compared with those carrying a high temperature formed film although the greater thickness of the latter will obviously affect the movement of electrons and metal cations. As examples of this enhanced reactivity, the stress-corrosion lives of susceptible Al–7% Mg and Al–4% Cu sheet tensile specimens when stressed at a high proportion of their Proof Stress in 3% NaCl solution can be cited.[18]

Material	Lives with thick heat-treated film present	Lives when tested after etching
		min
Al–7% Mg	~4 days	1½–3
Al–4% Cu	>1 week	18–30

Furthermore, etched Al–7% Mg will crack in completely deaerated 3% NaCl solution. This surprising result shows that when the metal carries only the thin room temperature air-formed film, corrosion can proceed without the presence of dissolved oxygen, at least in the early stages.

With regard to the patterns of copper deposition:

(*A*) I would not say that the spots are entirely random on the cold-rolled sample and could be visualized as sitting on the boundaries of elongated grains, although in a less continuous state than on the annealed sample; perhaps knowing the grain size and shape would help here.

(*B*) Is the pattern obtained with the annealed sample independent of heat treatment? Several workers have demonstrated that high purity aluminum can suffer from intense intercrystalline corrosion in hydrochloric acid after a particular heat treatment (usually quenching from a high temperature) and this is ascribed to segregation of impurity atoms such as iron and copper to the grain boundaries. If the annealed sample is in such a condition, an alternative explanation of the copper deposition along grain boundaries could be that the mixed oxide above such regions has a better electronic conductivity than the more pure alumina over the grain interiors and will therefore be more likely to function as a cathode.

It would be interesting to know whether similar patterns are obtained with no applied current and also with higher current densities than those mentioned.

Finally, I think the authors will agree that the patterns they obtain and the conclusions they draw apply mainly to surfaces carrying only a very thin film and that, if both samples had been tested as-received, in other words, with a high temperature formed film, there would have been much less difference in behavior.

M. J. Pryor and D. S. Keir: We thank Dr. Farmery for his interesting discussion and suggestions. It is, of course, implicit that one must consider the characteristics of oxide-covered aluminum in neutral solutions containing dissolved air, rather than those of the metal itself. We agree that the so-called "weak spots" in the air-formed film will probably constitute preferential sites not only for electron migration but also for anion migration. However, it is not necessarily true that impurity atoms in the metal must decrease the electronic resistance of thin oxide films. Very thin oxide films of up to about 50 Å on most metals will contain very substantial quantities of excess metal ions and therefore will show a high degree of *n* type semiconduction irrespective of whether the bulk oxide exhibits semiconduction of the *n* or the *p* types. Whether foreign atoms present in the metal will further enhance the conductivity of thin oxide films will depend among other things on whether they may be easily substituted in the oxide lattice. This may be achieved only if the cation is of similar size to that of the aluminum ion in the oxide lattice. Furthermore, the effect of small quantities of impurity atoms might well be masked by the larger quantities of excess metal ions in very thin oxide films.

It would appear more logical to attribute the greater electronic resistance of thicker thermally produced oxide film to the fact that the number of *n* type defects (due to

[17] Fulmer Research Institute, Stoke Poges, Bucks., England.

[18] H. K. Farmery and U. R. Evans, In press.

excess aluminum ions in the oxide lattice) will decrease with increasing distance from the metal/oxide interface. Therefore, the outer portions of the thermal films should be much less defective in nature and should exhibit much higher electronic resistances. It is of interest to point out that in fairly thick films of Cu_2O (which exhibits p type semiconduction in the bulk oxide) there will be a fairly well defined p-n junction some 50–100 Å from the oxide/metal interface.

With regard to the patterns of copper deposition on the cold-rolled aluminum, it is possible that a case could be made out for grain boundary deposition. However, if this is assumed then it must also be considered that the deposition is much less continuous than on the annealed specimens. We believe that the pattern of copper deposition on annealed aluminum is not markedly sensitive to annealing treatment. Whereas it has been postulated that the distribution of impurity atoms in aluminum is affected by heat treatment, we believe, for the reasons stated above, that the impurity atoms have rather little effect on the conductivity of thin aluminum oxide films. Such impurity atom effects might be more logically anticipated on the thicker thermal films where the effect of metal excess defects should be smaller.

Similar copper deposition patterns may be obtained with no applied current. However, as pointed out in the article, more general conduction of electrons occurs at higher current densities of around 20 $\mu a/cm^2$.

In conclusion, the results described are specific for aluminum carrying thin air-formed films (approximately 50 Å thick). With thicker thermal films we suspect somewhat different results would be obtained and that the problem would be greatly complicated, particularly on ferrous materials by the formation of multilayer scales.

THE ELECTROCHEMICAL BEHAVIOR, INCLUDING HYDROGEN OVERVOLTAGE, OF IRON IN ACID ENVIRONMENTS

Milton Stern (pp. 609–616)

J. O'M. Bockris[19]: I am most glad to have read Dr. Stern's stimulating paper. His approach is exceedingly clear and we have waited a long time for the kind of data which he has been measuring.

The pre-electrolysis carried out in the NaCl-HCl solution was only at 15 μa for 24 hr. It is, in my experience, rather better to carry out pre-electrolysis of such solutions at a current density corresponding to the highest potential which one is going to measure during the course of the work. Capillary active substances are then given to have the best possible opportunity to deposit.

It is quite easy to develop an expression for the corrosion rate in the absence of surface films and I believe that the one expression recently developed[20] would be applicable with little modification to most of Dr. Stern's results.

I agree strongly with Dr. Stern's remarks on the importance of concentration overpotential. It is, however, possible to stay away from this troublesome interference if one calculates that the actual current densities measured are always less than about one tenth of the limiting current densities for the species involved. An upper limit for i_L can always be calculated with some approximate appropriate value of δ, the diffusion layer thickness.

Regarding the mechanism of the hydrogen discharge reaction after the limiting current for the discharge process for hydroxonium ions has been reached, it is not so much that the dissociation of water is too low (which it is) but that it is too *slow*. It would be possible to have water dissociating near to the cathode and giving rise to protons, which then, after hydration, discharge, even though the equilibrium dissociation of water is very low. This is not the case as was shown by the calculations carried out by Watson.[21]

Milton Stern: We were well aware of the careful work of Professor Bockris and his associates concerning solution purification and pre-electrolysis. However, our purpose was to study the relations which exist between hydrogen overvoltage and the corrosion behavior of iron. Thus our system, of necessity, contained corrosion products. For many of the alloys studied, the corrosion products in solution undoubtedly played a significant role in determining the overvoltage behavior. Our experiments showed that cathodic polarization did not appreciably affect the corrosion potential after the applied current was stopped. The electrode rapidly assumed its initial steady-state potential. This was interpreted as an indication that deposition of capillary active substances during cathodic polarization played an insignificant role.

It is true that one may eliminate concentration polarization interference by maintaining current densities which are less than about one tenth the limiting diffusion current density. However, this in itself does not guarantee that a real Tafel slope will be observed. For a corroding electrode, it is necessary that one apply a current density many times greater than the corrosion current density in order to observe Tafel behavior. Thus the corrosion current density must be at least one hundredth of the limiting diffusion current density to permit an experimental determination of the constants β and i_o.

The clarification by Professor Bockris of the mechanism of hydrogen discharge at high current densities is sincerely appreciated. The concepts which he has presented in his many publications stimulated the approach taken in this investigation. Application of the principles presented in his most recent book will lead undoubtedly to marked advances in the understanding of corrosion mechanisms, polarography, and electrodeposition phenomena.

A. J. deBethune[22]: Referring to the diagram, how is the corrosion current $I_{corr.}$ determined without a knowledge of the anodic polarization curve?

Milton Stern: The answer to the question by Professor deBethune is adequately presented by equation (VIII) and its associated discussion on page 613 of the original paper. However, a general discussion of the method may prove more satisfactory. When a metal corrodes electrochemically, the total rate of all the reduction reactions which occur must equal the total rate of all the oxidation

[19] John Harrison Lab. of Chemistry, University of Pennsylvania, Philadelphia 4, Pa.

[20] J. O'M. Bockris, "Modern Aspects of Electrochemistry," Chapter IV, Academic Press, New York (1954).

[21] Watson, Thesis, London (1951).

[22] Boston College, Chestnut Hill 67, Mass.

reactions. For iron corroding in an acid, two electrochemical oxidation-reduction systems are operative. The first is the hydrogen ion–hydrogen gas system, while the second is the iron (metal)–iron (ferrous) system. The possible oxidation reactions are (*A*) Fe (metal) $\rightarrow Fe^{++} + 2e$ and (*B*) $H_2 \rightarrow 2H^+ + 2e$. The possible reduction reactions are (*C*) $Fe^{++} + 2e \rightarrow$ Fe (metal) and (*D*) $2H^+ + 2e \rightarrow H_2$.

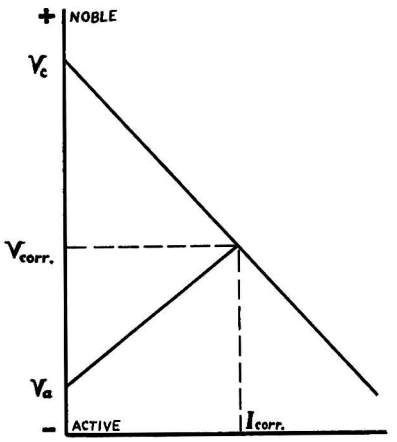

f(I)

At the corrosion potential, the sum of the rates *A* and *B* equals the sum of the rates of *C* and *D*. Since the corrosion potential is not close to the equilibrium potentials of either of the oxidation-reduction systems, reactions *B* and *C* proceed at negligible rates. Therefore, the total rate of reduction of hydrogen ions (reaction *D*) equals the total rate of oxidation of iron (reaction *A*). By definition, the corrosion rate is equal to the rate at which reaction *A* proceeds. Therefore, one may determine the corrosion rate by determining the rate of reduction of hydrogen ions at the corrosion potential. The Tafel constants β and i_o describe the rate of reduction of hydrogen ions at any potential in accordance with equation (VI) of the original paper.

$$\eta_a = -\beta \log \frac{i_{\text{reduction}}}{i_o}$$

If β, i_o, and $\eta_{corr.}$ are known, $i_{\text{reduction}}$ may be calculated. As stated above, this is equivalent to the corrosion rate.

ELECTRODEPOSITION OF TITANIUM ON BASE METALS

M. E. Sibert and M. A. Steinberg (pp. 641–647)

MORRIS EISENBERG[23]: 1. Did you determine the porosity of the titanium coating on steel?

2. You stated that as a result of the high temperature a TiC-layer formed between the steel base or coating. Wouldn't this cause brittleness in the substrata with a resulting poor adhesion? Was the adhesion of the coating measured?

M. E. SIBERT AND M. A. STEINBERG: 1. No absolute porosity determinations were made. Corrosion testing in HCl, H_2SO_4, HNO_3, and NaCl solution indicated that the coatings were essentially nonporous for practical purposes. Some surface porosity does exist, but in no case was this metallographically observed to be continuous through the coating to the base metal.

2. In the case of deposits applied to mild steel, a layer which is probably a Ti-C alloy is formed between base metal and the coating. Adhesion was excellent on as-deposited specimens in terms of resistance to peeling or flaking during cutting and grinding operations. Adhesion of worked coatings was not as satisfactory. This property was not measured quantitatively.

LEO GOLDENBERG[24]: The authors have presented a fine contribution to the knowledge of titanium deposition from a fused salt bath. I was particularly impressed with the description of the properties which the titanium plate was found to possess. At the same time I was somewhat disappointed that the bibliography did not include the citation of *Industrial and Engineering Chemistry*.[25] The similarity of the author's plate to what I had reported there is striking.

However, there are some features of the article about which I am curious. From a comparison of the amount of titanium plated to the number of ampere hours for each run as noted in Table I of the article under discussion, I have calculated a cathode current efficiency of less than 10%. Is this correct? How much, if any, metallic titanium is precipitated in the electrolyte as powder? At what point does the build-up of alkali metal fluorides interfere with cell operation? How stable is the K_2TiF_6 at plating temperatures in excess of 800°C? It would appear that any instability would add to the build-up of alkali metal fluorides in the electrolyte. What was the composition of the gaseous materials leaving the electrolyte during the plating operation?

M. E. SIBERT AND M. A. STEINBERG: Current efficiency based on the plate alone is only 5–15%. Over-all current efficiency including adhering titanium powder amounts to 40–60%. In this study no effort was made to avoid deposition of some powder. The powder is not precipitated in the electrolyte but deposits as an adherent mass after 0.002–0.003 in. of plate has been deposited.

The melt is operated satisfactorily with F^- contents up to 35%. At least 6–8 K_2TiF_6 charges (16 wt %) may be made before this occurs.

The K_2TiF_6 is increasingly unstable with temperature although dilution with NaCl and fluorides minimizes the loss of TiF_4. At 850°C with no current, the loss figure is <10% of initially charged Ti/hr. This figure is reduced considerably on application of a current and as fluoride concentration is built up.

Composition of the effluent gas during plating is approximately 1% CO, <0.5% CO_2, 20% Cl_2, and the balance argon.

[23] Stanford Research Institute, Stanford, Calif.

[24] 1005 Merrimac Drive, Silver Spring, Md.

[25] L. GOLDENBERG, *Ind. Eng. Chem.*, **46**, 13A (1954).

INFLUENCE OF THE K ABSORPTION EDGES OF CADMIUM AND SILVER ON THE X-RAY DIFFRACTION PATTERNS OF SOME CADMIUM COMPOUNDS

R. J. Robinson and F. Schossberger (pp. 685–686)

W. G. BURGERS[26]: In connection with the interesting results of their paper, it may be of interest to the authors that a similar "shifting-out" of a narrow spectral band due to the closeness of the K absorption edges of silver in the film emulsion and the substance matter of the specimen (in this case tin) was observed by Arlman and Kronig[27] in an investigation of diffuse x-ray reflections of a single crystal of tin.

[26] Laboratorium voor Physische Chemie, Technische Hogeschool, Julianalaan 136, Delft, Netherlands.

[27] J. J. ARLMAN AND R. KRONIG, *Physica*, **10**, 795 (1943).

FUTURE MEETINGS OF The Electrochemical Society

Cleveland, September 30, October 1, 2, 3, and 4, 1956

Headquarters at the Statler Hotel

Sessions will be scheduled on

Batteries, Corrosion, Electrodeposition, Electrothermics and Metallurgy, Theoretical Electrochemistry (joint with Electrodeposition), and Theoretical Electrochemistry

★ ★ ★

Washington, D. C, May 12, 13, 14, 15, and 16, 1957

Headquarters at the Statler Hotel

★ ★ ★

Buffalo, October 6, 7, 8, 9, and 10, 1957

Headquarters at the Statler Hotel

★ ★ ★

New York, April 27, 28, 29, 30, and May 1, 1958

Headquarters at the Statler Hotel

★ ★ ★

Ottawa, September 28, 29, 30, October 1, and 2, 1958

Headquarters at the Chateau Laurier

★ ★ ★

Papers are now being solicited for the meeting to be held in Cleveland. Triplicate copies of each abstract (*not exceeding 75 words in length*) are due at the Secretary's office, 216 West 102nd Street, New York 25, N. Y., *not later than June 15, 1956* in order to be included in the program. *Please indicate on abstract for which Division's symposium the paper is to be scheduled.* Complete manuscripts should be sent in triplicate to the Managing Editor of the JOURNAL at the same address.

ECS Sustaining Member

Pennsalt . . . Pioneer of the Electrochemical Industry

When the American Electrochemical Society was founded in April 1902, the Pennsylvania Salt Manufacturing Co. had been producing industrial chemicals for more than 50 years. Prominent among its early products was caustic soda (soda lye) made by chemical methods using common salt as a raw material. Pennsalt's charter, registered on September 25, 1850, described the company's business as "the manufacture of salt and articles resulting therefrom."

Older chemical companies in England and elsewhere in Europe had been studying for many years the effect of the passage of electricity through chemical compounds and solutions. One such process gave promise of becoming a better method of producing caustic alkalies. In this process, electric current was passed through solutions of salt brine held in tanks which were fitted with two electrodes. One of these was a pool of mercury which covered the bottom of the tank. Caustic soda was the product desired but two by-products resulted: chlorine, for which there was little demand except for making chloride of lime for bleaching and disinfecting, and hydrogen, also of little use but readily disposed of by release into the air.

This new caustic alkali process required a plentiful supply of salt, good transportation facilities, and a location giving promise of industrial growth and good markets. Pennsalt found such a site at Wyandotte, Mich., on the bank of the Detroit River just below the city of Detroit. Below the surface of the land Pennsalt purchased was an extensive bed of suitably pure salt. The first electrolytic process installed at the Wyandotte plant was one developed in England by George Bell. Pennsalt had purchased the patent rights. But the process proved difficult and inefficient, for large quantities of mercury were lost during the operation. When determined efforts to improve the operation failed, the use of this system was discontinued. Years later while excavating for a new building, hundreds of pounds of "lost" mercury were uncovered from cavities under the old plant site.

In 1904 a young Englishman, Arthur E. Gibbs, deeply interested in electrolytic processes and working for a Canadian chemical manufacturer near Niagara Falls, offered his services to Pennsalt, hoping to have an opportunity to study the electrolytic decomposition of salt. Although not a charter member of the American Electrochemical Society, he joined the organization six months after it was formed and was closely associated with it for over 45 years.

Gibbs developed a small experimental cell, only 12 in. high, which produced enough caustic soda to stimulate further work. Several larger cells were constructed and production became commercially important. These cells were of a cylindrical design having anode and cathode concentrically arranged with a semipermeable membrane or diaphragm of asbestos placed between them to prevent the products formed at the surface of the two electrodes from intermixing. The

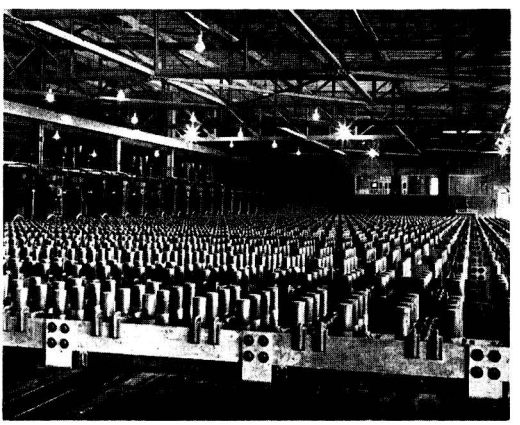

DeNora cell room, hub of Pennsalt's newest chlor-caustic plant at Calvert City, Ky.

anodes were of graphite, as in the Bell cell, but the cathode was of perforated iron, no mercury being used.

The first cells retained the weak caustic soda solution in the cathode chambers but soon the cathode solution was permitted to drain from that space as rapidly as it formed. Thus the "Gibbs Cell" was identified by its cylindrical construction and empty cathode chambers.

During the 15 years that followed, development of the Gibbs chlorine-producing cells proceeded rapidly. Others became interested in the design and operation of these units and sponsored the construction of similar electrolytic cells for use by other companies: the Tucker-Windecker Cell (used by Diamond Alkali), the Wheeler Cell (at Kimberly Clark Paper Co. and the Niagara Alkali Co.), and the Vorce Cell (Westvaco and elsewhere). Thus, for many years, the bulk of the chlorine produced in the United States came from the Gibbs cell, or derivatives of it.

Pennsalt has continued to use Gibbs cells of improved design, and has not only increased the installation at Wyandotte but has two other large chlorine-producing units equipped with these cells in the Pacific Northwest: one at Tacoma, Wash.; the other at Portland, Ore.

Although the Bell cell had shortcomings, the use of mercury for the cathode surface has been actively studied. Successful cells using it were developed years ago in Europe and England as well as more recently in the United States. Pennsalt constructed a plant using deNora mercury cells at its Calvert City, Ky., plant in 1953.

The products of the Gibbs cell furnish the raw materials for a large number of Pennsalt products. Caustic soda, which is first converted to sodium orthosilicate, is the base for a large number of detergents and cleaners. The chlorine, which

was considered as an obnoxious by-product 50 years ago, is now one of industry's most important chemicals. Reacting chlorine with hydrogen (also once a by-product of little value) forms a very pure hydrochloric acid. The acid in its anhydrous form is sold for conversion to vinyl chloride. With ammonia, hydrochloric acid forms ammonium chloride, used in large quantities in galvanizing iron. Causing chlorine to react with scrap iron forms ferric chloride, which is important in sewage treatment and water purification. Chlorine is also used in the manufacture of calcium hypochlorite bleaches. At first it was made into bleaching powder, but in recent years a greatly improved and more highly concentrated calcium hypochlorite has been produced.

Pennsalt's largest use for the electrolytic hydrogen produced in the Gibbs cells is in the production of ammonia. A portion of the hydrogen is sold as such to other chemical manufacturers.

Pennsalt has not limited its activities in the electrolytic field exclusively to the production of caustic alkali. In 1928 the company purchased a process for forming ammonium persulfate by electrolysis and has operated it continuously at Wyandotte since. In 1937, production of hydrogen peroxide was begun. The first step in this process consists of the formation of ammonium persulfate by electrolysis. Electrolytic production of sodium and potassium chlorate was started in 1941 at the Portland plant.

In addition to these chemicals, Pennsalt also produces benzene hexachloride and D.D.T. as an end product as well as special preparations in the form of dusts, sprays, and emulsions. Solutions of hydrofluoric acid are used in a variety of laundry soaps and rust removers. The list of products also includes acid and alkali resistant cements, paints, ceramic fluxes, and many other chemical specialties.

The vigorously active chemical element, fluorine, which belongs to the same family as chlorine, is also produced through the application of electrochemistry, although it is rather difficult to handle and special technique is required. This useful gas, first produced by Pennsalt at its Whitemarsh Research & Development Labs. in 1948, has a key role in the company's current expansion program.

While many of the products manufactured by Pennsalt result from strictly chemical operations, a large part of its activities involve the application of electrochemistry. It is natural, therefore, that the Pennsylvania Salt Manufacturing Co. should take pleasure and pride in its association with The Electrochemical Society as a Sustaining Member.

News Notes in the Electrochemical Field

First Patron Member

The International Nickel Co., Inc., New York, N. Y., which previously held two Sustaining Memberships in the Society, has become its first Patron Member.

New Sustaining Member

Shawinigan Chemicals Ltd., Montreal, Que., Canada, recently became a Sustaining Member of the Society.

M.I.T. Special Summer Program

Metallurgical Applications of X-Ray Diffraction will again be the subject of a two-week Special Summer Program from July 9 through July 20 during the 1956 Summer Session at the Massachusetts Institute of Technology.

According to Professor Ernest H. Huntress, director of M.I.T's Summer Session, the program will provide discussions of the principles of x-ray diffraction illustrated by examples of the practical techniques employed in metallurgical problems. It will be under the direction of Dr. John T. Norton, Professor of the Physics of Metals in the M.I.T. Dept. of Metallurgy. Professor Norton will be assisted in presenting the program by other members of the M.I.T. Faculty and staff and by a number of guest lecturers.

The program is not envisioned as a research conference. The lectures will be directed toward metallurgists who have not had advanced work or who may have been out of school for several years. Elementary knowledge of the nature of x-rays and the structure of metals will, however, be required.

Full details and application blanks may be obtained from the Summer Session Office, Rm. 7-103, Massachusetts Institute of Technology, Cambridge 39, Mass.

Foote Mineral–Electro Manganese Exchange

Foote Mineral Co., Philadelphia, Pa., has announced the exchange of 169,178 of its shares for the assets and business of the Electro Manganese Corp.

The operations of Electro Manganese in Knoxville are being handled as a division of Foote as of March 17.

Pennsalt Growth Program

The Pennsylvania Salt Manufacturing Co. has announced expansion of chlor-caustic facilities at its Calvert City, Ky., works as part of its $55 million growth program. "The new unit," President William P. Drake stated, "will increase chlorine production from 50 to 150 tons a day with accompanying increase of rayon grade caustic soda production. It is anticipated there will also be an increase in caustic potash production."

With preliminary engineering completed and construction scheduled to begin in the near future, the new unit will go into operation during 1957. It will utilize facilities and services incorporated in the existing plant which was completed in 1953. Under a licensing agreement with Monsanto, it will employ the newest type deNora cell.

Science Grants and Awards

Fifteen outstanding college students working for their doctor's degrees have been named to receive the 1956 Bell Telephone Laboratories Graduate Fellowships. The winners include 14 men and one woman.

The fellowships, awarded for the first time this year, were established to encourage study and research in engineering and science related to communications technology. Each fellowship is for one year and carries a grant of $2000 for the fellow and another $2000 for tuition, fees, and other costs of the academic institution he selects for his study.

An expanded program for Monsanto Chemical Co.'s financial aid to scientific education during the 1956–57 school year has been announced.

A total of 83 American colleges and universities will benefit from 111 separate direct aid awards under the program. This is an increase of 30 in the number of schools aided and 39 in the number of awards over the company's 1955–56 program.

The awards for the coming school year include 29 fellowships, 41 under-

graduate scholarships, and 41 cash grants. The fellowships are established for graduate study with the larger part of their $3000 average value going to the individual. The scholarships are intended to cover tuition costs. The company retains no control over the fellowships and scholarships. Choice of recipients is made by the administering schools on the basis of merit and need. The cash grants may be used at the schools' discretion to finance research, purchase equipment, or further any other scientific purpose.

ASTM Committee Week

Thirty-three technical committees of the American Society for Testing Materials held approximately 350 committee and subcommittee meetings at the society's annual Committee Week at the Statler Hotel, Buffalo, N. Y., February 27 to March 2. About 1300 technical men worked intensively during the five days of meetings discussing and correlating the great amount of research upon which ASTM specifications and methods of test are based, and putting into final shape new and revised tentatives and standards which the several committees will recommend to the society for adoption at its Annual Meeting at Atlantic City, June 16–21.

A reception and dinner in honor of ASTM President Claire H. Fellows was held Tuesday evening, February 28, sponsored by the Western New York–Ontario District.

An important highlight of the week's technical activities was an all-day symposium, Wednesday, February 29, on "Properties, Tests, and Performance of Electrodeposited Metallic Coatings." The symposium was sponsored by ASTM Committee B-8 on Electrodeposited Metallic Coatings. More than 300 attended the session.

Niagara Falls Plant Expansion

Stauffer Chemical Co. has announced plans to invest a million dollars in an expansion and modernization of its Niagara Falls, N. Y., plant. About $400,000 of the investment will be for additional facilities to manufacture 73% caustic soda. Approximately $150,000 will be spent to increase output of chlorinated solvents.

The company also plans to extend and improve several existing plant units which are now producing chlorine, caustic soda, titanium tetrachloride, silicon tetrachloride, and zirconium tetrachloride.

It is anticipated that the additions will be in operation by late summer.

SECTION NEWS

Midland Section

The first meeting of the year for the Midland Section was held on December 6, 1955. Professor H. H. Uhlig spoke on "Corrosion as an Electrochemical Process."

He traced the development of the electrochemical theory of corrosion from its early beginning to the present and discussed the various types of corrosion, explaining each in terms of theory.

The three kinds of cells functioning in corrosion were considered: (*a*) dissimilar metals, (*b*) concentration cells, and (*c*) differential temperature cells. Corrosion of aluminum, zinc, and magnesium containing cathodic impurities, galvanic couples, variable grain size are examples of the first kind.

Differential aeration is the most important example of type (*b*). Type (*c*) cells may be encountered in various kinds of heat exchangers.

The mechanism of pitting, particularly of stainless steel, postulates the transfer of chloride ion to the local anodic areas or pit nuclei under the influence of current. Accumulation of concentrated solutions of metal chlorides at the anodic sites destroys passivity of the adjacent metal and allows the pit to grow. A common method to inhibit pitting of stainless steel in sea water is by making the sea water more alkaline and precipitating the basic metal chlorides.

Polarization curves and potential measurements are helpful in a study of corrosion to supplement our knowledge of the mechanism involved. They are useful in measuring the degree of passivation and may be employed to calculate corrosion rates in some environments.

A dinner at the Midland Country Club preceded the meeting. President Uhlig gave a short talk outlining the achievements, goals, and problems of the Society.

The second meeting of the Midland Section was held January 17, 1956, with Dr. Ernest Yeager of Western Reserve University as guest speaker. He discussed recent advances in instrumental methods for the study of electrode processes.

Utilization of various applied current polarization techniques in the investigation of electrode processes is currently receiving widespread attention. However, Dr. Yeager cautioned that the direct polarization method, i.e., the measurement of the electrode potential while current is flowing, is subject to serious misinterpretation due to the inherent *IR* drop contribution which is included in this type of measurement. In a high impedance electrolyte this factor may completely mask, or, at best, severely distort the activation polarization phenomena.

Dr. Yeager discussed several recent improvements in commutator or interruptor circuits which permit the determination of the polarized electrode potential without the inclusion of *IR* drop effects. Instruments with interruption periods of 10^{-6} to 10^{-7} sec are now readily available. In the laboratory at Western Reserve University the interruptor circuit is utilized in exploratory studies on electrode processes at the oxygen electrode, the oxygen overvoltage phenomena, and in fundamental investigations of other electrode reactions. Several illustrations were shown on anodic, cathodic, and total cell polarization.

Decay of electrode polarization as a function of time after current interruption was considered on a rather general basis. *IR* drop polarization decays completely in 10^{-10} to 10^{-11} sec after current interruption, activation overvoltage decay is observed within 10^{-5} to 10^{-7} sec, while concentration polarization remains stable for approximately 10^{-3} sec. This latter effect and the corresponding ionic diffusion gradient involved in concentration polarization may be studied through the recently expounded Schlieren technique.

In the discussion that followed, Dr. Yeager replied to inquiries on the usefulness of the current interruptor circuit in polarization studies directed toward the evaluation of corrosion inhibitors, and to the investigation of the corrosion characteristics of stainless steels in passivating media. He also mentioned that this technique should be applicable to the study of electrode processes involved in the corrosion of magnesium as a galvanic anode.

A dinner at the Midland Country Club preceded the meeting.

H. W. SCHMIDT, *Secretary-Treasurer*

New York Metropolitan Section

The Metropolitan Section held a regular meeting on April 11. By unanimous vote the following were elected officers of the Section for the 1956–57 fiscal year:

Chairman—C. V. King, New York University, New York, N. Y.

Vice-Chairman—K. B. McCain, Wilbur B. Driver Co., Newark, N. J.

Secretary-Treasurer—Frances Lang, International Nickel Co., Inc., New York, N. Y.

The guest speaker for the evening was Dr. Robert M. Adams who spoke on the subject "Fluorocarbons—or the Taming of a Shrew."

Although Moissan succeeded in releasing fluorine from inorganic materials in 1886, and claimed to have produced C_2F_4, it remained for Schwarz in the early 1900's to do work which has led to present-day activity in fluorocarbons. Midgely and Henny, making full use of Schwarz's studies, were able to produce chlorofluorocarbons, which are known today as the Freons. The elements carbon, fluorine, and chlorine combine to form stable, nontoxic, noncorrosive compounds. Some of these compounds have been discovered accidentally, such as polyfluoroethylene, generally known as Teflon. A similar compound that was developed is perfluorovinyl chloride or Kelef. Through the work of Simonds an electrochemical method was devised for producing completely fluorinated materials. Hydrocarbon and anhydrous hydrogen fluoride are passed into an iron cell where an electric current is passed through the mixture. The products are fluorocarbons and hydrogen. Through the discovery of perfluorobutyramine a way was found for adding groups to the molecule. In the production of fluorocarbons it is difficult to control processes employing reactions of elements and simple groups. The electrochemical process is a practical, economic way of producing desirable products. The fluorocarbons have found acceptance because of three important properties: stability, incompatibility, and surface activity. Some of these properties are very important in determining the uses of these compounds. A preparation containing one of these compounds is the first commercial material available for use in chromium plating baths to control misting. The fluorocarbons have found extensive use in refrigerants, propellants, lubricants, in rubbers, and in the impregnation of paper and fabrics. These compounds are water and oil repellent. The fluorinated rubbers are resistant to attack by oils. While the price of the fluorinated compounds is relatively high, improvements in manufacturing processes and increasing use will tend to bring prices down.

M. F. QUAELY, *Acting Secretary*

Ontario–Quebec Section

The winter meeting of the Ontario–Quebec Section was held on February 10 at McGill University, Montreal. About 60 were in attendance.

Mr. P. E. Cavanagh, Director, Dept. of Engineering and Metallurgy, Ontario Research Foundation, presented a paper on "How to Use More Canadian Iron Ore in Canada." He stated that the production of iron ore, pig iron, and steel are a basic index of the general wealth, industrialization, and strength of any country. Since the 1930's the production of iron ore in Canada has increased from zero to about 15,000,000 tons per year. In the same short period of about 25 years, the steel industry has doubled in output, while the consumption of steel also has doubled. Canada is now third in steel consumption per capita behind the United States and Sweden. In the 1930's all our iron ore was imported in order to make steel, whereas today Canada is exporting considerably more iron ore than she imports.

It appears certain that production of iron ore in Canada will at least double in the near future, and it is not beyond the realm of possibility that the rate of production will be at the level of about 45,000,000 tons per year at the end of the next 25 year period, in 1980. It also appears certain that most of this iron ore will be exported to the United States, with some proportion going to Europe. In this situation it is logical and proper at the present time for Canadians to consider means of converting a considerable part of this Canadian iron ore into semifinished or finished products here in Canada.

Mr. Cavanagh estimated that, in 1980, 67% of the iron ore produced in Canada will be exported, 27% will be used by the orthodox steel industry.

Dr. M. Sem, the second speaker, is Technical Director of Elektrokemisk A/S, Oslo, Norway. He presented a paper entitled "Latest Developments in Electric Pig Iron Smelting." He stated that in the spring of last year the Norwegian Government's new integrated iron and steel works at Mo i Rana commenced operation. These works are, at the present initial stage, scheduled to produce annually about 180,000 metric tons of iron and steel products, based on the electric smelting of domestic iron ores. For this purpose Elektrokemisk A/S have designed a

MANUSCRIPTS AND ABSTRACTS FOR FALL MEETING

Papers are now being solicited for the Fall Meeting of the Society, to be held at the Statler Hotel in Cleveland, September 30, October 1, 2, 3, and 4, 1956. Technical sessions will be scheduled on Batteries, Corrosion, Electrodeposition, Electrothermics and Metallurgy, Theoretical Electrochemistry (joint symposium with Electrodeposition), and Theoretical Electrochemistry.

To be considered for this meeting, triplicate copies of abstracts (not to exceed 75 words in length) must be received at Society Headquarters, 216 West 102nd St., New York 25, N. Y., *not later than June 15, 1956. Please indicate on abstract for which Division's symposium the paper is to be scheduled.* Complete manuscripts should be sent in triplicate to the Managing Editor of the JOURNAL at the same address.

***

The Spring 1957 Meeting will be held in Washington D. C., May 12, 13, 14, 15, and 16, at the Statler Hotel. Sessions will be announced in a later issue.

new closed electric low shaft furnace of the Tysland-Hole type, with a capacity of about 20,000 kw and a daily production of approximately 200 metric tons of pig iron. This capacity is about twice as large as that of any electric pig iron furnace which has been in operation to date. Three of these furnaces have been erected. The hydroelectric power supplied has a frequency of 50 cycles and, for correction of the power factor, large capacitor batteries have been installed in connection with the furnace transformers. A description of furnace design and layout was included in the paper. The furnaces have shown very satisfactory results during the first period of operation. The reported power consumption per ton of pig iron is favorable, and electrode consumption is lower than previously obtained in this field of smelting. From the start, the furnaces have operated without disturbances. It is hoped that arrangements can be made to publish Dr. Sem's complete paper in the JOURNAL.

R. R. ROGERS, *Secretary-Treasurer*

San Francisco Section

A regular Section meeting was held on March 21 at the Faculty Club of the University of California, in Berkeley. The speaker for the occasion was Mr. Joseph C. Schumacher, Director of Research of American Potash and Chemical Corp. and Regional Editor of the JOURNAL for the Los Angeles area.

At the business meeting preceding the technical paper of the evening, a report on the preparations for the Spring 1956 Convention was given. It was also announced that the Section had become one of the participating members of the "San Francisco Engineer," a publication which reaches most of the Bay area engineers. Mr. Schumacher reported that considerable progress is being made toward organization of a Los Angeles Section of the Society.

The technical topic covered by Mr. Schumacher was the "Commercial Electrolytic Production of Manganese Dioxide." The paper covered development of a process to make battery-grade MnO_2 from the laboratory stage to plant-scale production.

The γ-form of MnO_2, which is the battery-active form, is rarely found in nature; the largest deposit of this material is located in the Gold Coast, in Africa. Its exact nature is still the subject of many debates, although it can be identified by means such as the electron microscope or x-ray diffraction.

Synthetic battery-active MnO_2 is better than the natural product, but, as late as 1950, its production constituted less than 2% of the 60,000 tons required annually in the U. S. Under the impetus of the Signal Corps, Western Electrochemical Co. (now part of American Potash and Chemical) started to investigate, on a laboratory scale, production of active MnO_2 from an abundant source of domestic, inactive MnO_2. The basic process consists in reducing the ore to MnO, leaching the ore with H_2SO_4, then electrolyzing the $MnSO_4$ solution to re-form an active grade of MnO_2 at the anode.

Laboratory studies showed that best results and highest efficiencies were obtained at about 10 amp/ft², 95°C, and higher $MnSO_4$ concentrations (say 150 g/l). Graphite anodes were used. Cells can be run for as high as 30 to 60 days, and MnO_2 deposits as thick as 1 in. can be built up, with little change in current or cell voltage over this period. The product is rather difficult to remove from its graphite base, but, since some graphite can be tolerated in the final product, the starting anode and deposit are ground up together. Electrolyte purity was found to be important, and such contaminants as Cu or Fe are harmful.

Mr. Schumacher next described the prototype cells built at Culver City, Calif., and then the full-scale plant which is located in Henderson, Nev. This plant uses 30 cells, and each cell operates for approximately 30 days, so that every day one of the cells is shut down, the product removed, and new anodes installed; this makes for good use of all plant facilities. In 30 days, each cell builds up 10 tons of product, so that the plant capacity is 10 tons per day. The product is about 91-92% MnO_2, contains some combined water, and exceeds Signal Corps specifications.

The audience manifested its interest with a series of questions, and a lively discussion of some of the phases of anodic MnO_2 deposition followed.

MORRIS FEINLEIB, *Vice-Chairman*

Washington-Baltimore Section

The Section held its 39th technical meeting on March 15 at the National Bureau of Standards. James R. Nall of the National Bureau of Standards spoke on "Electroprecipitation of Barium and Strontium Carbonates on a Nickel Base." The alkaline earth carbonates are commonly deposited on nickel by spray or by electrophoresis for use as electron emitters in electron tubes. Coatings obtained by these means are not completely reproducible, and Dr. Nall described a new method for deposition by electrolysis. On a properly prepared nickel cathode in bicarbonate solutions, a dense coating of the normal carbonates will form during electrolysis owing to the change in *p*H in the vicinity of the electrode. Coatings produced by this technique are at present being tested in electron tubes.

Leo Waldron of the Naval Research Lab. presented a film on "Marine Cathodic Protection." Protection of steel hulls of ships from galvanic corrosion in sea water is of great importance in maintaining the seaworthiness of our fleet. The film showed the intricacies of the installation of both impressed and galvanic current systems of cathodic protection.

Russell D. Kirk of the Naval Research Lab. spoke on "Charge Compensation in Luminescence and Coloration." Normal lattice vacancies are thought to be the source of luminescent and color phenomena in many materials, and, by modification of the number of vacancies in the crystal lattice, these effects may be enhanced or suppressed. Synthetic vacancies may be created by introducing foreign ions of unusual valence that induce corresponding changes in the number of oppositely charged ions in the lattice; the entire assembly remains electrically neutral. Several examples of intensification of the luminescent and coloration phenomena were demonstrated.

JEANNE BURBANK, *Secretary*

NEW MEMBERS

In April 1956 the following were approved for membership in The Electrochemical Society by the Admissions Committee:

Active Members

HAROLD L. CREAMER, Mallinckrodt Chemical Works; Mail add: 410 Prospect St., Fall River, Mass. (Electronics)

A recent action of the Board of Directors of the Society requires that, commencing January 1, 1956, all prospective members include first year's dues with their applications for membership.

Also, please note that, if sponsors sign the application form itself, processing can be expedited considerably.

HENDRIK D. ERASMUS, Metals Research Labs., Electro Metallurgical Co., P. O. Box 580, Niagara Falls, N. Y. (Electrothermics & Metallurgy)

ROBERT P. FRANKENTHAL, Applied Research Lab., U. S. Steel Corp., Monroeville, Pa. (Theoretical Electrochemistry, Corrosion)

JOHN W. HENSLEY, U. S. Naval Ordnance Test Station; Mail add: 74 A. Franklin, China Lake, Calif. (Corrosion, Electrodeposition, Theoretical Electrochemistry)

FRANCIS L. HOLDERREED, Anaconda Reduction Dept., The Anaconda Co., Anaconda, Mont. (Electrothermics & Metallurgy)

HERBERT MILLER, Sylvania Electric Products Inc.; Mail add: 63 Broadway, Newtonville 60, Mass. (Electronics)

WILLIAM T. MONAGLE, Reaction Motors, Inc., Ford Rd., Denville, N. J. (Electrothermics & Metallurgy)

JAMES D. PATRICK, Frigidaire Div., Materials & Process Engineering, General Motors Corp., Dayton 1, Ohio (Corrosion, Electrodeposition)

JOHN R. STONE, American Smelting & Refining Co., Barber, N. J. (Electrodeposition, Electrothermics & Metallurgy, Industrial Electrolytic)

JOHN D. STRICKLAND, The British Columbia Research Council, Vancouver 8, B. C., Canada (Electrodeposition)

ROBERT C. WADE, Metal Hydrides, Inc.; Mail add: 18 Congress St., Beverly, Mass. (Electrothermics & Metallurgy)

THOMAS B. WALKER, Canadian Carborundum Co., Ltd., Stanley Ave., Niagara Falls, Ont., Canada (Electrothermics & Metallurgy)

HERBERT C. WINKEL, Engineering Dept., Winkel Machine Co., Inc., Watervliet, Mich. (Battery)

FRANK WORMWELL, Dept. of Scientific and Industrial Research, Chemical Research Lab., Teddington, Middlesex, England (Corrosion)

Student Associate Members

JOHN R. AYLWARD, Western Reserve University; Mail add: 2320 E. 30th, Apt. 14-1156, Cleveland 15, Ohio (Battery, Electro-Organic, Theoretical Electrochemistry)

MINAS ENSANIAN, Western Reserve University; Mail add: 2027 East 115 St., Cleveland 6, Ohio (Battery, Electronics, Electro-Organic, Theoretical Electrochemistry)

NORBERT D. GREENE, JR., Ohio State University, 208 Engineering Experiment Station, Columbus 10, Ohio (Corrosion)

Reinstatements to Active Membership

ELDRED C. BRACE, Infilco, Inc., Tucson, Ariz. (Electrodeposition, Industrial Electrolytic)

MERRITT L. KASTENS, Stanford Research Institute; Mail add: 250 West Floreata Way, Menlo Park, Calif. (Electronics)

Transfer from Associate to Active Membership

DEMETRIUS N. TRIADIS, Research Lab., International Nickel Co., Inc., Bayonne, N. J. (Corrosion, Electrodeposition)

Transfer from Student Associate to Active Membership

ARTHUR C. DOUMAS, Dow Chemical Co.; Mail add: 125 Pecan Lane, Lake Jackson, Texas (Industrial Electrolytic)

Deceased Reported in March

KIRK H. LOGAN, Washington, D. C.
BERNARD W. MILLER, Chicago, Ill.
RICHARD M. WICK, Allentown, Pa.

PERSONALS

E. KEITH MCMAHON has been appointed director of development for the Chemical, Paint, and Metallurgical Dept. of the Merritt-Chapman & Scott Corp. Dr. McMahon will serve under Carl McFarlin, Sr., M-C&S Executive Vice-President for the Chemical, Paint, and Metallurgical Dept., which is comprised of Devoe & Raynolds Co., Inc., Louisville, Ky., and Tennessee Products & Chemical Corp., Nashville, Tenn. Dr. McMahon will be responsible for projecting and coordinating plans for the further growth and expansion of Devoe and Tennessee operations in the chemical, paint, and metallurgical fields.

HERBERT KAY has been named manager of catalyst development for the Climax Molybdenum Co. Previously he had been in charge of new chemical development. In his new position Mr. Kay will be responsible for the development of uses of molybdenum in corrosion inhibitors, intermetallic compounds, and ceramics, as well as in catalysts.

DONATO J. BRACCO has been appointed manager of the Chemistry Lab. of Sylvania Electric Products Inc. In his new post Mr. Bracco has responsibility for the company's research programs in such fields as surface chemistry, electrochemistry, solid state chemistry, re-

action kinetics, diffusion, and analytical research, including radioactive chemical procedures.

LUKE THORINGTON, previously with the Westinghouse Electric Corp. in Bloomfield, is now affiliated with the Engineering Div. of the Duro-Test Corp., North Bergen, N. J.

BOOK REVIEW

THE PRINCIPLES OF CHEMICAL EQUILIBRIUM by K. G. Denbigh. New York: Cambridge University Press, 32 E. 57 St., 1955. xxi + 491 pages, $7.50.

This is essentially a textbook of chemical thermodynamics for students of chemistry and chemical engineering, although the author does not hesitate to introduce molecular and kinetic theory, theories of nonideality, and a long section on statistical mechanics. The level is about that of first-year graduate students in American universities. There is only minor emphasis on specific problems of chemical engineering, not enough to detract from general use.

Part I (two chapters, 108 pages) is devoted to the first and second laws, auxiliary functions, development of thermodynamic formulas, discussion of chemical potential, partial molar quantities, etc. Part II (Chapters 3–10, 223 pages) contains chapters on applications to gases and gas reaction equilibria, phase rule and phase equilibria, ideal and nonideal solutions, and reaction equilibria in solutions. The treatment is in terms of the Gibbs chemical potential so far as practical. The concepts of fugacity, activity, and activity coefficients are introduced and illustrated logically. Part III (Chapters 11–15, 147 pages) deals mostly with statistical mechanics, which is used as an introduction to theory of heat capacity of crystals, to presentation of the third law, and for brief treatment of "regular solutions" and of adsorption. The last chapter discusses kinetics. Part III is probably written at too high a level, by comparison, or is too brief for its subject matter.

The book contains a great deal of well-written, provocative exposition and discussion. In comparison with other leading books in its field it merits high rating. This is not to say that it does not also deserve severe criticism. For example, the treatment of heat theory and the second law is entirely classical, and the usual confusion between "heat" and "thermal energy" is maintained. There is considerable pressure today, especially among the followers of Brönsted, to revise and broaden the interpretation of the second law to cover all forms of energy. Work cannot be obtained from systems all of whose energy is equipotential; entropy is the "quantity" in thermal energy which, to obtain work, must be degraded in "potential." The unique position of thermal energy is that entropy can be created, not that there is a special conversion factor in "transforming heat into work."

In such respects, Denbigh's book is quite disappointing. It is difficult to criticize individual statements when they are made from an outmoded point of view. It is pointed out (p. 21) that we do not expect a vessel of water to cool spontaneously while lifting a weight from the floor. It would seem equally important to point out that we do not expect to obtain electrical energy from two identical electrodes immersed in the same solution. We do not expect the vanes of a radiometer to turn if they are equally blackened and equally illuminated on all sides, etc.

In discussing oxidation of carbon (pp. 71–72) the author points out that ΔG is about 94 kcal/mole, and that an equivalent amount of useful work could be approached with suitable experimental arrangement. He then points out that ΔH has nearly the same value, and that on burning the carbon ". . . almost as much energy is obtained as heat as would have been obtained as work, if the process had been carried out reversibly. The wastefulness of the process is in the subsequent conversion of the thermal into mechanical energy."

Obviously this is wrong; the wastefulness is in the irreversible combustion. The author has already expressed the view (p. 32) that the ratio w/q in a Carnot cycle should be called a "conversion factor" rather than "efficiency," because the cycle is already 100% efficient. Certainly the entire viewpoint should be changed. In burning the carbon a certain amount of entropy has been created, and the production of work is now dependent on transferral of the entropy through a temperature interval.

We must also object to certain statements about electrical cells (pp. 161–162). "The essential aspect of the cell is the fact that the equilibrium composition of the reaction system is not the same as it would be in the absence of a potential difference between the two electrodes; if the potential difference is E the reactants and products come to a certain state of equilibrium, whereas if the cell is short-circuited they come to a quite different state of equilibrium. . . . the electrons in one electrode do not have the same chemical potential as those in the other electrode, and this difference of chemical potential can only exist because the liquid phase of the cell is a very poor *electronic* conductor."

Actually, of course, the contents of an electrical cell are *never* in a state of equilibrium; the materials are so chosen that reaction is negligible until the circuit is completed. In the example cited, hydrogen and mercurous chloride are quite capable of direct reaction, from a thermodynamic viewpoint. That direct reaction is negligible is a matter of kinetics and is not dependent on lack of electronic conduction in the medium.

Readers will surely deplore the fact that the third law is not developed before p. 414 and loses its perspective among the methods of calculating equilibrium constants. There is no mention

DECEMBER 1956 DISCUSSION SECTION

A Discussion Section, covering papers published in the January–June 1956 JOURNALS, is scheduled for publication in the December 1956 issue. Any discussion which did not reach the Editor in time for inclusion in the June 1956 Discussion Section will be included in the December 1956 issue. Those who plan to contribute remarks for this Discussion Section should submit their comments or questions in triplicate to the Managing Editor of the JOURNAL, 216 W. 102nd St., New York 25, N. Y., *not later than September 1, 1956*. All discussions will be forwarded to the author, or authors, for reply before being printed in the JOURNAL.

of the enthalpy and free energy functions such as $(G^0 - H_0^0)/T$, although these are new compiled from thermal as well as from statistical and spectroscopic data.

We repeat that this book compares very favorably with others in its field. It will be of best use under the guidance of an alert and experienced teacher.

CECIL V. KING

LITERATURE FROM INDUSTRY

CATALOGUES OF AEC REPORTS. Two free price lists of technical reports released by the Atomic Energy Commission for sale to the public are now available on request: Price List No. 25, superseding Price List No. 24 issued last August, and TID-1901, the AEC's "Report Announcement Bulletin." *Office of Technical Services*, U. S. Dept. of Commerce, Washington 25, D. C.

G-E HEATERS AND HEATING DEVICES. Bulletin GEC-1005G, 60 pages, contains application index, calculating data, specifications, operating information, and list prices of standard G-E heaters and heating devices. *General Electric Co.*, Schenectaday 5, N. Y.

"TERGITOL" SURFACTANTS. New 40-page data folder on Tergitol surfactants describes 7 nonionics and 4 anionics. Information given on physical properties, shipping data, specifications, and on wetting, penetrating, cleaning, and sudsing action, and lime soap dispersing power. *Carbide & Carbon Chemicals Co.*, A Div. of Union Carbide & Carbon Corp., 30 East 42 St., New York 17, N. Y.

NEW PRODUCTS

SENSITIVE D-C VACUUM-TUBE VOLTMETER. New Model 200B combines the high input impedance of earlier Keithley electrometers in a compact, battery-operated d-c vacuum-tube voltmeter with much greater sensitivity. *Keithley Instruments, Inc.*, 3868 Carnegie Ave., Cleveland 15, Ohio.

TRANSISTOR OSCILLATOR. Recently developed crystal controlled transistor oscillator offers a complete plug-in signal source with fixed temperature and humidity environment for transistor and circuitry elements. *James Knights Co.*, Sandwich, Ill.

IMMERSION HEATER. A single-unit immersion heater-thermostat, prewired and ready to be connected into any available circuit, has been introduced. The versatile ThermX "QT" Heater is ideal for use in both small plating tanks and in an independent series in large tank installations. *N. J. Thermex Co., Inc.*, 533 Bergen St., Harrison, N. J.

UNIVERSAL POTENTIOMETER. "Type K-3" Universal potentiometer has a unique reading window that centralizes 3 or 4 dial readings into a single row of digits plus a scale value. Used for measurement of d-c voltage. *Leeds & Northrup Co.*, 4934 Stenton Ave., Philadelphia 44, Pa.

RAPID INDUCTROL. The Rapid Inductrol is a motor-driven, oil immersed, continuously variable, full-range voltage control. Oil immersion minimizes maintenance, adds to the safety factor, and saves space. Available in both selenium and germanium rectifier models. *Rapid Electric Co.*, 2881 Middletown Rd., New York 61, N. Y.

ABRASIVE BUFF. A new Sectional Impregnated Abrasive Buff, for buffing of all ferrous and nonferrous metals, has been developed. The buffs are engineered of specially treated biased cloth, impregnated with selected abrasive grains bonded throughout its entire construction. *Coated Abrasives Div., The Carborundum Co.*, Niagara Falls, N. Y.

To receive further information on any New Product or Literature from Industry listed, write directly to the company at the address given in each item.

EMPLOYMENT SITUATIONS

Please address replies to box shown, % The Electrochemical Society, Inc., 216 W. 102nd St., New York 25, N. Y.

Positions Available

ELECTROCHEMIST

Internationally known research organization requires electrochemist for research and development work in corrosion, plating, batteries, etc. Training in physical chemistry, metallurgy, chemical engineering, or electrochemistry is required.

This is a permanent position with an organization offering excellent opportunities for personal and professional growth. Liberal benefits include generous tuition refund for graduate study. *Send resumé to Box A-264.*

METALLURGISTS

Company engaged in basic process and pyrometallurgy requires several men for Production, Development, and Quality Control who have some experience in one or more of the following: Smelting and Refining, Steelmaking, or Electric Furnace Operation. Excellent opportunities for qualified men. Hospitalization, insurance, and pension plan provided by Company. Plants located midwest, north, and south. All replies held strictly confidential. *Submit detailed resumé to Box A-265.*

Positions Wanted

CHEMIST, 36, 11 years' experience, including batteries, electroplating, general physical and chemical commerical testing, seeks New Jersey, Philadelphia, New York City position. *Reply to Box 357.*

CHEMICAL ENGINEER, 40, B.S. degree, 14 years' experience, including materials engineering and research, electrodeposition processes, product engineering and development work involving capacitors. *Reply to Box 358.*

CHEMICAL ENGINEER, experience in high temperature process development, including fused salt electrolysis, electric furnaces, metals extraction, B.Ch.E. 1939, married, age 38, seeking challenging, mature position. *Reply to Box 359.*

ADVERTISERS' INDEX

The Electrochemical Society

Patron Member

International Nickel Co., Inc., New York, N. Y.

Sustaining Members

Air Reduction Co., Inc., New York, N. Y.
Ajax Electro Metallurgical Corp., Philadelphia, Pa.
Allied Chemical & Dye Corp.
General Chemical Div., New York, N. Y.
Solvay Process Div., Syracuse, N. Y. (3 memberships)
Alloy Steel Products Co., Inc., Linden, N. J.
Aluminum Co. of America, New Kensington, Pa.
Aluminum Co. of Canada, Ltd., Montreal, Que., Canada
American Machine & Foundry Co., Raleigh, N. C.
American Platinum Works, Newark, N. J. (2 memberships)
American Potash & Chemical Corp., Los Angeles, Calif.
American Potash & Chemical Corp. (Nevada), Henderson, Nev.
American Zinc, Lead & Smelting Co., St. Louis, Mo.
Auto City Plating Co. Foundation, Detroit, Mich.
Bart Manufacturing Co., Bellville, N. J.
Bell Telephone Laboratories, Inc., New York, N. Y.
Bethlehem Steel Co., Bethlehem, Pa. (2 memberships)
Burgess Battery Co., Freeport, Ill. (4 memberships)
Canadian Industries (1954) Ltd., Montreal, Que., Canada
Carborundum Co., Niagara Falls, N. Y.
Chrysler Corp., Detroit, Mich.
Columbia-Southern Chemical Corp., Pittsburgh, Pa.
Consolidated Mining & Smelting Co. of Canada, Ltd., Trail, B. C., Canada (2 memberships)
Corning Glass Works, Corning, N. Y.
Crane Co., Chicago, Ill.
Diamond Alkali Co., Cleveland, Ohio (2 memberships)
Dow Chemical Co., Midland, Mich.
Wilbur B. Driver Co., Newark, N. J.
E. I. du Pont de Nemours & Co., Inc., Wilmington, Del.
Eagle-Picher Co., Joplin, Mo.
Eaton Manufacturing Co.
Stamping Div., Cleveland, Ohio
Electric Auto-Lite Co., Toledo, Ohio
Electric Storage Battery Co., Philadelphia, Pa.
The Eppley Laboratory, Newport, R. I.
Food Machinery & Chemical Corp.
Becco Chemical Div., Buffalo, N. Y.
Ford Motor Co., Dearborn, Mich.
General Electric Co., Schenectady, N. Y.
General Motors Corp.
Research Laboratories Div., Detroit, Mich.
Gould-National Batteries, Inc., Depew, N. Y.
Graham, Crowley & Associates, Inc., Chicago, Ill.
Great Lakes Carbon Corp., Niagara Falls, N. Y.
Hanson-Van Winkle-Munning Co., Matawan, N. J. (3 memberships)
Harshaw Chemical Co., Cleveland, Ohio (2 memberships)
Hooker Electrochemical Co., Niagara Falls, N. Y. (3 memberships)
Houdaille-Hershey Corp., Detroit, Mich.
Kaiser Aluminum & Chemical Corp.
Div. of Metallurgical Research, Spokane, Wash.
McGean Chemical Co., Cleveland, Ohio
Merck & Co., Inc., Rahway, N. J.
Metal & Thermit Corp., New York, N. Y.
Michelin Tire Manufacturing Co., Clermont-Ferrand, Puy-de-Dome, France
Monsanto Chemical Co., St. Louis, Mo.
National Cash Register Co., Dayton, Ohio
National Lead Co., New York, N. Y.
National Research Corp., Cambridge, Mass.
Norton Co., Worcester, Mass.
Olin Mathieson Chemical Corp., Niagara Falls, N. Y. (4 memberships)
Pennsylvania Salt Manufacturing Co., Philadelphia, Pa.
Philco Corp., Lansdale, Pa.
Philips Laboratories, Inc., Irvington-on-Hudson, N. Y.
Poor & Co.
Promat Div., Waukegan, Ill.
Potash Co. of America, Carlsbad, N. Mex.
Radio Corp. of America
RCA Victor Div., Harrison, N. J.
Ray-O-Vac Co., Madison, Wis.
Rockwell Spring & Axle Co.
Standard Steel Spring Div., Coraopolis, Pa.
Shawinigan Chemicals Ltd., Montreal, Que., Canada
Speer Carbon Co.
International Graphite & Electrode Div., St. Marys, Pa. (2 memberships)
Stackpole Carbon Co., St. Marys, Pa.
Stauffer Chemical Co., San Francisco, Calif.
Sylvania Electric Products Inc., Bayside, N. Y. (2 memberships)
Sarkes Tarzian, Inc., Bloomington, Ind.
Tennessee Products & Chemical Corp., Nashville, Tenn.
Udylite Corp., Detroit, Mich. (4 memberships)
Union Carbide & Carbon Corp.
Electro Metallurgical Co., New York, N. Y.
National Carbon Div., New York, N. Y. (2 memberships)
United Chromium, Inc., New York, N. Y.
Vanadium Corp., of America, New York, N. Y.
Victor Chemical Works, Chicago, Ill.
Wagner Brothers, Inc., Detroit, Mich.
Western Electric Co., Inc., Chicago, Ill.
Westinghouse Electric Corp., E. Pittsburgh, Pa.
Wyandotte Chemicals Corp., Wyandotte, Mich.
Yardney Electric Corp., New York, N. Y.

STRIPPING ENAMEL . . .

SAVING TIME

Enthonics* AT WORK

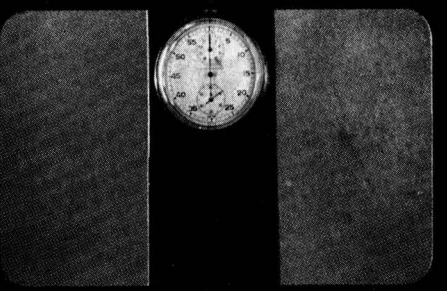

IMMERSED . . . THE WATCH STARTS!

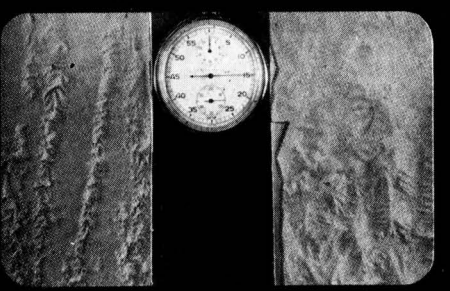

15 SECONDS . . . WRINKLING TAKES PLACE!

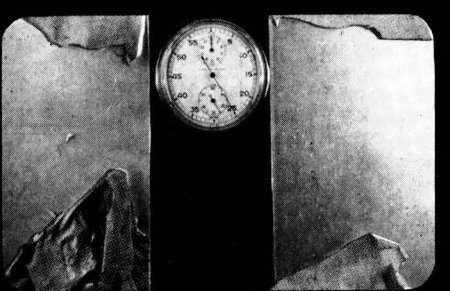

25 SECONDS . . . STRIPPING COMPLETED!

25 seconds from immersion to completed stripping!

That's the fast, dramatic story of ENTHONE Enamel Stripper S-18 in action — another example of *Enthonics at work.**

Enthone Enamel Stripper S-18 is the modern organic stripper developed for removing the newest organic finishes such as Epon or Epoxy coatings and many synthetic enamels from copper, copper alloys, steel and aluminum.

For the right strippers to solve your organic stripping problems fill out a questionnaire we'll send at your request; return it with typical samples of your work. Enthonics will find the answer . . . without obligation!

And ask for your copy of the "Enthone Check List" of literature covering more than 60 products and processes developed for modern electroplating and metal finishing.

* *The Scientific Solution of Metal Finishing Problems*

ENTHONE INCORPORATED

442 ELM STREET, NEW HAVEN, CONNECTICUT

ELECTROPLATING CHEMICALS METAL FINISHING PROCESSES

Service Representatives and Stock Points in Principal Cities of U.S.A. and Canada, Brazil, England, France, Sweden, and Germany